ABSTRACT

Title: STANDARDIZING AND SIMPLIFYING SAFETY SERVICE PATROL BENEFIT-COST RATIO ESTIMATION

Mersedeh TariVerdi, M.S., 2012

Directed By: Prof. E. Miller-Hooks, Department of Civil and Environmental Engineering

Safety Service Patrol (SSP) programs operate nationwide with the aim of mitigating the impact of traffic incidents, especially along urban freeways. The central mission of the SPP programs is to reduce incident duration thereby reducing congestion related travel delays, fuel consumption, emission pollutants, and the likelihood of secondary incidents. The SSP-BC Tool was developed herein to fill the need for a standardized benefit-cost ratio estimation methodology for SSP programs with wide applicability and substantiated and needed updatable monetary conversion rates. The developed tool is designed to capture characteristics of incident, traffic, roadway geometry, and weather particular to the state area. VISSIM, a traffic microsimulation platform, was used to develop several multiple regression models with R-square values of 0.7 to 0.9 to assess the impact of travel delay, fuel consumption, and emission pollutants. Separate approaches were employed to estimate the savings in secondary incidents. In addition, a comprehensive method to compute fuel consumption and emissions is presented.

STANDARDIZING AND SIMPLIFYING SAFETY SERVICE PATROL BENEFIT-COST RATIO ESTIMATION

.

Mersedeh TariVerdi

Thesis submitted to the Faculty of the Graduate School of the
University of Maryland, College Park, in partial fulfillment
of the requirements for the degree of
Master of Science
2012

Advisory Committee:
Professor Elise Miller-Hooks, Chair
Professor Paul Schonfeld
Assistant Professor Lei Zhang

Acknowledgments

First and foremost I offer my sincerest gratitude to my supervisor, Prof Elise Miller-Hooks, who has supported me throughout my thesis with her patience and knowledge. No doubt that without her this thesis would not have been completed or written. I am deeply indebted to my committee members Prof. Paul Schonfeld and Dr. Zhang for their time and effort in reviewing this work.

I acknowledge the I-95 Corridor Coalition for their financial support for this project and Tier 1 center (CTSM) for the 9-month fellowship.

I would like to thank my team-mates, Suvish, Xiadong, and Kara for sharing the literature and invaluable assistance; to my best friends, Nezam, Alireza and many others for their support.

I am deeply and forever indebted to my parents for their love, support and encouragement throughout my entire life. I am very grateful to my brothers Sam and Amir.

Contents

List of Tables

List of Figures

CHAPTER 1. Introduction

Traffic congestion adversely effects traveler safety, cost, quality of life and the environment. Traffic congestion can be recurring or non-recurring, i.e. due to randomly arising events. Congestion caused by recurring events is a result of traffic demand exceeding the fixed capacity of a road segment during every day traffic patterns. Conversely, when the available capacity of a road segment decreases due to unpredictable events, such as vehicle incidents or adverse weather conditions, it is categorized as non-recurrent congestion. The Federal Highway Administration (FHWA) sites non-recurrent congestion as the cause of approximately 60 percent of all road traffic in the United States.

Traffic incidents (e.g. accidents, breakdowns), in particular, are a major cause of non-recurring traffic congestion. In fact, Caltrans' Division of Research and Innovation claims that traffic incidents cause about 25 percent of this type of congestion on freeways (Caltrans, 2010). Therefore, incidents are counted as one of the most significant reasons for congestion in vehicular transportation. Increased travel time, increased risk of secondary accidents and decreased safety to other drivers and responders were identified as the most serious problems associated with an incident in a road segment. Additional problems, such as increased fuel consumption, pollutant emissions, cost of goods and services and negative impact on emergency response time, are also considered by decision-makers to be significant issues arising from traffic incidents. Moreover, the longer the incident duration and the time of impact to traffic flow, the greater the incident's negative impacts. It is evident that traffic incidents have a strong adverse effect on urban areas. As such, reducing incident clearance time can mitigate its impacts (see, for example, Blumentritt et al., 1981).

To control the impact of traffic incidents, Traffic Incident Management (TIM) programs that aim to reduce the duration and consequences of incidents and improve the safety of motorways have been introduced nationwide. A significant goal of most TIM programs is to coordinate the response by a number of public and private organizations to incidents. For example, transportation agencies are typically called to the incident scene by first responders, including law enforcement. Freeway Service Patrol (FSP) and similar Safety Service Patrol (SSP) programs are often components of a large TIM program. These programs have been widely cited as very effective. In these programs, the service patrol vehicles may roam the roadways to which they are assigned (i.e. their beats), monitoring and responding to observed incidents. Alternatively, they may be dispatched to a call while roaming or from a traffic incident management center. The trained drivers of patrol vehicles may call for assistance from law enforcement and/or emergency responders, or may directly assist with motorists' needs.

SSPs receive most of their funding from state and federal taxes. Therefore, they are must have public support and may be scrutinized when budgets are limited. While states work to provide essential services they must consider their budget limitations. As such, quantifying the benefits of SSPs is important to legislators determine the effectiveness of such programs in terms of improving safety and increasing public benefits. Thus, even in times of budget crises, the benefits of these programs may be great enough that funding them is encouraged.

This research effort builds on recent I-95 Corridor Coalition efforts (Chou and Miller-Hooks, 2008) in which a procedure was developed to determine the benefits (i.e. reduction in congestion, secondary incidents, fuel consumption and pollution, along with their monetary equivalents) of an existing SSP program. The methodology was employed to estimate the B/C ratio for the Highway Emergency Local Patrol (H.E.L.P.) program in New York. This prior effort revealed the need for additional study in identifying a set of best performance measures and monetary conversion rates to accurately depict the benefits and costs of such programs. Moreover, the developed approach, like other comparable methods with similar accuracy used around the country, requires significant computational effort and is, therefore, costly and time-consuming. A quicker and less data-intensive approach is desired so that it can be readily and widely utilized by all states around the US Such an approach is developed within the effort described herein.

When attempting to compare an SSP program to its alternatives, it is common to compare the benefits of the program with its costs through a benefit - cost (B/C) ratio. This ratio has been estimated for many SSP programs operating around the nation. These ratios, however, range dramatically (e.g. from 2-to-1 to 36-to-1). The majority of this variability is likely due to the wide range of estimation methodologies and monetary equivalent conversion factors employed within these techniques, rather than to actual differences between the program benefits. This great variability also opens these findings to questions about their accuracy. A standardized methodology that can be universally and equitably employed in such B/C ratio estimation is essential as it would aid in creating consistency and, therefore, greater confidence in the validity of the results.

The main objective of this study was to develop a user-friendly tool, referred to as the SSP-BC Tool, based on consistent performance measures and monetary conversion rates that can quickly compute the B/C ratio of an existing or planned SSP program. In Chapter two, a review of existing US SSP programs and other relevant studies that evaluate their performance, as well as reported B/C ratios, are presented.

There are numerous factors that might be considered in evaluating the benefits to society of a SSP program. The most common are: savings in travel time, fuel consumption, pollutant emissions and secondary incidents. These are described in detail in Chapter three. In the same chapter, a review of factors that have the greatest effect on these measures is also provided. Components of weather, roadway gradient and curvature, density of ramps in the roadway segment, and traffic composition, all of which influence the available capacity of a roadway segment and fuel consumption rates, are considered in this study.

To quantify these benefits of a SSP program, VISSIM, a microscopic traffic simulation product, is employed. The Component Object Module (COM) interface of VISSIM was used for modeling freeway incidents. The COM interface permits controlled experiments with altered spatial and temporal incident characteristics. To provide a realist portrayal of an incident in a simulation environment, all factors that have been found to affect travel delay, fuel consumption and emissions must be considered in the experimental design criteria. A methodology for modeling traffic incidents is adopted that exploits this COM interface. Within this methodology factors, such as roadway length and gradient, are directly set in VISSIM, while other factors, such as volume, traffic composition and incident attributes, are defined through the interface. The effect of weather on roadway performance is captured through changes to free flow speed. This methodology is described in Chapter three.

Replicating real-world conditions within a simulation environment requires a primary study into the capabilities of the software and creation of specific methods needed to adequately capture desired effects. Chapter four highlights the necessity of this investigation and describes these methods. Initial runs were made to study trends in travel delay and fuel consumption estimates resulting from univariate changes in factors. Whether variables are dependent was also verified through runs in which the state of two or three factors were permitted to change simultaneously.

Upon analyzing outputs from the simulation runs, and after discussion with PTV America's support, it was determined that the built-in fuel consumption tool available within VISSIM was not suitable for this study. The tool did not provide repeatable estimates. Moreover, it seems that it overestimates fuel efficiency of vehicles available within the US and its equations were developed for emissions estimation from traffic on arterials. Specific methods for calculating fuel consumption and emissions from vehicular modal parameters gathered for each VISSIM run are presented in Chapter four. A review of factors affecting fuel consumption and emissions is given in Chapter three.

Analysis of results from the initial runs provided insights into the response of the vehicles in VISSIM to changes in characteristics of the roadway segment, traffic volume and the roadway environment. As an example, these runs revealed that traffic performance was unaffected by changes in roadway curvature, an important input. Thus, efforts associated with these runs indicated that the effects of significant curvature could not be captured directly and a suitable methodology would be needed.

Additional restrictions on combinations permitted in batch runs were identified, (i.e. when speed was set through code and grade was non-zero) that preclude the possibility of conducting simulation runs to capture all combinations of input. Because it was not possible to create batch runs to run all combinations of inputs, regression analysis was employed. Specifically, regression models of travel delay and fuel consumption were developed and calibrated based on simulation results from 1200 runs on a typical stretch of a three lane freeway. For each run, a randomly generated traffic incident was created. The incident scenarios involved one of three states of lane blockage (shoulder, one lane and two lane blockage) with equal likelihood. For each incident, the incident duration was set according to a statistical distribution identified in previous studies. This culminated in 7 regression models capturing the response of dependent variables associated with travel delay and fuel consumption to incident duration, traffic volume, gradient and percentage of trucks. To reduce the error terms in the regression models, and improve overall fitness, an additional 73,290 runs were designed and conducted. The runs involved all possible combinations of 16 categories of incident duration, 11 categories of traffic volume and 6 speed categories, resulting in 1,056 combinations. For each combination, runs including one of 3 types of lane blockage and one of 5 possible roadway sizes in terms of number of lanes and 5 random seed for each were made. Note that no complete road closure scenario was considered. Other spatial and temporal incident characteristics were held constant.

At the heart of the SSP-BC Tool is a database of five tables: tables of travel delays for light and heavy duty vehicles, average driver and police officer wages, and fuel costs. The tool pulls data from these tables to complete computations related to the benefits and costs of the studied system. Data in these tables are derived directly from the simulation run results (travel delays, fuel consumption), through regression-based estimates (travel delays, fuel consumption), computations (emissions, secondary incidents) or from publically available sources (wages, fuel costs, traffic composition, and monetary conversion rates). The regression models were used specifically to capture the effects of traffic compositions (i.e. percentage of trucks in traffic mix) and roadway grade.

While Chapters three and four focus on individual incident characteristics and impacts, Chapter five describes calculations and assumptions used to obtain program benefit estimates, and ultimately the B/C ratio. Chapter six includes snapshots of the tool and a brief explanation of how the tool works through an illustrative example. Results of a case study involving the H.E.L.P program are presented Chapter seven. General findings follow in Chapter eight.

CHAPTER 2. Background and Literature Review

SSP programs exist in a large portion of the US SSP drivers can provide free assistance to motorists. Examples of service include: providing a gallon of gasoline, changing flat tires, jump starting dead batteries, pushing vehicles off the road, providing minor mechanical repairs, and helping motorists call for other emergency services. In the case of severe accidents, SSP drivers are trained to help police redirect traffic. These services are crucial for shortening the duration of incidents and, thus, diminishing their impact, and improving safety for other drivers on the roadway segment. Furthermore, SSPs can be used as probe vehicles, providing real-time updates on traffic conditions (Traffic Incident Management Handbook).

In this chapter, evaluation studies on SSP programs around the nation reported in the literature are reviewed. B/C ratio computation approaches and estimates by program are reported.

1.1 Factors to Consider in Benefit-Cost Estimation

The first step of estimating the benefits and costs of a SSP program is to determine the components that should be considered in the calculations. The reduction in travel delay and corresponding economic benefits for the motorists plays a significant role in the benefit estimation. Some studies also consider prevention of secondary incidents due to decreased incident duration; they assume a direct relation between number of potential secondary incidents and incident duration. In addition, environmental concerns, such as fuel consumption and pollutant emissions, are included in savings. Some studies derive an estimate for fuel consumption from delay time or use the computational tools available in some simulation software packages. There are other savings that should be counted in the benefits of a SSP program. For example, costs of towing if SSP vehicles were not at the scene, lawsuits from secondary incidents that are prevented, and additional time available for troopers for more urgent tasks that the SSP programs cannot handle.

1.2 Evaluation and Estimation Methodologies

The most accurate way to evaluate the benefits of a SSP program is to conduct a "before-and-after" study that compares the incident detection, response, clearance and recovery times (often marked by a return in traffic state to pre-incident flow rates) for a comparable period before and after the deployment of the SSP program. Donnell et al. (1999) evaluated the Penn-Lincoln Parkway Service Patrol in this way. The study recorded similar incidents that occurred prior to and following the implementation of SSPs, the collected data was compared to compute possible savings. Respectively, incident response time and clearance time were found to be reduced by an average of 8.7 and 8.3 minutes (17.1 minutes overall savings in incident duration), yielding a B/C ratio of 30:1. In another study, Skabardonis et al. (1995) analyzed the operation of SSP programs in San Francisco, California using field data from 24 weekdays before the SSP and 22 weekdays after the SSP program was implemented. The B/C ratio was shown to be 3.4. An assessment that was carried out by Bertini et. al. (2001) in one region of Oregon showed that the regional SSP program reduced the average cost of delay-causing incidents to travelers by 36 to 66 percent when it was upgraded from part-time to full-time.

In many circumstances, however, the "before" dataset is not available as it usually requires a well-maintained and long-term managed database. Therefore, researchers adopt a "with-and-without" approach. This method compares a SSP managed incident to a similar incident that was managed by state or local police. Commissioned by the Safety Service Patrol (SSP) program in Northern Virginia (NOVA), Dougald et. al. (2008) compared the average durations of various episodes with similar incident types and roadway and traffic conditions. The main difference between each episode was whether or not the SSP program responded. The data that was compared came from two databases: 1) the incident management database (IMD) and 2) the Virginia State Police (VSP) computer-aided-dispatch (CAD) system. This type of study has been applied to investigations conducted in other states, including Indiana (1999), Minnesota (2004), Florida (2005), California (1995, 2005), Maryland (2006), New York (2008) and Missouri (2010).

In these circumstances where no "before" data was maintained, it is necessary to make assumptions surrounding how long the incident would last had such a SSP program not existed. In this way, the potential savings of SSP-assisted incidents can be calculated. Sensitivity analysis can be conducted to examine how the B/C ratio responds to varying incident duration savings. Generally, the range of assumed duration reduction is between

10 and 20 minutes. A study of the evaluation of the SSP program in Los Angeles, assumed that the SSPs would reduce incident duration by 10, 12.5, or 15 minutes, resulting in a B/C ratio that ranged from 3.75:1 to 5.5:1 (Skabardonis et al., 1998). Moreover, the average duration of crashes and in-lane incidents handled with the Hoosier Helper SSP were assumed to be lowered by 10 min while all other incident durations were reduced by 15 minutes (Latoski et al. 1999). Chou et al. (2008) lengthened the duration of without FSP-assist incidents by between 5 and 25 minutes in 5-minute increments for studies on SSP program of New York State, H.E.L.P.

The estimation methods of incident delay and delay savings of SSP programs draw on methods such as statistical, deterministic queuing, or simulation-based models, or surveys. Examples of studies involving each are given next.

Mauch et al. (2005) examined the Big-rig SSP pilot program that provides services including heavy-duty tow trucks along the I-710 freeway in California through use of statistical modeling. Regression analysis was completed and correlations between average vehicular delay per day and big-rig and non-big-rig incidents were noted. A calibrated regression-based function was given to describe the relationship between traffic delay and incident duration. They combined the response time savings with delay estimates to forecast delay savings. It was assumed that for comparison purposes if conventional services would be required, 45 minutes of response time would be needed for dispatch of the big-rig tow truck. Expected benefits from the program were estimated to be $14,700/day with a benefit-cost ratio of 5:1, where benefit computations include travel delay only. Other studies employing statistical approaches to evaluating the benefits of SSP programs include: Mauch et al. (2005), Haghani et al.(2006).

Where traffic volume profiles over the incident duration are available, a deterministic queuing model can be applied to predict travel delay. Skabardonis et al. (1995, 1998) estimated delay as the difference in travel times under normal and incident conditions using data from loop detectors and probe vehicles. Guin et al. (2007) used extrapolated capacity reduction factors during the response and clearance of incidents associated with cumulative traffic volume as inputs to the queuing model for the Georgia NaviGAtor SSP program. This approach was also employed in the evaluations of SSP programs in Oregon (Bertini et al., 2001), Florida (Hadi and Zhan, 2006; Hagen et al, 2005), Virginia (Dougald wt. al, 2007) and Missouri (Sun et Al., 2010).

The majority of SSP program evaluation studies rely on simulation, because it is often the case that traffic volume data and other traffic characteristics are limited and, thus, effects on traffic must be estimated. Traffic simulation models have become quite advanced, permitting control of roadway design, traffic volumes, and incident characterization, including incident duration, number of lanes blocked, and location. Latoski et al. (1999) estimated delay using the XXEXQ macroscopic traffic simulation model in studying the Hoosier Helper program in Northern Indiana. The study yielded B/C ratio of 4.71 if the program operates only in the day time and 13.28 for 24 hour operations of the program considering travel delay in benefits and annual investment, employee salaries and benefits, overhead and maintenance costs. 120 incidents were replicated in the microscopic CORSIM traffic simulation platform for the purposes of studying their effects on travel delay for Coordinated Highways Action Response Team (CHART) in Maryland (Chang et al., 2006). Benefits in reduction of travel delay, fuel consumption and emissions were estimated to be 1,006.50 million dollars in a similar study in 2009. Representative incidents with varying duration and lane blockage were simulated in the PARAMICS microscopic traffic simulation platform to analyze the Freeway Incident Response Safety Team (FIRST) program in Minnesota (MnDOT, 2004). Total incident delay was plotted against volume corresponding to different incident durations ranging from 4 to 40 minutes. Based on the plot, delay reductions can be predicted given the incident duration reduction caused by the FIRST program. The B/C ratio estimated for FIRST was 15.8, including travel delay and crash avoidance in the benefit estimation. More recently, Chou and Miller-Hooks (2008) replicated 693 actual incidents in CORSIM to analyze the B/C ratio of the H.E.L.P. program in New York. Incidents were simulated with H.E.L.P-assist and without H.E.L.P-assist circumstances. The rubbernecking effect set up in CORSIM was computed from capacity reduction estimates associated with number of lanes, lane blockage, and incident type. It was found that the B/C ratio range was between 2.14 and 2.68 (for different costs) using conservative monetary conversion rates for travel delay, fuel consumption, emission pollutants and avoided secondary incidents. The B/C ratio would increase to between 13.2 and 16.2 if vehicle occupancy, traffic composition, and higher incident severity level were included in benefit evaluation.

1.3 Overview of Service Patrol Benefit/Cost Ratios per State

The first SSP program with annual operations originated in 1960 in Chicago, Illinois. In 2006, the US DOT and Intelligent Transportation System (ITS) Joint Program Office (JPO) conducted a survey regarding service patrol programs in 106 metropolitan areas. At the time, 73 out of 99 areas that responded had a service patrol program in operation and more than 40 states had implemented at least one SSP program.

From review of the literature, including journal articles, research reports and web pages from state departments of transportation, it can be concluded that service patrols reduce incident duration, improve safety, and help reduce fuel consumption and emissions. It was proved that its benefit outweighed its cost with the B/C ratio ranging from 1.48:1 to 38.25:1. A summary of B/C ratio estimates noted in the literature can be found in Table 2.1. It is evident from the table that the ratios vary widely. This is in part because there are inconsistencies in not only analysis methods and monetary conversion rates used to obtain the ratios, but also in the factors they include in benefit estimation. In fact, each state or city adopts its own set of factors that it deems relevant to calculate the B/C ratio. Underestimation may result from ignoring certain benefits while overestimation may occur from over-counting low probability events. Differences in monetary conversion rates, that provide monetary values for estimated benefits, can also greatly impact the final ratio values.

Table 1.1 Freeway service patrol B/C ratio

State	Program name	Location/service area	Year	Included benefits	B/C
California	I710 Big-Rig	I-710 south of ocean blvd to the I-5 interchang	2005	Travel delay	5
California	FSP	LA	1998	Travel delay, fuel consumption	5 for 15 min duration reduction
California	FSP	SF	1995	Travel delay	3.4
Florida	Road Ranger	district 1-7, except dis.3, Turnpike	2005	Travel delay, fuel consumption	2.3-41.5, 25.1 overall

Georgia	NaviGAtor	Atlanta	2007	Travel delay, fuel consumption, emissions, avoided secondary incidents	4.4
Indiana	Hoosier Helper	Northwest Indiana	1999	Travel delay	4.7 daytime ,13.3 24h
Michigan	Freeway courtesy Patrol	Southest Michigan	2009	Travel delay Air quality	15.2
Minnesota	FIRST	Minneapolis, St. Paul	2004	Travel delay, crash avoidance	15.8
Missouri	Freeway motorist assist program	St.Louis	2010	Travel delay, secondary crashes	38.25
New York	H.E.L.P	Long Island; in New York City; the Lower Hudson Valley; Buffalo; Rochester; and the Albany Capital District	2009	Travel delay, fuel consumption, emissions, avoided secondary incidents	2.14-16.5 for 20 min reduction
Oregon	FSP	Region 2	2001	Travel delay Fuel consumption	32.52-3.68
Virginia	SSP	Hampton Road	2007	Travel delay, fuel consumption, emissions	overall 4.71, range of 1.48-10.17 Vs. V/C
Virginia	NOVE SSP	Northern Virginia	2006	Travel delay, fuel consumption, emissions	6.2

Each mentioned previous study was conducted for a unique location given data for a specified time period and each such study typically required enormous effort to complete. These studies, however, are needed to defend and secure financial support for continued program operations. It is often the case that studies in one area re-invent methodologies created for studies in other areas. Moreover, their estimated B/C ratios cannot be directly compared, because they rarely use similar factors or monetary conversion rates.

The Freeway Service Patrol Evaluation (FSPE) model, developed by the University of California at Berkeley (Skabardonis et al., 2005) for California, is a dedicated SSP evaluation tool. That can be applied more widely. The FSPE model was implemented in Excel workbook using Visual Basic for Application (VBA). This tool computes daily, annual or specified time period savings with respect to incident delay, fuel consumption and emission, as well as the B/C ratio. The tool relies on a deterministic queuing model for calculating incident delay. Benefits of SSPs are dependent on the beat’s geometric and traffic characteristics, and the frequency and type of assisted incidents. Default model parameters are provided, but they can be modified by the users if empirical field data are available. This SSP model can analyze 24/7 SSP services, or can accommodate more limited weekday or weekend services, although the best final prediction model was found to be for 24 hour SSP services. They applied the 24 hour model to estimate the benefits. They count for limited operational hours and used the proportion of vehicle miles traveled (VMT) in fewer than 24 hours. Each beat is divided into segments for each travel direction and data are input accordingly. The FSPE model distributes the FSP-assists per incident type proportionally to the VMT per beat. It is assumed that the response time without the SSP is 30 minutes. The SSP response time is computed based on the beat length, average tow-truck speed, and number of trucks operating on the beat.

The FSPP model later was developed based on the FSPE model to evaluate the roadway segments which does not have SSP assistance. The saving in response times are estimated based on a statewide weighted average of all incidents from the fisical year 2002-2003 FSP-assists database. One of the strengths of this SSP evaluation tool is the consideration of directional effects of daily traffic volume along each patrolled beat. The tool was calibrated for use in California. Significant effort and data are required to calibrate the queuing model for use in other locations (Skabardonis et al., 2005).

1.4 Summary

While B/C ratio estimation models, specifically FSPP and FSPE, exist that might have general utility in B/C ratio estimation for SSP programs, the SSP-BC Tool proposed herein accounts for a wider array of traffic, environmental and program characteristics that influence benefit and cost estimates. The SSP-BC Tool accounts for factors, such as ramp density, horizontal and vertical alignments, traffic composition, and weather conditions, that have been identified as important to travel delay, fuel consumption and emissions estimation. Moreover, fuel consumption and pollutant emissions estimates used in prior related studies, when included, are made based on simplistic regionally developed rates for travel day to fuel consumption and emissions. For example, in the FSPP tool, the fuel consumption and emission calculation factors are developed for California conditions. The tool uses average vehicular speed; thus, driving modes such as acceleration or deceleration and stops of vehicles are not captured in the computations. In the proposed SSP-BC tool, estimates of these factors are made from these modal parameters. The SSP-BC Tool also has the advantage of including up to two lanes blockage in the freeway segment. The FSPP and FSPE tools include at most one lane that is blocked. On the other hand, the FSPP and FSPE tools can be used to compute incident response time savings due to a SSP program. As such, they can provide needed input to the SSP-BC tool. The SSP-BC Tool also accounts for secondary incidents that statistically would arise with longer incident durations than can be expected where SSP exist, which FSPE and FSPP tools do not.

CHAPTER 3. Factors Affecting SSP Benefits and Their Calculation

Numerous methods are practiced by incident program managers for measuring and evaluating SSP program performance. Results of such studies are often used to justify the expenses of these programs, but can also provide insights that can be used to improve performance and ultimately reduce the number and impact of traffic incidents. The first step to evaluate a SSP program is to identify the contributing factors to benefit values as will be discussed in this chapter. In the first Section, MOEs employed in benefit estimation are identified. Factors effecting the estimation of these MOEs are discussed in Section 3.2. Methodologies used for their computation are described in Subsections 3.3-3.5. This is followed by a summary in Section 3.6.

2.1 Measures of Effectiveness (MOEs)

A myriad of MOEs may be used in evaluating the benefits of a SSP program. Typical measures include: operational performance measures (e.g. incident response time), traffic performance measures (e.g. travel delay), environmental impacts, safety (secondary incident prevention), reliability, maintainability, and ease of use. In the context of this study, travel delay, fuel consumption, pollutant emissions, and prevention of secondary incidents have been chosen as the MOEs of interest.

2.2 Factors Contributing to Travel Delay and Fuel Consumption

Numerous factors, like roadway geometry and weather, affecting MOEs have been identified in studies on travel delay, fuel consumption and emissions. A comprehensive set of factors has been used in this study for estimating all MOEs; although, some factors are more significant for one MOE than others. For example, roadway grade will have greater impact on fuel consumption than occurrence of secondary incidents. To identify the factors of greatest importance for travel delay estimation, works in the literature were reviewed. The majority of statistical and deterministic queuing methods developed for this application area assume that the most significant factor in reducing incident-induced delays is to reduce incident duration. One of the formulae most widely used to compute travel delay was developed by Wirasinghe (1978) as described in (Qi et al, 2002). For a given roadway segment, Wirasinghe's formula is given in equation (1). This equation includes factors of incident duration (T), total capacity (S_1), traffic demand (S_2), and bottleneck capacity (S_3).

$$\boldsymbol{Travel\ Delay} = \frac{T^2(S_1-S_3)(S_2-S_3)}{2(S_1-S_2)} \qquad \textbf{Eq.3.1}$$

In equation 3.1, incident duration and bottleneck capacity are directly related to travel delay resulting from an incident. The number of lanes blocked and severity of the incident is a function of available capacities at bottlenecks at the time of the incident. Incident duration estimation is required within equation 3.1 for travel delay computation. Since 1987 many techniques have been developed to predict incident duration based on collected data. However, the site-specific nature of the collected data has caused disagreement as to the validity of the results. The majority of prior studies have employed different statistical models to estimate incident duration, travel delay, and similar required data to evaluate traffic conditions and the efficiency of an SSP or similar program while they can be applied in studies of roadways with similar traffic characteristics, geometry and weather. These models are neither suitable nor applicable to other regions with different traffic circumstances. A goal of the proposed SSP-BC Tool is, thus, to provide a method to uniformly estimate and compare travel delay savings associated with SSP programs.

To address the need for regional or even roadway-specific estimates, microscopic traffic simulation methods are employed. In general microscopic traffic simulation can be used to estimate the consequences of an incident on travel performance. In developing the SSP-BC tool, to produce realistic estimates, its application to a nationwide model, calibrated parameters for typical US highways, comprehensive information and details of the typical incident sites were considered.

When considering travel delay, it is important to analyze congestion, incident duration and the causes of both. Geometry of the roadway, traffic characteristics, demand, construction and major maintenance operations, traffic accidents or vehicular breakdowns, and weather conditions are the factors suggested in the Highway Capacity Manual that affect the actual capacity of a highway segment. Table 3.1 shows factors that have been considered in some studies of incident duration and travel delay. In this study, the simulation experiments were designed to account for nearly all of these suggested factors.

Table 2.1 Previous studies on travel delay and incident duration

Authors, year	Dependent variable	Variables used in the model development
Zhao et al. 2010	Incident delay	Peak-hour Character of incident Severity level Disposal type
Boyles wt al. 2006	Incident duration	Number of lanes blocked Personal injuries Response units(fire department, police, FSP)
Qi (2002)	Incident duration	Temporal characteristics Weather (snow, rain) Incident location (with respect to ramps) Incident characteristics Involved vehicle Response source
Smith et al. (2001)	Clearance time	Physical variables: accident time of the day, the day of the week, weather Vehicle variables: number of vehicles, truck involvement, Response variables
Garib et al. (1997)	Incident duration	Number of lanes affected Presence of trucks Time of the day Police response time Weather

A basic freeway segment is chosen as the control sample for simulation designs herein as it is in HCM for estimating the capacity of a roadway under different circumstances (HCM, 2010, 10-1). The method of the HCM 2010 assumes that under basic conditions a freeway segment can reach its full capacity. These basic conditions include clear fine weather and visibility, no congestion due to incidents, no work zone activity (short- or long-term), and acceptable pavement conditions which support normal operations. In addition, presumably all the drivers are familiar with the area.

Models of typical base geometries and additional estimates to account for special roadway features, such as curvature and weather, were developed. The frequency and severity level of incidents were permitted to vary over time and space. Temporal characteristics include season, day of week, and time of day of an incident. Other attributes, such as location of the incident in the roadway and lane blockage due to incident occurrence, are considered as spatial characteristics. Regardless of the time or location that an incident occurs, as long as there is at least one vehicle traveling behind the incident, the result is capacity and/or speed reduction, which affects time delay. A list of factors that are studied herein is given as follows.

- Geometry of the roadway segment
    - Segment length
    - Number of lanes and average lane width
    - Lateral clearance (shoulder)
    - Ramps
    - General terrain
    - Horizontal curves
    - Segment gradient
- Traffic Characteristics
    - FFS
    - Ramp FFS
    - Traffic flow rate
    - Percentages of trucks in traffic flow
- Incident attributes
    - Incident severity
    - Incident duration
    - Average incident duration
    - Rubbernecking effect
- Weather conditions

These factors are discussed in the following subsections. As this study uses a simulation estimation method, The range associated with each chosen factor within the simulation estimation method is based on information from the literature as discussed in proceeding subsections. These factors affect not only travel delay, but fuel consumption and emissions. Some factors affect these latter MOEs directly and, thus, are not only a consequence of added delay.

2.2.1 Geometry of Roadway Segment

2.2.1.1 Segment Length

A large number of studies have used simulation to study the impact of traffic incidents on travel delay using a model of a generic fixed-length homogeneous section of roadway. The homogeneity of a Section relates to its traffic, geometry and weather. Chou and Miller-Hooks (2008), Saka et al. (2004), and Hobeika and Dhulipala (2004) examined a 10-mile segment. This length was typically chosen to ensure that the effects of a traffic incident could be entirely captured within the model. A similar length, thus, is used for simulation runs of this study. Greater homogeneity may exist for shorter roadway segments, especially where there is significant horizontal curvature and vertical changes; however, using a shorter length segment can lead to errors in estimates. Additionally, it has been noted that there can be an undesirable increase in accident location reporting errors and other types of errors for shorter roadway segments (Shankar et al., 1994).

2.2.1.2 Number of Lanes and Average Lane Width

As the study focuses on freeways, 2 to 6 lane highway segments in each direction are considered. It is assumed that the standard minimum lane width of 12 feet is available based on the default value of lane width of urban and rural highways in HCM 2010.

2.2.1.3 Lateral Clearance (Shoulder)

To ensure full operational capacity, basic freeway segments require a minimum 6-feet right-side shoulder. As VISSIM does not offer the capability to model shoulders, initial numerical experiment were conducted to investigate VISSIM’s ability to capture the impact of shoulder characteristics. This is done by adding an additional lane that is closed to traffic. It was noted that VISSIM does not capture the effects of shoulder existence. Therefore, no interruption in flow or reduction to capacity due to either shoulder width or closure was modeled. Note that impact of capacity reduction due to incidents occurring in the shoulder has been studied in this effort.

2.2.1.4 Ramps

Only major junctions were modeled and all on- and off-ramps were assumed to be located at the right-edge of the roadway. According to the HCM 2010, merge and diverge influence areas are 1500 feet downstream from the merge and 1500 feet upstream from diverge points. Thus, route decisions used within VISSIM to model vehicle movements towards off-ramps started from 1500 feet before the off-ramps. Qi (2002) considered the possibility of incorporating relationships between incident and ramp locations in incident duration modeling. Qi was unable to obtain the needed data to ascertain details of this relationship. Moreover, no other studies of this relationship could be found in the literature. Preliminarily experiments were designed here to study this relationship, but based on the results, (Section 4.2.2) only ramp density was used to capture the impact of ramps.

Ramp density is defined in HCM to explain the impact of merging and diverging vehicles on the free flow speed and the capacity of the segment. Ramp density is the average number of on-ramps and off-ramps in a 6-mile segment based on the midpoint of the study segment. It varies from 0 (occurs in rural areas) to 6 (possible in dense urban areas) total ramps per mile. The free flow speed of a basic freeway segment is most sensitive to ramp density as discussed in Chapters 10 and 11 of the HCM. The HCM does not discuss the impact of the number of main lanes on ramp operations or the percentage of traffic separating\entering from\to the main lane. However, the HCM (2010), states that on average, an increase of 2 ramps per mile in total ramp density causes approximately 5 miles per hour reduction of speed in the basic segment (FFS of 75 miles per hour having zero ramp density, standard lane width and right-side clearance) , because of approximate linear relation of free flow speed and ramp density. Numerical experiments were made in this study to compare travel delay and fuel consumption due to different exiting flows.

2.2.2 General Terrain

There are three categories of general terrain: level, rolling, and mountainous. Level terrain contains any combination of horizontal or vertical alignments that enables heavy vehicles to operate at the same speed as passenger cars. Typically, this terrain contains short grades with a maximum 2% incline/decline. In rolling terrain, there is a combination of vertical or horizontal grades which cause heavy vehicles to operate slightly poorer than passenger cars, but still they have not reached crawl speed (i.e. the maximum constant speed that trucks can maintain on a specific grade over a given length on an uphill stretch). In mountainous terrain, heavy vehicles operate at crawl speed for significant distances or frequent intervals. The impact of horizontal curves and vertical grades were studied separately in this effort. If data pertaining to roadway grade are not available, default values for each terrain are made available in the tool.

2.2.2.1 Horizontal Curves

Curvature is a signification factor in the incident duration estimation studies (Gomes et al, 2008). In most of the relevant statistical studies, however, existence of curvature enters the incident duration estimation models as a dummy variable regardless of its degree. The degree of a curve relates to its design speed. The sharper the curve, the slower the design speed. For safety related reasons, posted speed limits on curves are usually lower than the design speed of the curves based on the minimum radii.

Super elevation change in horizontal curves of a road segment can vary from 0 percent for areas with severe weather conditions to 8 percent for drier areas and regions with favorable weather conditions. For areas of high-speed, such as freeways, a maximum super elevation of 6% in horizontal curvature is typical and is employed in this study. In the US it is customary that the design speed range for curves be set between 45 and 80 mile per hour (Roadway Design Manual 2010). Shankar et al. (1994) completed one of the few studies that considered this curvature in estimating incident duration. They categorized horizontal curves by their design speeds and determined an explanatory variable for each category. This method, however, requires a level of detail that is not practical for the users of the SSP-BC Tool developed herein. Within the tool, in a segment with free flow speed of 70 mph, thus, curvatures having design speeds of 70 to 75 mph were assumed as straight, 60 to 65 mph as mild and 50 to 55 mph as sharp. To capture this, 5 and 10 mile per hour speed reductions were applied for mild and sharp curvatures, respectively.

2.2.2.2 Segment gradient

Roadway gradient is one of the highway-related factors known to significantly affect fuel consumption and emission rates (Park and Rakha, 2005), since vehicles need more power on uphill climbs to maintain their speed and less power in descending downhill.

The Roadway Design Manual has 4 percent maximum allowable grade for urban freeways as shown in Table 3.2. However, since SSP programs also operate on mountainous roads with higher grades, the impact of grade in the range of -10% to 10% is considered in this study.

Table 2.2 Maximum grade table (Adopted from roadway design manual 2010,

Functional Classification	Type of Terrain	15	20	25	30	35	40	45	50	55	60	65	70	75	80
Urban and Suburban															
Local	All	<15	<15	<15	<15	<15	<15	<15	--	--		--	--	--	--
-	-	-	-	-	-	-	-	-	-	-		-	-	-	-
Collector	Level	9	9	9	9	9	9	8	7	7		--	--	--	--
-	Rolling	12	12	12	11	10	10	9	8	8		--	--	--	--
-	-	-	-	-	-	-	-	-	-	-		-	-	-	-
Arterial	Level	--	--	--	8	7	7	6	6	5		--	--	--	--
-	Rolling	--	--	--	9	8	8	7	7	6		--	--	--	--
-	-	-	-	-	-	-	-	-	-	-		-	-	-	-
Freeway	Level	--	--	--	--	--	--	--	4	4		3	3	3	3
-	Rolling	--	--	--	--	--	--	--	5	5		4	4	4	4

2.2.3 Traffic Characteristics

2.2.3.1 Free-Flow Speed (FFS) and Roadway Capacity

FFS is the most important factor defining the roadway capacity. Theoretically, when the density and flow rate in the segment is zero, vehicles travel with FFS. In practice, it is defined as the desired speed at flow rates between 0 and 1000 passenger cars per hour per lane. Using a systematic simple (e.g every tenth vehicles in each lane and a minimum of 100 vehicles) the mean speed of all passenger cars can be reported as FFS (HCM, 2010). The factors affecting FFS are: lane width, lateral clearance and ramp density, all of which were considered in simulation designs herein under geometric characteristics of the segment.

The HCM defines capacity as the "average flow rate across all lanes." VISSIM does not have direct input for capacity. Consequently, by using the FFS as the initial desired speed, suggested reduced capacities under various circumstances can be modeled. For example, to include ramp density in the model, instead of running all the possible number of ramps, the equivalent reduced speed for capacity reduction percentages due to ramp density provided by the HCM is used.

The maximum posted speed limit in US freeways varies from 55 to 80 mph according to Highway Safety Research and Communications (2012). Considering capacities in the HCM 2010 and their relationship with other factors, a 70 mph FFS was employed in the simulation runs herein. This is because speed reduction is generally taken from a base FFS of 70 mph.

Table 2.3 FFS vs. Base capacity for freeways (Adopted from HCM 2010)

FFS (mile/h)	Base Capacity (pc/h/ln)
75	2400
70	2400
65	2350
60	2300
55	2250

The capacity-speed relationship shown in Table 3.3 is based on national norms, but this relationship can change locally. Furthermore, upon review of data from the National Motorist Association it is observed that, in urban facilities, speed limits for passenger cars and trucks are identical. There are roadways in some states such as California, where the speed limits differ by vehicle class. In this study, it was assumed that speed limits are identical for all vehicle types. To consider impact of weather condition on speeds and existence of ramps, the study range of the vehicle speed is chosen to be 35 to 75 mph in this study.

2.2.3.2 Ramp FFS

For simulating ramps in VISSIM, their FFS must be set. Typical speeds for ramps are in the range of 20 to 50 mph according to the HCM. 25 and 35 mph were considered in this study. The impact of ramp density was taken into account using base capacity reduction due to increase in number of ramps in a segment. The relationship between base capacity and total ramp density is shown in Figure 3.1, assuming drivers are familiar with the area and no trucks are present (HCM, 2010).

Figure 2.1 Base capacity vs. Total ramp density (adapted from HCM, 2010, P. 10-7)

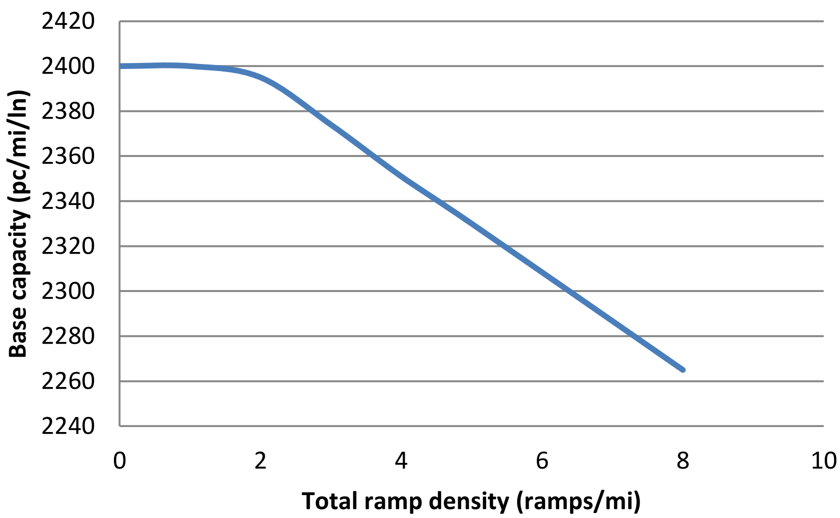

2.2.3.3 Traffic Flow Rate (Demand)

Traffic volume directly affects level of service of the freeway segment and savings from reduced incident duration. The hourly traffic (in each direction) was used as traffic volume. A range of maximum capacities between 200 and 2200 vehicles per lane per hour (vplph) on average was used for simulation runs. For traffic flows of less than 1000 vplph, vehicular speeds are nearly constant. At a 75 mph FFS, the minimum breakpoint of speed reduction due to flow growths occurs at a volume of 1000 vplph (HCM 2010). Thus, for each case, 11 different traffic volume categories from 200 to 2200 vplph were simulated.

2.2.3.4 Truck Percentages in Traffic Flow

Traffic composition, including the percentage of heavy vehicles, is one of the details required to complete an operational analysis of a freeway segment. In addition, the rate of fuel consumption is highly dependent on truck percentages. A range between 0 and 20% trucks is used in developing the SSP-BS Tool. This range was based on information involving truck percentages in specific areas. Specifically, a 3 percent truck composition value was noted for the I-270 freeway in Maryland (Miller-Hooks et al., 2010).

2.2.4 Incident Attributes

Incident-caused congestion and incident duration are greatly affected by incident severity. As a factor in statistical analyses related to incident duration estimation models, severity is most often noted to be significant. However, SSP program savings are typically derived from more frequent, low severity incidents.

2.2.4.1 Incident Severity

In most studies on freeway capacity reduction and incident duration, traffic accidents or vehicular breakdown are modeled based on lane and shoulder blockage (Hadi et al. 2000; Saka et al.,2008; Chou and Miller-Hooks, 2008; Khattak et al., 2010 ; HCM 2010). In this study, shoulder, one lane, and two lanes blockage events are used to model incidents with different severity levels. The greater the severity, the more lanes blocked.

2.2.4.2 Incident Duration

The main objectives of SSPs are to identify incidents or other causes of disruption in the traffic stream and minimize incident duration. Thus, a standard method to calculate incident duration is essential for SSP program evaluation.

Incident duration is often defined as the time between incident occurrence and when response vehicles leave the scene (Garib et al. 1997, Nam and Mannering, 2000; smith and smith, 2001). The Traffic Incident Management Handbook describes incident duration based on the time required to detect an incident, time from incident report to on-scene response, and time required to clear the incident. A widely used approach to defining incident duration is depicted through timestamps in Figure 3.1.

Figure 2.2 Incident timestamp flow chart (Chou and Miller-Hooks, 2008)

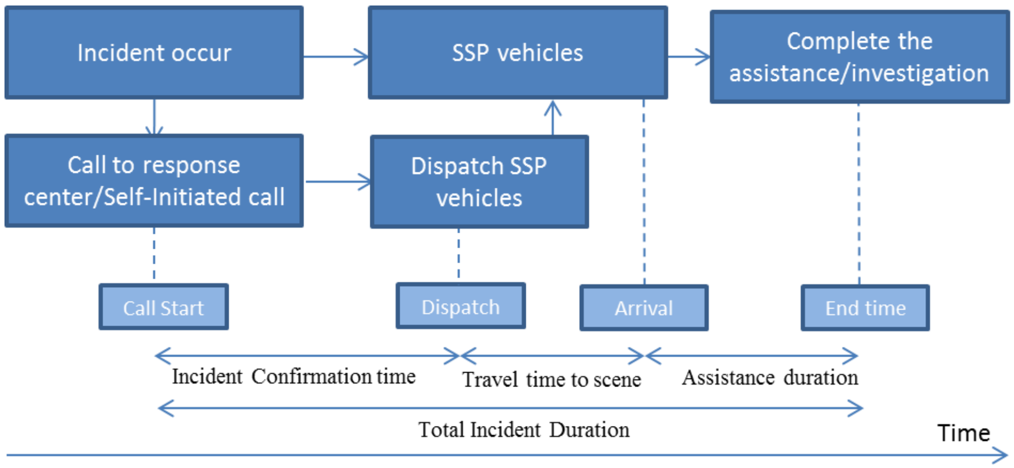

As described in (Chou and Miller-Hooks, 2008), at the moment the incident occurs, the driver will call the management center and the "Call Start Timestamp" will be logged. Once confirmation of the incident is received, a SSP vehicle driver will be dispatched to the scene and the "Dispatched Timestamp" is logged. The "Arrival Timestamp" is marked when the patrol unit arrives at the scene. Finally, once the event is cleared, the "End Timestamp" is recorded. Thus, time for confirmation, response time, assistance duration, and incident duration can be determined from the difference between two timestamps as follows:

Confirmation time = Dispatch time - Call Start time

Response time = Arrival time - Dispatch time

Assistance duration = End time - Arrival time

Incident duration = End time - Call Start time

When an incident is identified by a patrolling vehicle, i.e. is self-initiated, both the time for incident confirmation and response time will be zero.

The majority of SSP program responses are made to incidents with durations of 90 minutes or less. SSP programs may also assist state troopers or local police in response to more severe, typically longer, incidents. Although the frequency of these long duration incidents is low (often less than 2%), these incidents cause very significant travel delay. In fact, in some cases, it is necessary for law enforcement to close the entire freeway.

Including these extreme cases in the evaluation, study of SSPs often results in an overestimation of the benefits of such programs, particularly since they play a supporting, rather than leading, role in these events. Therefore, incidents with durations greater than 90 minutes were not modeled within this study and benefit estimations can be considered conservative in this respect.

2.2.4.3 Average Incident Duration

To quantify the benefits of a SSP program in New York State, Chou and Miller-Hooks (2008) studied the incident data for the study region. In the first phase of their study, the average incident durations over all incidents arising within a six-month period along four roadways, i.e. I-287, I-684, the Taconic State Parkway and the Sprain Brook Parkway, were calculated. In Table 3.4, a summary of the computed incident durations is shown. Savings from the SSP program can be computed from the difference between the average duration of incidents to which the SSP vehicles responded and those to which it did not.

Table 2.4 Average incident duration (Chou and Miller-Hooks, 2008)

Responds	Taconic State Parkway	Sprain Brook Parkway	I-684	I-287
With SSP	17.60	12.10	26.24	17.70
Without SSP	39.56	21.96	40.61	68.21
Savings	21.96	18.12	14.37	50.52

As shown in the table, for those incidents to which the SSP program did not respond, the average incident duration varied between 22 and 68 minutes. The range is smaller where the program is involved in the response. In a study on traffic recovery time, Saka et al. (2004) used VISSIM to simulate incidents that lasted between 10 and 60 minutes. Skabardonis et al. (2005) assumed that the average incident time without SSP response would be 30 minutes. Taken from a report in CHART in 2009 the average incident durations of incidents involving property damage and disabled vehicles were reported to be 33 and 20 minutes, respectively. Therefore, incident durations of 5 to 90 minutes with 5-minute increments were studied for the SSP-BC Tool herein. It is assumed that during this 5 minute time period, estimated savings change linearly.

2.2.4.4 Rubbernecking Effect

When an incident occurs in a freeway, vehicles in unaffected lanes often reduce their speeds. The effect of these speed reductions is called the rubbernecking effect. Assuming that a warning sign is set up for upstream traffic to inform other drivers of the incident, the rubbernecking effect can be modeled by a reduced speed area in the segment from the warning sign to the incident location. It is assumed in the models developed herein that warning signs are set up 500 feet prior to the incident as is recommended in emergency traffic control guidelines.

The effect of rubbernecking is an important piece of an incident to consider. It is often the case that many accidents are caused by drivers looking at other vehicle crashes and other roadside traffic incidents. A 2003 study by the Virginia Commonwealth University's Transportation Safety Training Center (TSTC) revealed that rubbernecking was the leading cause of vehicle crashes. It accounted for 16 percent of all vehicle crashes. Other distractions arising external to the vehicle, such as the presence of deer, accounted for 35 percent (Masinick and Teng, 2004) of such crashes.

2.2.5 Weather Conditions

A growing concern of roadway management agencies is the impact of adverse weather on freeway traffic operations. It is understood that severe weather conditions reduce freeway capacities, but few works have studied its precise impact. In addition, the results obtained from many studies are from outside the US or relate to rural freeway segments within the US. These statistics may not be applicable to urban freeway segments due to different roadway geometries, driver behaviors, and traffic characteristics.

In pertinent studies, weather conditions are classified into one of three types: "rain", "snow" and "others" (wind, fog, etc.). Each category is divided in terms of intensity (light versus heavy). The effect of each classification of weather on FFS is summarized in Table 3.5.

Table 2.5 Weather-Speed relation

Researcher/year	Light rain	Heavy Rain	Light snow	Heavy Snow	visibility	Wind
Ibrahim and Hall/ 1994	1.2-8 mph	3-10 mph	0.6 mph	26.4 mph	N/A	N/A
HCM 2000	2-14%	5-17%	8-10%	30-40%	N/A	N/A
Kyte/ 2001	15.3 mph	15.3 mph	23-26 mph	26.4 mph	N/A	N/A
Manish et al. /2005	1-5 %	4-7%	3-10 %	11-15%	6-11%	1-1.5%
Rakha et al./ 2007	N/A	N/A	13%	40%	13%	10%
N/A Not Availble						

It has been shown that that the impacts of weather on traffic flow and its parameters are dependent on the class of road. Chin et al. (2004) used loop detector data from different regions of the US. These data were linked to different weather. The weather conditions were classified into 6 categories: light rain, heavy rain, light snow, heavy snow, fog, and ice. The impact of each adverse weather condition was then translated into loss of capacity and speed as shown in Table 3.6.

2.6 Speed and capacity reduction based on road type (Chin et al. 2004))

Weather Condition	Urban Freeway		Rural Freeway	
	Capacity (%)	Speed (%)	Capacity (%)	Speed
Light rain	4	10	4	10
Heavy rain	8	16	10	25
Light snow	7.5	15	7.5	15
Heavy snow	27.5	38	27.5	38
Fog	6	13	6	13
Ice	27.5	38	27.5	38

The impact of weather can be modeled through its effects on speed and capacity reduction. Because VISSIM does not have explicit capacity input, suggested speed reduction along urban freeways due to adverse weather conditions was used for this study. Table 3.6 shows no significant difference between urban and rural freeways except under the condition of heavy rain.

To categorize intensity of weather conditions, thresholds have been developed in the HCM as follows.

Light rain: perception below 0.25 inch/hour

Heavy rain: Perception greater than .25 inch/hour

Light snow: perception below 0.5 inch/hour

Heavy snow: Perception greater than 0.5 inch/hour

In this study, using this knowledge from previous studies, speed reduction on urban freeways was based on the 6 different adverse weather conditions. For this investigation, the levels are selected as: 5% speed reduction due to light rain, 10% for heavy rain, light snow, and low visibility, 15% for fog, 35% for heavy snow, and 40% for icy conditions. Table 3.7 shows suggested speeds under different weather states.

Table 2.7 Actual speed under adverse weather conditions

speed limit	**speed reduction percentage**				
	5	10	15	35	40
75	71.25	67.5	63.75	48.75	45
70	66.5	63	59.5	45.5	42
65	61.75	58.5	55.25	42.25	39
60	57	54	51	39	36
55	52.25	49.5	46.75	35.75	33

It is assumed that weather conditions are uniform along a segment. In addition, simulated weather does not change during the simulation. In other words, a specified speed reduction value was used for any simulation run.

The focus of this section has been primarily on factors affecting travel delay. However, many of the factors that affect travel delay also directly impact fuel consumption and emissions of air pollutants. For example, grade is a roadway characteristic with its greatest effect on fuel consumption. Travel factors, such as speed, were also found to significantly impact fuel consumption and emissions.

2.3 Calculating Travel Delay

A simulation-based evaluation method was developed to estimate travel delay and input data needed to compute fuel consumption and emissions. The platform employed in this study is PTV America's VISSIM (version 5.3) software, a micro-simulation tool for traffic operations modeling. VISSIM is used to obtain estimates of travel characteristics and other metrics for roadways with operational SSP programs and those without (for comparison) through a host of simulation runs in which solitary incidents are simulated and their effects are estimated.

VISSIM computes the travel delay of each vehicle and total travel delay in the network in terms of the average total delay per vehicle (in seconds). Total delay is computed over all vehicles passing through a travel segment. For a given vehicle, its value is determined by subtracting the ideal travel time (assuming FFSs can be maintained) from the realized travel time.

2.4 Calculating Fuel Consumption and Air Pollutants

While VISSIM could be applied directly in estimating travel delay, it was found that it could not reliably compute fuel consumption for freeways and no module is available for computing pollutant emissions. PTV offers external (in the form of add-ons) fuel consumption and emission calculation modules for VISSIM. The user manual describes a process in which emissions data can be obtained from node evaluation at a network level. For this study, necessary licenses needed to use the emissions and fuel consumption add-ons were available and several preliminary tests were designed and run in an effort to validate fuel consumption and emissions output from these modules. Unfortunately, the modules did not function as designed. In most runs, fuel consumption and emissions were not reported. Results of those runs for which results were obtained revealed that the fuel economy estimates from VISSIM were over-estimated for US vehicle markets. In fact, an average fuel efficiency of 35 miles per gallon was obtained from the successful runs. Through discussions with the PTV America, Inc. support staff, it was determined that these tools would not be reliable, nor necessarily available, for this study. More generally, the fuel consumption and emissions models were specifically designed for signalized intersections and not freeways.

A comprehensive method to calculate fuel consumption and emissions from all vehicle movements in vehicle record output files of VISSIM was adopted in this study. After recording the actual speed, acceleration, and mass of all vehicles, the data was entered into the network at one second intervals during a simulation period. For each run, calculations for the run were made to obtain fuel consumption and emissions.

2.4.1 Emissions Calculation

Emissions in the transportation sector are primarily due to the combustion of fossil fuels. Carbon dioxide (CO_2) and hydrocarbons, such as methane (CH_4), are produced from the combustion products of fossil fuels, like petroleum, diesel and biofuels, as a result of the fuel's high carbon content [USEPA, 2010a]. Nitro gases or NO_x emissions are formed when nitrogen (N), either in the air or in fuel, combines with oxygen (O_2) at high temperatures. Other pollutants, such as PM and CO, are formed due to incomplete combustion of fuel; whereas, SO_x emissions are formed as a result of the sulfur content in the fuel [USEPA, 2009].

CO_2 emissions are proportional to the carbon content of the fuel. Logically, this would mean emissions vary by fuel type. These emissions can be calculated using a simple relationship associating the amount of fuel consumed, the carbon content of the fuel (or carbon coefficient) and the fraction oxidized (usually estimated to be 99%) [USEPA, 2006]:

$$COCO_2\ Emissions = \frac{44}{12}\ Fuel\ Consumped\ Fuuel\ Carbon\ Content\ Fraction\ Oxidized$$

On the other hand, non-CO_2 emissions (CH_4, NOx, PM, SOx, etc.) are not directly proportional to fuel consumption and are affected by vehicle characteristics. Therefore, to accurately determine the effects, vehicle-specific emission rates/factors (e.g. mass of pollutant/mile) are used in combination with vehicle activity. These factors are a function of vehicle type, age, fuel, and emission control technology. Vehicle activity can be defined by vehicle miles travelled (VMT) or hours of operation, and depend on the units of the emission factor [NCHRP, 2006]. Vehicle activity can be used directly to calculate emissions by either using the vehicle fuel economy (miles per gallon) or fuel-based emission factors (grams per mile).

$$Non - CO_2\ Emission = Activity_{(Fuel,Vehicle.Technology)}.\ Emission\ Factor_{(Fuel,Vehicle,Techonology)}$$

While these general mathematical relationships are typically used to calculate emissions, the level of accuracy is dependent on the approach used to define emission production processes and number of variables considered in determining emission factors [IPCC, 2006]. With a top-down approach, emission estimates are obtained using aggregate fuel consumption. These estimates can be reasonable when emissions calculation at the macro-scale level is needed (e.g. national emissions inventory). With a bottom-up approach, often used at a micro-scale level (e.g. project level emissions), more detailed inputs for fuel consumption and emission factors are required. It must be noted that while the bottom-up approach may also be used for inventory purposes, obtaining large-scale, detailed data inputs for emissions calculations often proves to be difficult.

Both fuel consumption and emission factors are associated with/dependent on several variables which influence the performance of a vehicle and, therefore, the amount of fuel consumed or mass of pollutants emitted. The power-demand of a vehicle is dependent on various inter-linked parameters, such as vehicle characteristics (type, age, mass, etc.), operating mode (start/stop, running, idle and vehicular speed) and environmental parameters (road characteristics, temperature, humidity, etc.). A schematic illustrating the relationships of these factors to emissions is shown in Figure 3.1.

Figure 3.1. Schematic illustrating relationship of variables to vehicular emissions (SHA)

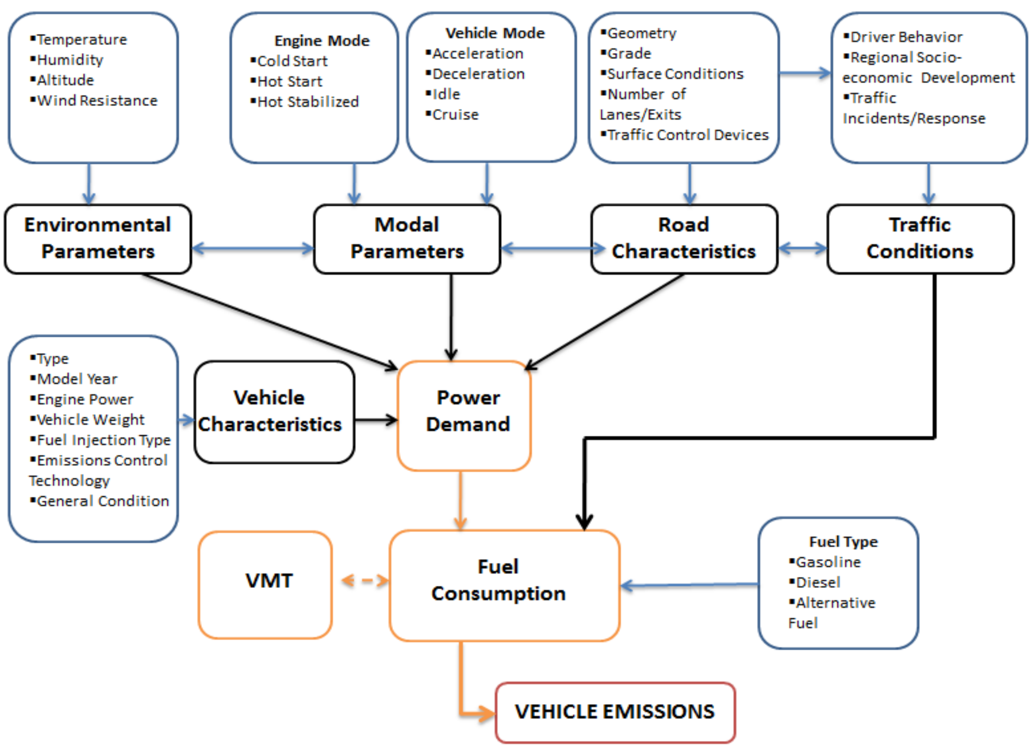

As illustrated in the figure, modal and environmental parameters, vehicle and road characteristics, fuel type, and traffic conditions, all affect a vehicle's power demand, which in turn affects the resulting emissions produced. For example, use of alternative fuels or newer and more efficient vehicles or driving on a relatively flat road would typically produce lower emissions. Also, modal parameters significantly affect emissions. For example, emissions produced when a vehicle is turned off and restarted before the engine has cooled down (hot start) are lower as compared with those when the vehicle is initially turned on (cold start). Depending on traffic conditions and road characteristics, vehicles at higher speeds or accelerating from low speeds produce more emissions as compared to at higher speeds. Moreover, road characteristics (e.g. road grade, number of lanes, the number and type of specific traffic control devices, surface conditions, etc.) also influence the traffic flow and density. For example, large road grade and high traffic volume result in a large number of stops and starts and, therefore, emissions [Bachman, 1997]. The incorporation of these variables in determining emission factors and fuel consumption, that is, working on a micro-scale level, would produce more accurate and realistic results.

Of the many models that currently offer emission estimates for on-road vehicles are traffic simulation models, like CORSIM, S-PARAMICS, INTEGRATION, and TRANSIMS. These are some of the most widely used traffic simulation models. These, along with other models, such as DYNASMART-P, represent driver behavior and vehicle kinematics for individual vehicles and trips, and are able to replicate and enable analysis of a variety of traffic-related activities. Many of these traffic simulation models account for environmental impacts of traffic related activities either by using emissions estimation modules integrated within the model or by using external microscopic emissions estimation models as plug-ins to determine emission outputs. The plug-ins provides instantaneous emission rates based on the vehicular inputs from the simulation models. However, a major disadvantage of using these models is that these models use averages for speeds, acceleration, deceleration and fuel consumption in order to generate emissions output. In most cases, the methodology employed to estimate emissions is not described. Therefore, while these models that best simulate traffic have the potential to provide a level of detail required for micro-level emissions estimation, they use a macroscopic or undefined methodology for emissions estimation.

Of the external microscopic emissions estimation models (sometimes used as plug-ins with traffic simulation models), CMEM and MOVES created by University of California-Riverside and USEPA, respectively, are the most notable and comprehensive. These models use a power demand approach to capture the physical processes of emissions production, incorporating a vehicle's modal parameters, and hence, provide more accurate emission estimates [CMEM, 2010; USEPA, 2011]. Although both models have many benefits and are capable of producing microscopic, modal emission results, neither accounts for several important factors relevant to assessing the effects on emissions produced from traffic conditions and changes to vehicle composition on roadways. Some of the disadvantages of using these models lie in the scope of the variables they cover, level of detail captured in the outputs, and the limited flexibility they offer users.

2.4.2 Fuel Consumption and Emission Calculation Methodology

Similar to MOVES and CMEM, a power-based approach was used for this research project to estimate emissions wherein vehicle characteristics and modal parameters, namely vehicle mass, velocity and acceleration, are used to calculate the instantaneous power demand ($P_{v,t}$) for a vehicle type category. When combined with the speed-based engine parameters (e.g. K, N, V), this approach provides an instantaneous fuel rate (FR_t). The fuel rate is then multiplied by fuel-based emission factors (EF) to produce emission estimates for criteria air pollutants, such as HC, CO, NOx, CO_2. Furthermore, the calculated instantaneous fuel rate (FR) when multiplied by the fuel-based sulfur content and other variables provides the associated instantaneous SOx emissions output for the vehicle. The equations and related data used to determine second-by-second emissions output for this research project are described next. The nomenclature used in the Equations (Eq. 3.1) is listed in Table 3.1.

Table 2.8 Nomenclature for variables used in equations

LDV	:	Light-duty Vehicle (e.g. passenger cars, SUV, etc)
LDT	:	Light-duty Trucks
$P_{V,t}$	:	Instantaneous Tractive Power of vehicle V at time t (KW)
M	:	Vehicle mass (metric tonne)
v_t	:	Vehicle speed at time t (mph)
a_t	:	Vehicle acceleration at time t (mph/s)
c_1	:	Conversion factor for speed: $0.447ms^{-1}$/mph
A	:	Rolling resistance coefficient (KW/mps)

B	:	Rotational resistance coefficient (KW/mps^2)
C	:	Aerodynamic drag coefficient (KW/mps^3)
r	:	Road grade i.e. slope (%)
g	:	Gravitational constant: 9.81 m/s2
FR_t	:	Fuel consumption rate (g of fuel/s)
HV	:	Heating Value (KJ/g)
η	:	Engine Efficiency = 0.4
K_t	:	Engine friction factor at time t (KJ/rev*L)
N_t	:	Engine speed at time t (rps)
V	:	Engine displacement volume (L)
S	:	Engine Speed to Vehicle Speed Ratio (rpm/mph)
g/g_{top}	:	Gear ratio
K_0	:	0.22 KJ/rev-litre (average based on range 0.19-0.25 KJ/rev-L)
EM_{Pol}	:	Emission for pollutant (g)
EF_{Pol}	:	Emission factor for pollutant (g/mile)
ρ_{Fuel}	:	Denisty of fuel (g/gal)
Fuel $Economy_{LDV/LDT}$	:	Fuel Economy for vehicle category (gal/mile)
T	:	Total time travelled by vehicle category (s)
EM_{SOX}	:	SOx Emission (g)
SC_{Fuel}	:	Sulfur Content of Fuel (ppm)

2.4.3 Power Demand ($P_{v,t}$) and Instantaneous Fuel Consumption (FR_t) Calculation

The power-demand approach breaks down the emissions generation process of a vehicle into the physical processes of the vehicle's engine that correspond with vehicle operation and emissions production. As previously discussed vehicle performance during various driving conditions directly contributes to fuel consumption and resulting emissions. For example, vehicle characteristics, like age and engine size, would determine how quickly the vehicle can move in and out of periods of high power demand (e.g. overcoming high gradients or reaching desired speeds by accelerating). Therefore, estimating the physical processes that a vehicle undergoes during operation can provide higher resolution in defining a vehicle's emissions production process. These processes are best captured by the engine's tractive power ($P_{v,t}$), which in turn is based on the vehicle's modal parameters (e.g. v_t and a_t) and road characteristics (i.e. r). At a given time t, the instantaneous tractive power is defined as:

$$\boldsymbol{P_{V,t} = A.v_t.c_1 + B.v_t^2.c_1^2 + C.v_t^3.c_1^3 + M.v_t.c_1.\left[(a_t.c_1) + g.\sin\{arctan(r/_{100})\}\right],} \quad \textbf{Eq. 3.2}$$

The instantaneous modal parameters, speed (v_t) and acceleration (a_t) at time t, were obtained directly from VISSIM outputs (or by other means); whereas, the vehicle parameters, such as mass (M) and the vehicle track road-load coefficients (A, B and C) for each vehicle category were obtained from USEPA's MOVES model. These values were estimated by USEPA using vehicular data for LDVs and LDTs from inspection and maintenance programs and developing linear models to determine the coefficients from vehicle mass, M [Koupal et al, 2004]. The vehicle parameters used here are listed in Table 3.9.

Table 2.9 Calculation of Road -Load coefficients [Source: USEPA, 2011c]

Vehicle Category	Source mass(metric tons)	A(KW/mps)	B(KW/mps2)	C(MW/mps3)
LDV(passenger cars)	1.4788	0.156461	0.00200193	0.000492646
LDT(Trucks, SUVs,etc)	1.86686	0.22112	0.00283757	0.000698282
LHD<=14K	7.64159	0.561933	0	0.00160302
LHD<=19.5K	6.25047	0.498699	0	0.00147383

The vehicle's power demand directly influences the amount of fuel consumed, and therefore the mass of pollutant produced. The fuel consumption rate (FR_t) or the energy used per second to operate the vehicle is a function of engine speed (N_t) and the engine friction factor (K_t), which captures the energy used to overcome engine friction per engine revolution and unit displacement. Both N_t and K_t are dependent on various speed-related vehicle parameters. The simplified equation used to calculate FR appropriate for meso-scale emissions estimation (as required here) was obtained from Barth et al. (2000) and is expressed as:

$$\boldsymbol{FR = \frac{1}{HV} \cdot \left[\frac{P_{V,t}}{\eta} + (K.N_t.V\right],} \qquad \textbf{Eq. 2.3}$$

where

$$\boldsymbol{N_t = \frac{1}{60} \cdot S \cdot \frac{g}{g_{top}} \cdot v_t}\ , \qquad \textbf{Eq. 2.4}$$

$$\boldsymbol{K = K_0 \cdot \left[1 + (N_t - 33)^2 \cdot 10^{-4}\right]}. \qquad \textbf{Eq. 2.5}$$

The values for S (based on vehicle type category) and g/g_{top} (based on vehicle speed, v_t) and fuel based variables (i.e. HV) are recorded in Table A.4 and Table A.3 of Appendix A respectively.

2.4.4 CO_2, CO, HC, CO & NOx Emissions Calculation

For the purpose of this project, fuel-based emission factors (i.e. mass of pollutant produced per unit of vehicle activity), EF_{Pol}, for the LDV and LDT vehicle categories for major fuel types (i.e. gasoline and diesel) were obtained from the USEPA (refer to Table A.2 in Appendix A). These emission factors in combination with other variables specific to the vehicle categories (e.g. fuel economy, time spent on roads, etc) and fuel (i.e. density, EF_{Pol}) were then used to calculate the emissions output for each pollutant (EM_{Pol}) using Equation 3.6.

$$\boldsymbol{EM_{Pol} = EF_{Pol}.FR.Fuel\ Economy_{\frac{LDV}{LDT}}.\left(\frac{1}{\rho_{Fuel}}\right).T,\quad Pol \in \{CO_2, HC, CO, NO_x\}} \qquad \textbf{Eq.3.6}$$

2.4.5 SOx Emissions Calculation

The sulfur-content in a fuel affects the amount of SOx emissions produced when fuel is consumed. Therefore, the sulfur content (SC_{Fuel} as obtained from Table A.3 in Appendix A) for gasoline and diesel were used to estimate the SOx emissions for a vehicle category using the following relationship:

$$\boldsymbol{EM_{SOX} = 2.FR.\left(\frac{SC_{Fuel}}{1{,}000{,}000}\right).T,} \qquad \textbf{Eq. 2.6}$$

2.4.6 Fuel Consumption

To estimate the total fuel consumed by a vehicle category due to effects on its modal profile caused by changes within the traffic scenario, the power-demand based FR as calculated previously was used as shown in Equation 3.8.

$$\boldsymbol{FC_{LDV/LDT} = \sum FR_{LDV/LDT}\cdot\left(\frac{1}{\rho_{Fuel}}\right),} \qquad \textbf{Eq. 2.7}$$

2.4.7 Assumptions

While there are many other variables that might have been considered, such as engine speed, air-to-fuel ratio, fuel use and catalyst pass fraction, vehicle emissions are most influenced by engine power and fuel use. Also, since the scale of this project requires meso-scale emission results, and since all other variables require additional detailed vehicle-specific parameters (based on dynamometer measurements of each vehicle type by brand), these variables were not used in determining $P_{v,t}$ [Barth et al., 2000].

2.5 Secondary Incident Savings

An incident is called "secondary" if it is a consequence of a primary incident. The occurrence of such a secondary incident is related to the duration of a primary incident (Khattak et al., 2008; Zhan et al., 2008). Therefore, as SSP programs aim to decrease the duration of primary incidents, they also decrease the risk of secondary incidents. In fact, it was noted in Karlaftis et al. (1998) that for every minute of additional incident duration, the risk of occurrence of a secondary incident increases by 1.7% in the winter and 3.1% in all other seasons, for an average of 2.8%. They fitted two logistic regression models to primary crashes assisted by SSP vehicles associated with the Hoosier Helper program in Indiana. Crashes within 3 miles upstream and within the clearance time plus15 minutes of a primary crash were classified as secondary. The odds ratio, which measures the strength of connotation between a primary incident characteristic and the probability of secondary incident occurrence, is presented. Odd ratios of clearance time in winter and all other seasons are estimated as 1.018 and 1.032, respectively. In other words, the SSP program could reduce the probability of secondary incident occurrence by 18.5% in the winter and 36.3% in all other seasons per incident to which they respond.

The first step in quantifying the savings in secondary incidents is to estimate the number of incidents that are secondary. However, there is little agreement among researchers in terms of the validity of methods aimed at identifying and classifying secondary incidents. The primary approaches to such identification and classification are static threshold, dynamic threshold, and simulation-based filtering methods. Table 3.10 lists the classification methods in the literature.

Raub (1997) employed temporal and spatial thresholds to classify incidents. Any incident that occurs within 15 minutes of the resolution of another incident and within 1 mile is defined as a secondary incident. Applying this method, 15-percent of all incidents reported by police were found to be secondary. Other studies used similar fixed thresholds,. For example, Moore et al. (2004) defined incidents as secondary if they occurred within 2 hours and 2 miles from incident identification. This static method is also adopted by Karlaftis et al. (1999), Hirunyanitiwattana et al. (2006) and Zhan et al. (2008). One drawback of the static threshold method is that it cannot capture field conditions (i.e. changing demand), and therefore, leads to misclassification.

The dynamic threshold method was developed to compensate for the shortcomings of the static approach. Sun et al. (2007, 2010) proposed a master incident progression curve to identify secondary incidents. The progression curve is constructed from affected distance, which is measured from incident location to the end of its queue. Instead of using a static maximum or average queue length, the author marked the end of varying queue throughout the entire incident duration. Incidents that fall under the curve are considered to be secondary. It was concluded that the method reduced Type I errors by 24.38-percent and Type II errors by 3.13-percent. Similarly, Zhang and Khattak (2010) employed a dynamic queue-based method in which queue length is calculated by a deterministic queuing model (D/D/1). Zhan et al. (2009) classified secondary incidents as those that occur within the boundary of the estimated maximum queue length and dissipation time of a lane-blocked primary incident. To arrive at this conclusion they used a cumulative arrival and departure traffic delay model.

A simulation-based secondary incident filtering (SBSIF) method was proposed by Chou and Miller-Hooks (2008). This model used geometric boundaries to analyze the incident impact area in a time-space contour map of traffic speeds. Regression models are established for identifying the corner points of the impact area. The authors conclude that the SBSIF method can reduce the misclassifications by up to 58-percent. They noted that 4% of 693 incidents to which H.E.L.P. responded to were secondary using this approach.

Regardless of the method used in distinguishing secondary incidents from primary incidents, once the number of secondary incidents as a fraction of primary incidents is known, the next step is to estimate savings in secondary incidents, i.e. the number of incidents that did not arise secondary to a primary incident as a result of reduction in incident duration. Chou and Miller-Hooks (2008) assumed the number of secondary incidents without SSP is linearly correlated with the total delay ratio between with and without SSP response cases. Similarly, Guin et al. (2007) employed an equation based on the ratio of average incident duration of SSP versus non-SSP incident responded cases.

Table 3.10 provides an overview of secondary incident methodologies, assumptions and assumed rates from the literature. In general, Federal Highway Administration (FHWA) noted that approximately 20% of all incidents are secondary incidents. They include not only crashes, but engine stalls, overheating, and running out of gas as types of secondary incidents.

Table 2.10 Secondary incident classification methods

Authors (Year)	Definition	Method	Claimed Percentage/Main Finding	Data Sample Size	Data Source	Data Time and Location
Raub (1997)	Occur within 15 min from incident resolution and within 1 mile	Fixed temporal and spatial parameters	>15% of all incidents reported, average secondary crash occurs within 36.4 min, 600 meters after primary accident, average primary accident duration is 45 min, added of delay 69 min	1,796	Police reports	1995 Northern Chicago, IL
Karlaftis et al. (1999)	Occur within 15 min from incident resolution and within 1 mile	Fixed temporal and spatial parameters	>15% of all incidents reported		Indiana DOT	1992-1995, Borman Expressway
Moore et al. (2004)	Occur within 2 hrs and 2 miles from incident identification	Fixed temporal and spatial parameters	Secondary accidents are considerably rarer events than previous studies suggest, lower frequency of secondary crashes, 1.5%~3% per primary incident	84,684	CA Highway patrol	March, May, July 1999 and Dec.1998, LA Freeway
Hirunyanitiwattana et al. (2006)	Occur within 1 hrs and 2 miles from incident identification	Fixed temporal and spatial parameters	Secondary crashes occur more often during rush hour traffic in the morning and evening, rear-end collision is the predominant secondary collision type, accounting for 2/3 of all secondary crashes.	70,6 in 1999 and 183,988 in 2000	FHWA	1999 and 2000, CA highway system

Sun (2007,2010)	Occur under a master incident progression curve	Dynamic threshold method by marking the end of varying queue throughout the entire incident	dynamic method reduce Type I error by 24.38% and Type II by 3.13%; Results from using dynamic method versUSstatic method can differ by more than 30% in identifying secondary incidents	5,514	Highway patrol in St. Louis, MO	2002, I-70, MO
Zhan et al. (2008)	Occur within 2 miles and 15 min from incident resolution	Fixed temporal and spatial parameters	Average rate of 7.94% as primary incidents, 5.22% as secondary crashes, secondary crashes are usually much less severe than other crashes. Traveler sight conditions and lane blockage durations of primary incidents are significant contributing factors for determining the severity of secondary crashes	4,435	SMART database of FDOT	Jan 2005-Jan 2007 Fort Lauderdale, FL
Zhan et al. (2009)	Occur within the boundary of estimated maximum queue length and dissipation time of the potential lane-blockage primary incident	Cumulative arrival and departure traffic delay model to Estimate maximum queue length and associated queue recovery time	5% as primary incidents , 3.23% as secondary crash, accidents occur in daytime and with long lane-blockage duration increase the possibility of secondary crashes	4,435	SMART database of FDOT	Jan 2005-Jan 2007 Fort Lauderdale, FL

Zhang and Khattak (2010)	Occur within the a queue associated with primary incident and duration of primary incident, contained event duration: durations of all secondary incidents are contained within primary incident duration, extended event duration: duration of one or more secondary incidents partially overlaps with primary incident duration but extend beyond it	Dynamic queue-based method which queue length is calculated through a deterministic queuing model(D/D/1)	Contained and extended events show different characteristics and operational response patterns. Factors associated with durations of longer cascading events include primary incident being a crash, secondary incident being crash, multiple vehicles involved in secondary incidents, and longer time gap between primary and secondary incidents	37,379	Traffic Operations Center, VDOT	2005, Hampton Roads
Zhang and Khattak (2010)	Occur within a queue associated with primary incident and duration of primary incident	Dynamic queue-based method which queue length is calculated through a deterministic queuing model(D/D/1)	96.93% independent incidents with average of 14 min primary incident duration, 2.7% primary-secondary pairs of 40 min duration of primary incident, 0.37% primary-multiple secondary events of 68 min primary incident duration, characteristics of primary incident including crash, long duration, multiple-vehicle involvement and lane blockage and road geometric variable increase secondary incident frequency	37,379	Traffic Operations Center, VDOT	2005, Hampton Roads, VA
Chou (2010)	Occur within the incident impact area on time-space traffic speed contour map	Simulation based secondary incident filtering method	24 and 27 out of 630 potential secondary incidents are identified employing visual and regression implementations for corner point identification with SBSIF method	693	New York DOT	2006, I-287, NY

2.6 Summary

In this chapter, the essential measures required to evaluate the benefits of a SSP program are identified. Factors affecting travel delay, fuel consumption, and pollutant emissions were reviewed. Assumptions and computational methodologies for computing the MOEs were also introduced. In the next chapter, the importance and ability to experimentally capture the effects of each factor in MOE estimation is studied.

CHAPTER 4. Implementation of Variables in Simulation Designs

The SSP-BC Tool must be comprehensive to enable the estimation of program benefits under all possible incident scenarios for which any user may require results. A simulation-based method was developed to estimate travel delay and fuel consumption of an incident scenario. Travel delay is a direct output of the simulation software, but fuel consumption is derived from modal parameters related to vehicular movement details, obtained from the simulation (e.g., velocity, acceleration, mass, etc.). Savings in emissions are computed from total fuel consumption. Savings calculation in secondary incidents partially benefits from obtained travel delay values.

Any given incident falls into one combination of the identified factors as each incident is defined by its location, lanes blocked, and duration, as well as by the settings related to roadway grade, weather and other contributing factors discussed in Chapter 3. To account for all combinations of these factors related to incidents on freeways with between 2 and 6 lanes, up to 2 lanes blocked (no road closure considered), and clearance times of less than 90 minutes, i.e. all combinations within the study scope, combinations over 8,000,000 simulation runs would need to be conducted. Additionally, some of the factors cannot be controlled through code and thus, automating all of the runs through batch runs is not possible. Even using a powerful computer and even if all runs could be automated; it would take more than a year to complete. This means that simulating all incident scenarios is impractical. Instead, simulation runs are supplemented through statistical approaches described in this chapter.

A set of preliminary experiments were conducted to gain insight into the impact of each factor on travel delay and fuel consumption and to choose appropriate statistical estimation (i.e. supplemental) models to employ and methodologies for their calibration. A control case was designed and simulation runs were taken in which the state of a single factor was changed univeriately. These experiments were designed to answer two questions: (1) Does the simulation technique replicate the factors appropriately in the simulation environment? (2) What form should the statistical model take and it include?

Multiple-regression modeling was chosen to estimate travel delay and fuel consumption of a given incident from a sample of the possible incident characteristic combinations (i.e. incident scenarios). Results of this initial set of experiments showed that it is best to develop different regression models for shoulder, one- and two-lane blockage scenarios. Moreover, travel delay for LDVs and LDTs must be computed separately, because the monetary benefits associated with savings incurred by trucks is incorporated within the truck driver's hourly costs. Therefore, for travel delay, one multi-regression model was developed for each of the six categories of incidents and vehicle types as shown in Figure 4.1. Based on results of additional preliminary experiments to assess the impact of the various factors on fuel consumption estimation, one general model was calibrated to account for all incident scenarios.

Figure 3.1 Estimation model development progress

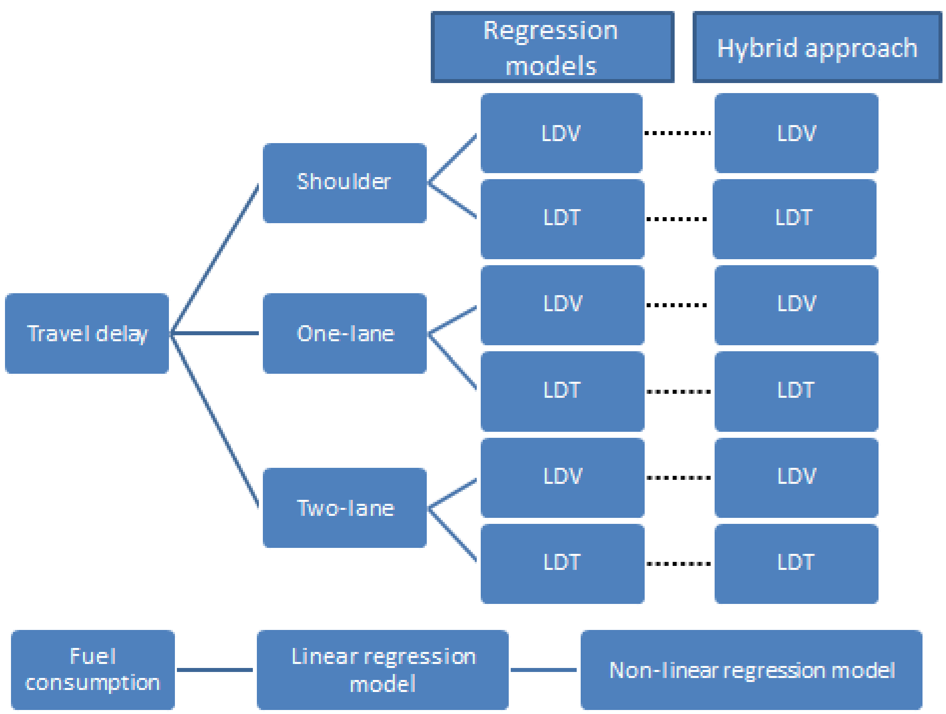

The goodness-of-fit and modeling assumptions were tested. Results from these tests indicated that the developed models needed improvement. Thus, a hybrid statistical-simulation data approach was introduced for improving the travel delay regression models, and a non-linear regression model was calibrated to improve the goodness-of-fit of the fuel consumption estimation model. This progression is also shown in Figure 4.1.

The simulation platform, general settings and incident simulation techniques are described in Section 4.1. Results of single-factor experiments are described in Section 4.2. Regression models and investigation of their goodness-of-fit are presented in Section 4.3. This is followed by a summary in Section 4.4.

3.1 General Simulation Settings and Incident Modeling

While many high quality microscopic simulation software programs, like PARMICS, VISSIM and CORSIM, areavailable that for many purposes adequately model traffic (Brockfield et al., 2004; Ranjitkar et al., 2004; Jones et al., 2004; Bloomberg et al., 2003), some studies have revealed that some platforms, like VISSIM and PARAMICS are better than others, specifically CORSIM (Choa et al., 2002). Given positive experience with VISSIM in the literature, as well as prior experience, including extensive calibration studies (Miller-Hooks et al, 2010), by the authors with VISSIM, VISSM was chosen as the simulation modeling platform. . An additional benefit of working with VISSIM is its COM interface. The interface provides great flexibility in controlling various aspects of the simulation environment.

Primary calibrated VISSIM parameters, assumptions, and method for modeling incidents are described in Section 4.1. In Section 4.2, methods of implementation for each of the factors in the simulation environment and their impacts on travel delay and fuel consumption given by results of numerical experiments on individual factors are explained. Results of these experiments are combined to reproduce more realistic incident scenarios in which multiple factors change concurrently. Multiple-regression modeling is employed to estimate travel delay and fuel consumption as explained in Section 4.4. This is followed by an improved estimation model for travel delay exhibited in Section 4.5 and a summary of the Chapter in Section 4.6.

3.1.1 Simulation Settings

For each incident scenario and seed, one run of VISSIM involves 7,200 seconds of simulation time. A typical incident scenario is explained in next section and shown in

Figure 4.1. The software user manual suggests the use of a warm-up period. This period includes the first 1,800 seconds of each run; this period is also required to achieve a steady traffic flow along the segment from the start of the analysis period. Incidents are designed to occur 300 seconds after the end of the warm-up period or 2,100 seconds into the simulation. To get more accurate results, the VISSIM user manual suggests running a minimum of three runs with different random seeds for each simulation model and reporting the average over random seeds in the final results. Average results, based on the 5,400 seconds of simulation run time, over runs with five randomly chosen seeds were collected. The software user manual suggests 1 time step per simulation second in terms of simulation resolution for models that contain only vehicles (i.e. that are not multimodal). However, five time steps per simulation second was used in this study. It was observed in preliminary runs that in modeling congested roadway conditions, using a higher resolution reduces loss of vehicles due to difficulty by the vehicles in entering the network.

Each run required approximately 2.5 minutes on a Dell Precision T7500 personal computer with a 3.20 gigahertz quad core processor and 12 gigabytes of RAM, running a 64 bit Windows 7 operating system.

3.1.2 Control Case

A typical incident to which SSP vehicles responded was selected and designed based on the information in Chapters 2 and 3 to be the control case incident for the single-factor experiment runs. The studied segment is a three lane, 10-mile, unidirectional straight freeway segment with no on-ramps, off-ramps, grade, or lane drops as shown in Figure 4.1. The incident duration is 20 minutes (described in Section 4.1.3) which would not change with experiments, the traffic volume is set to be 1200 vplph. The FFS of vehicles is set to be 75 mph. In each experiment, all characteristics are set as base except for the factor under study.

3.1.3 Simulating Incidents and Rubbernecking Effect

The COM interface of VISSIM allows users to control various aspects of the simulation, which makes the software highly flexible. However, VISSIM and its COM interface do not include a specific feature for modeling traffic incidents. Simulation-based traffic studies relying on the VISSIM platform have used a variety of methods to model incidents, including: defining a parking lot with one space and assigning a car to park in the space for a fixed time period (Wang et al. ,2003; Pulugurtha et al. , 2002), setting a bus stop at the incident location in which the bus stops for a fixed period of time (Hadi et al.,2000), using active traffic signal control in the affected lanes for the duration of an incident (Saka et al. 2004) and setting a passenger vehicle with speed of zero in the incident location from the start time of the incident to the end of clearance time (Chou and Miller-Hooks, 2010). In this study, two cars with zero speed are co-located at the incident location (lane, and location with respect to ramp) from the start time of the incident for a pre-set incident duration time.

VISSIM provides a function that allows users to set a temporary reduced speed area on a link. Such reduced speed areas can capture the effects of rubbernecking during an incident. That is, they can be used to model the reduction in speed in unblocked lanes during the incident time period. Hadi et al. (2000) found that a speed of 20 mph for vehicles modeled in VISSIM in which an incident is active results in the suggested available capacity by the HCM.

At the end of the incident period, vehicles involved in the incident are removed from the blocked lanes. Once the reduced speed areas become inactive, vehicles traveling in the affected lanes accelerate until they reach their initial desired speed (Figure 4.2).

Figure 3.2 Incident layout on typical three-lane unidirectional freeway segment

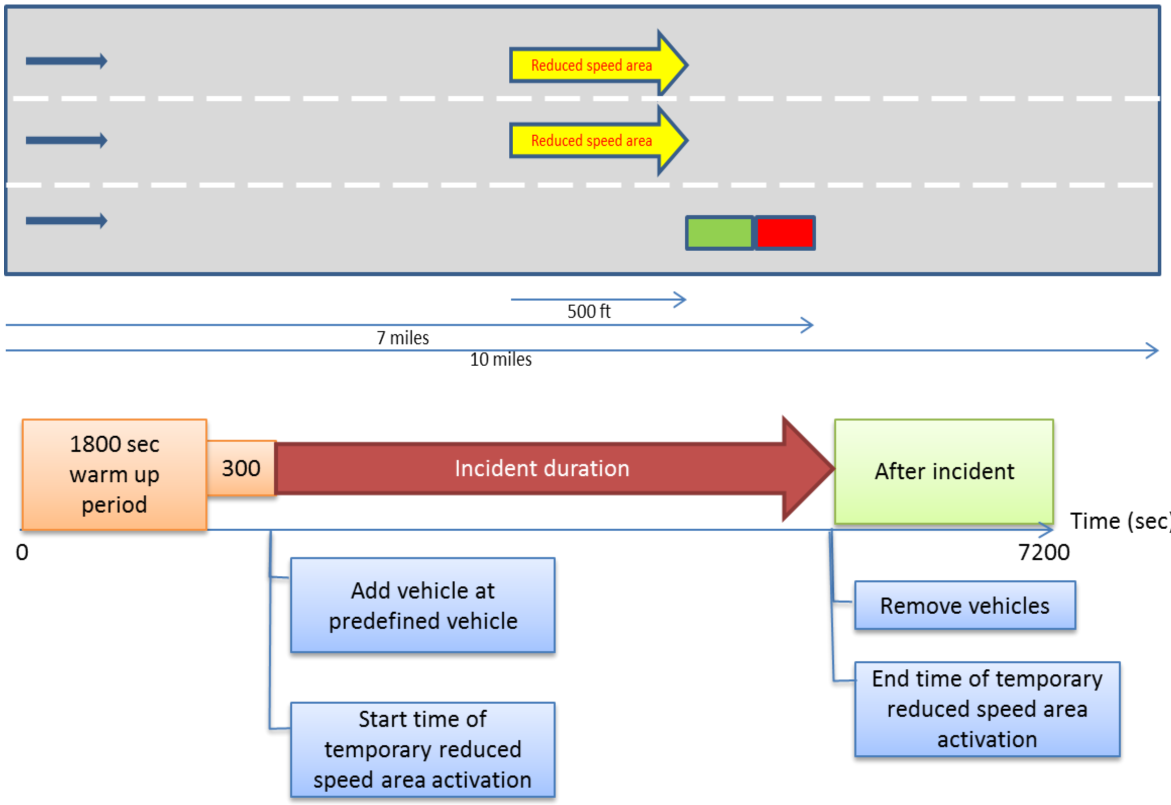

3.1.4 VISSIM Calibration

To correctly predict system response, it is essential to calibrate the simulation software to existing traffic conditions. Miller-Hooks et al. (2010) identified five car-following and lane-changing parameters in VISSIM that had very significant effect on travel delay estimation. After completing an extensive effort to calibrate a model of a 41-mile Maryland freeway (82 miles in both directions) against actual travel time measurements, they suggested changes to four of the five values. The suggested parameter settings are: 'Following' Variation (CC2), 'Following' Thresholds (CC4&5), Safety Distance Reduced Factor (SDRF), and Look Back Distance (LBD). Their definitions, default values, possible range in VISSIM, and the final set that are used in this study are listed in Table 4.1. CC2 to CC5 belong to the Wiedmann 99 car following model, which is mainly suitable for interurban and freeways. SDRF and LBD are lane-changing parameters associated with driver behavior.

Table 3.1 Driver behavior parameters, adopted from Miller-Hooks et al. (2010)

Parameter	**Definition**	**Default Value**	**Range**	**Final**
CC2	Following variation: desired safety following distance	4 meters	1.5-20 meters (16.40-65.62 ft)	39.37 (ft)
CC4&5	Lower & Upper following threshold	0.35 mph	0.1-2.0	0.1
SDRF	Safety distance reduced factor: effects safety distance during lane changing	0.6	0.1-0.9	0.1
LBD	Look back distance: defines the distance at which vehicles will begin to attempt to change lanes	200 meters	50-1000 meters	3280.83

Note: the sign of Lower following threshold (CC4) is '-' and the sign of Upper following threshold (CC5) is '+'.

3.2 Single-Factor Experiments

Finding a way to model significant factors of travel delay and fuel consumption in VISSIM simulation environment and monitoring their impact on travel delay and fuel consumption are discussed in this subsection. Results of this section helped to choose the appropriate explanatory variables for estimating travel delay and fuel consumption. When a factor was identified as insignificant in the relevant travel delay or fuel consumption estimation model, it was not included in the estimation model or the approach used to capture the impact of that factor in the simulation environment was changed. Factors were designed to change univariantly in the control case in various simulation runs. Results in terms of travel delay and fuel consumption estimates were analyzed for a set of experiments associated with each factor. A summary of the studied factors and ranges on their values is presented in Table 4.2.

Table 3.2 Summary of variables used in numerical experiments

General Attributes	Factors	Rang used
Geometry of the roadway segment	Segment length	10 mile
	Number of lanes and average lane width	2-6 lane, 12 feet
	Lateral clearance (shoulder)	6 feet
	Ramps	0 to 10 ramp/mile
	Horizontal curves	Straight, Mild, Sharp
	Segment gradient	-10 to +10 percent
Traffic characteristics	FFS	55 to 75 mph
	Ramp FFS	25 and 35 mph
	Traffic flow rate	200 to 2200 vplph
	Percentages of trucks in traffic flow	0 to 18 percent
Incident attributes	Incident severity	Shoulder, 1-lane and 2-lane Blockage
	Average incident duration	0 to 90 minutes (5-minute increment)
	Rubbernecking effect	500 feet Upstream of Incident Location
Weather conditions	Clear, Light Rain, Heavy Rain, Snow, Fog, Icy condition, Low Visibility, Wind	

3.2.1 Geometry Factors: Number of Lane and Lane Blockages

To describe the number of main lanes that are blocked due to an incident, average travel delay per vehicle is calculated for possible combinations of number of lanes and lane blockage within the study range (Table 4.3). Total travel delay divided by total number of vehicles gives average travel delay per vehicle in a simulation run.

Table 4.3 indicates a decrease in the average travel delay per vehicle when the number of lanes in a segment increases. The impact of one lane closure on travel delay is much higher in freeways with fewer of lanes, but the difference between travel delay of one lane and two lanes blockage scenarios was not large. One closed lane due to an incident results in a travel delay increase of approximately 13 times that in a two-lane freeway and 5 times that for a six-lane freeway. However, when two lanes are closed due to an incident, travel delay is approximately two times larger compare to one lane blockage for a comparable roadway segment. It is shown in Table 4.3 that fuel consumption is not very sensitive to the number of lanes blocked. This is because the relationship between fuel consumption and vehicular speed has a parabolic shape. Fuel consumption at lower speeds in a stop-and-start mode due to congestion is nearly the same as at higher speeds (e.g. an average speed of 70 mph) with no stops and starts. Therefore, number of lanes blocked due to incident can be eliminated from the fuel consumption estimation model. An approximate trend for travel delay versus fuel consumption is shown in Figure 4.4.

Table 3.3 Number of lanes and lane blockage analysis

state of factor	Travel delay (hour/vehicle)			Fuel consumption (gallon)		
	shoulder blockage	1-lane blockage	2-lane blockage	shoulder blockage	1-lane blockage	2-lane blockage
two lane	7.44	100.23	N/A	307.5198	305.4774	N/A
three lane	10.12	110.34	240.76	275.2585	331.2327	319.7124
four lane	13.94	104.45	199.53	614.0988	613.5244	614.5162
five lane	14.93	88.543	129.87	775.1365	777.0599	781.0039
six lane	17.35	77.84	109.45	925.1616	923.8499	933.9603

N/A: Not Applicable

Figure 3.3 Number of lanes and lane blockage analysis

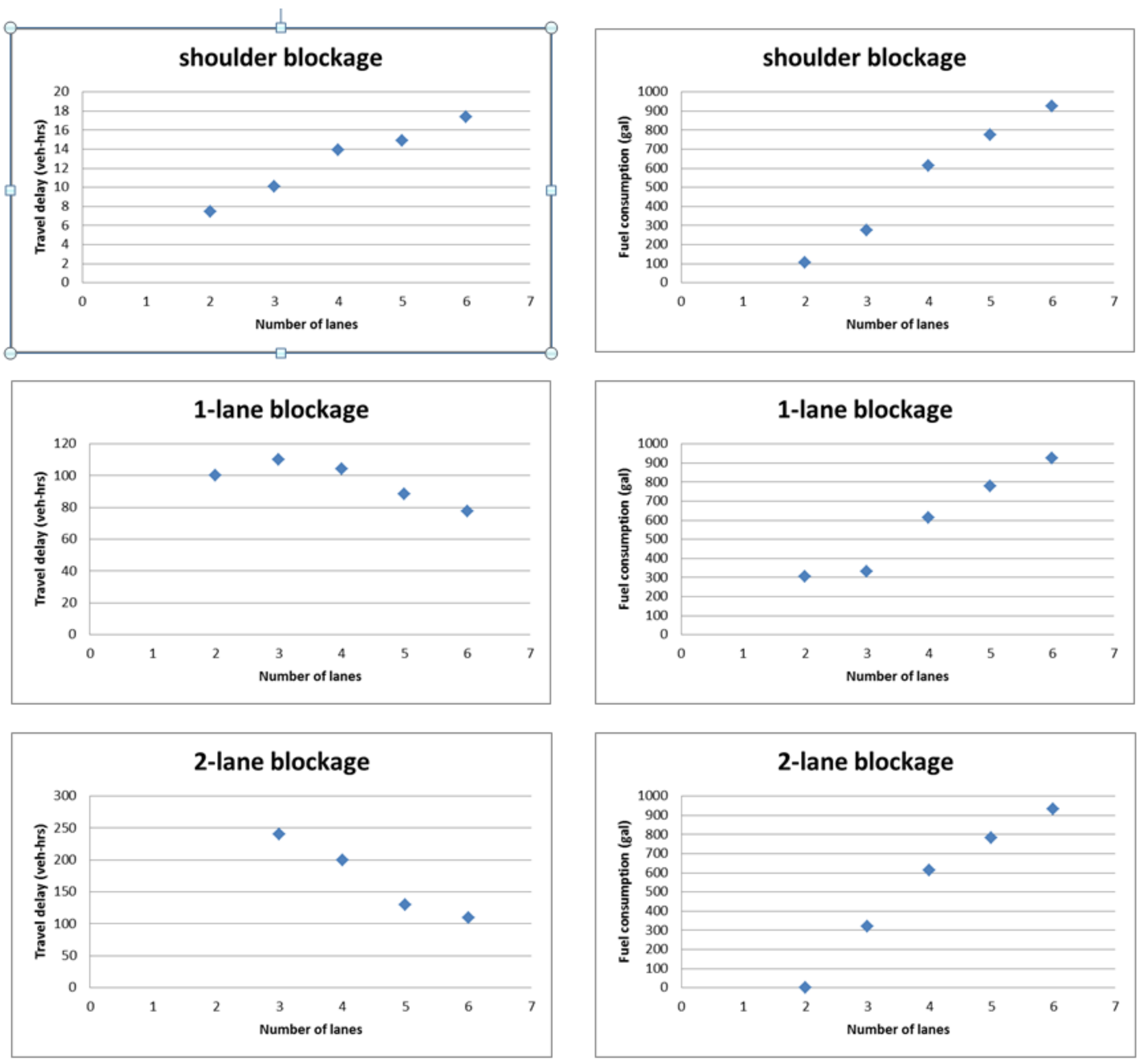

A linear trend can be seen in both travel delay and fuel consumption graphs given in Figure 4.3. However, travel delay is greatly affected by lane blockage. Therefore, it was necessary to develop separate estimation models for travel delay for different lane blockage incident scenarios.

3.2.2 Geometry Factors: Ramps

The FFS along the ramps, exiting traffic flow and location of incident with respect to ramp locations are important aspects that have been considered in simulating incidents in close proximity to ramps. The impact of incident-ramp proximity on travel delay and fuel consumption is studied. The simulation roadway segment is set to have one off-ramp. (Figure 4.2 compare to Figure 4.1). Two ramp FFSs (25 and 35 mph) are tested. Additionally, two exiting flow percentages (25 and 50) of the main lane traffic volumes are considered. Studies have shown that ramps are significant sources of bottlenecks in freeway operations, affecting traffic as far as a quarter-mile upstream and downstream of merge and diverge points (Zhang et all, 2009). Five incident locations, each set within a half-mile of the off-ramp location, are modeled as depicted in Figure4.4. The average travel delays and fuel consumption over 5 random seeds for each case are reported in Table 4.4.

Figure 3.4 Simulating incidents close to an off-ramp

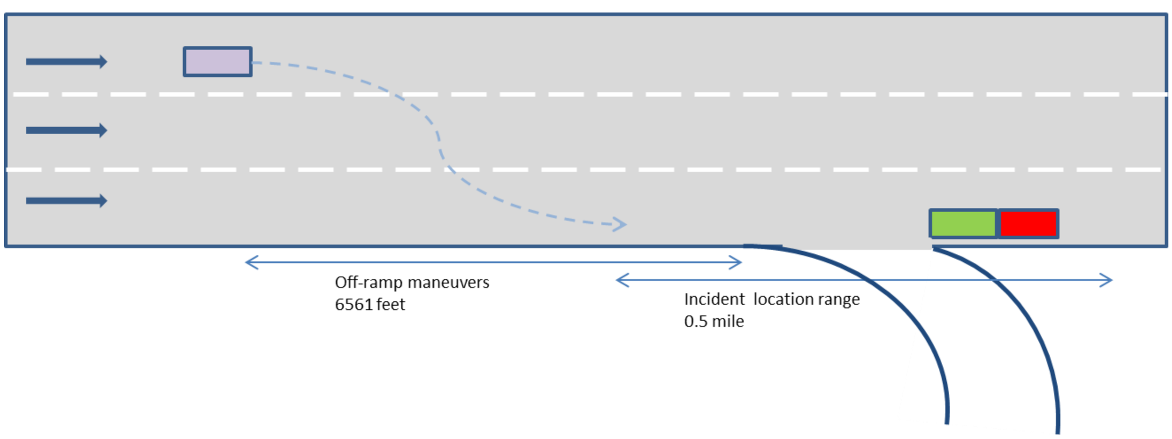

The distance needed for a vehicle to start a diverging maneuver is set as the number of lanes the vehicle must pass multiplied by the look-back distance. For example, if the look-back distance is set as 200 feet, a vehicle in lane three will start changing lanes to reach the right-most lane beginning from 400 feet upstream of the off-ramp.

Table 3.4 Ramp analysis

State of the factor	Travel delay (vehicle-hour)		Fuel consumption (gal)	
(ramp speed-exiting volume)	Passenger cars	Trucks	Passenger cars	Trucks
25mph- 25%	13.106	0.180	613.1	15.4
25mph- 50%	13.106	0.180	613.3	15.7
35mph- 25%	10.484	0.131	614.2	15.6
35mph- 50%	10.484	0.131	614.1	15.7
base case	10.295	0.116	614.1	15.8

As anticipated, the lower the ramp FFS, the higher the travel delays incurred and greater the fuel consumed. However, even for arising incidents close to the ramp with design speed of 35 mph and the main lane FFS 70 mph, the ramp does not affect travel delay significantly. However, fuel consumption decrease since portion of vehicles moves slower nearer to ramp and vehicles generally have higher fuel efficacy in the range of 30 to 50 mph range than at 70 mph.

To include the incident-ramp proximity impact on travel delay and fuel consumption in SSP-BC Tool, the speed design of every ramp on the study segment should be included as input. However, the information does not make significant difference in travel delay and fuel consumption outputs. A more practical way to include the impact of ramps, therefore, was selected for the SSP-BC Tool as explain in Sections 3.2.1.4 and 3.2.3.2 in which capacity reduction due to ramp density is applied.

3.2.3 General Terrain: Horizontal Curves

Given a specific number of points, VISSIM provides an option to draw a Bezier curve when creating connector links. To assess whether or not the software adequately captures the effects of curvature in freeway operations on speed, preliminary simulation runs were conducted in which the travel time of vehicles traversing two similar segments, one curvy and one straight, were compared. No significant difference was noted between travel times in these runs. Thus, it was concluded that the operational effects of roadway curvature are not captured. To capture these effects, reduced speed areas and lower approaching desired speeds were used within curved areas of the test segment. This is consistent with freeways where speed limits are reduced around curvy roadway segments.

1000 feet of the base segment is modeled with curvature. Curves with three design speed were considered. The effect of the curvature is captured by setting speeds of 65, 55, and 50 mph along the 1000-foot length of the 70 mph segment. Incidents were placed randomly in different positions within the curve.

Results of test cases were not significantly different from the base case in lower speed categories. Therefore, for roads with mild and sharp curves, 5 mph and 10 mph speed reduction respectively were applied to posted speed limits if the exact speed limit of the segment close to a curve is not available in detail.

3.2.4 General Terrain: Vertical Curves

The gradient of the segment can be set manually in VISSIM. According to HCM 2010, the maximum grade in level terrain is 2% (-2%), in rolling terrain is 5% (-5%), and in mountainous terrain is 10% (-10%) as discussed in Section 3.2.2.2. The base case has 0% gradient. The results for different grades are shown in Table 4.5.

Travel delay increases significantly as the gradient of the segment increases. Negative grades (downhill) do not have a significant impact on travel delay. The impact of grade on average vehicular speed can be discerned from results given in Table 4.6. The average speed of trucks is more affected by grade. The difference between average speeds of passenger vehicles and trucks widens as the grade increases.

Table 3.5 Segment grade analysis

percentage of grade	Travel delay (vehicle-hour)		Fuel consumption (gal)	
	Passenger cars	Trucks	Passenger cars	Trucks
-5%	10.5	0.1	515.5	12.9
5%	26.1	0.2	397.4	9.6
10%	83.6	5.3	289.6	14.5
base case	10.295	0.116	614.1	15.8

Table 3.6 Impact of gradient on average speed

percentage of grade	Average Speed (mph)	
	Passenger cars	Trucks
-5%	61	52
5%	52	35
10%	37	23
base case	60	51

Fuel consumption reduces with reduced speed resulting from higher grades. The VISSIM manual explains that the impact of gradient on traffic flow is found in acceleration and deceleration of vehicles, "The possible acceleration decreases by 0.1 m/s^2 per percent of positive gradient (road incline)." To capture the effects of gradient and not changes in speed, on fuel consumption, all other factors, including speed, remain constant in this set of experiments. Thus, for different gradient settings, a constant speed is forced. This permits analysis of travel delay fuel consumption and emissions changes due to changes in gradient. Results are provided in Table 4.7. To maintain a constant speed along a gradient, a significant increase in fuel consumption rate is required.

Table 3.7 Fuel economy changes due segment grade

percentage of grade	**Fuel Economy (mpg)**	
	Passenger cars	Trucks
0	22.06	21.34
5%	16.18	16.27
10%	11.50	10.09

3.2.5 Traffic Characteristics: Speed of Vehicles

In the simulation runs, the speed of vehicles is defined by the desired speed. VISSIM has a speed distribution for desired speeds from which it assigns a speed to every entering vehicle. If the speed of any vehicle for any reason (e.s. lane blockage) changes, vehicles reach their assigned desired speed after passing the obstacle. Four different speed regimes from 37.5 mph (60kmh) to 75 mph (120 kmh) were modeled.

It was found that fuel consumption is highly sensitive to desired speed. In fact almost 50% reduction in fuel consumption was noted when desired speed changes from 120 to 60 kmh. Travel delay, however, slightly decreased with decreasing desired speed.

Table 3.8 Travel delay and fuel consumption changes by FFS

FFS (kmh)	**Travel delay (vehicle-hour)**		**Fuel consumption (gal)**	
	Passenger cars	Trucks	Passenger cars	Trucks
60.00	7.66	1.64	257.82	9.36
80.00	8.16	0.4	306.46	11.04
100.00	8.42	0.14	397.98	12.54
Base Case (120)	10.295	0.116	614.1	15.8

3.2.6 Traffic Characteristics: Demand Flow Rate

The average speed of vehicles in incident cases with prevailing traffic volumes prior to incidents between 200 and 2200 vplph, were obtained through simulation runs, results from which are shown in Figure 4.5. The sold line depicts the HCM-suggested speed for a basic freeway segment with FFS of 70 mph. The dash-square line Indicates VISSIM average speed, obtained from this study for the base segment under different flow rates. The dash-triangle shows average speed over the segment for an incident with 90-minute duration. The dot line indicates the boundary of Level of Service E and F when density passes 45 passenger car per mile per hour (pc/mi/hr).

Figure 3.5 Average speed Vs. Traffic flow rate

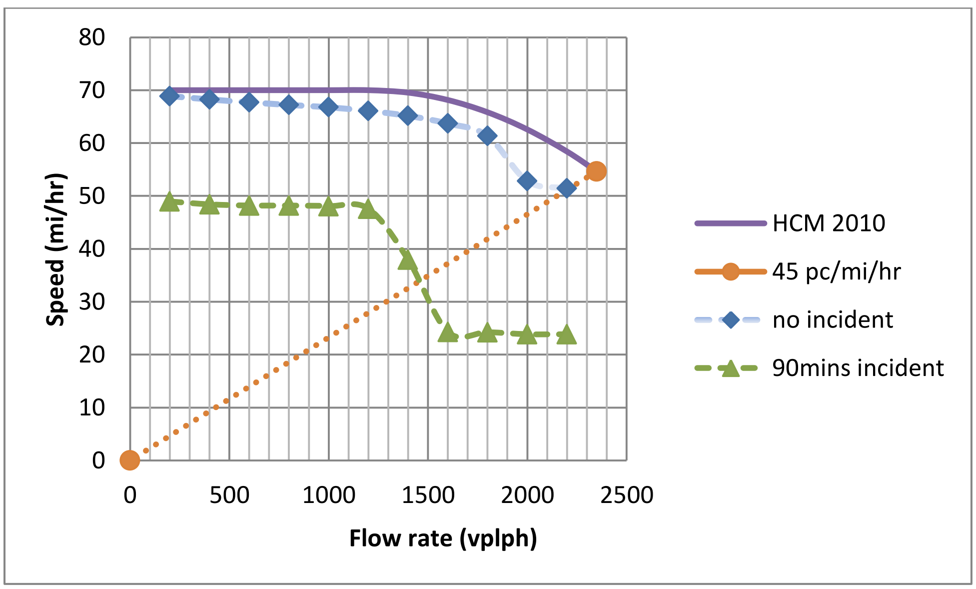

From the 90-minute incident line, the average speed reported for the study segment with incident at a density of 45 pc/mi/hr, where 90-minute incident line passes the dot line, is approximately 35 mph. The HCM suggests a 15% capacity reduction due to shoulder incidents in a 4-lane freeway. It, also, provides adjusted speed-flow curves for indicated capacity reductions (i.e. due to incidents, Exhibit 10-9, HCM 2010). From the mentioned graph in HCM, the average vehicular speed under 15% capacity reduction in a basic segment at 45 pc/mi/hr is approximately 40 mph (FFS of 70 mph, capacity of 2400 pcplph). This indicates that for the simulated segment, capacities associated with lower traffic flow rates are reached in comparison to ideal conditions in a basic freeway segment suggested in the HCM. Furthermore, from the "no incident" line in Figure 4.3, the capacity of the simulated segment closes in on 2000 vplph as average speeds for higher traffic flows become almost constant from this flow rate. Also, after 2000 vplph, the travel times don't change significantly as traffic flow increases (Figure 4.6). Having 2000 vplph capacity in mind for the study segment under normal conditions, the corresponding average speed of vehicles to the capacity given a 15% capacity reduction in case of incident must be in the range of 35 to 38 mph. 35 mph value has been found from simulated incident case.

Figure 3.6 Travel time vs. Traffic flow

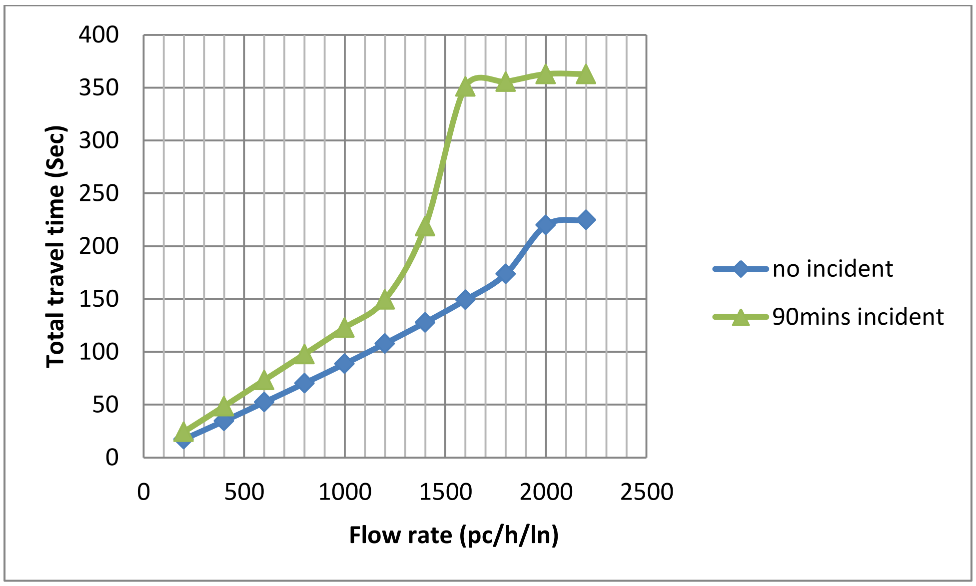

Findings reported in Figure 4.5 also indicate lower average speeds resulting from the simulation runs under lower traffic volumes as compared with expectations given in the HCM suggested values because the gap between previously mentioned adjusted speed-flow curve and actual speed-flow curves is smaller as low flow rates (Exhibit 10-9, HCM 2010). From Section 4.2.5, it was found that travel delay slightly decreased with desired speed. Thus, if maintaining the suggested speeds of at in lower flow rates, higher travel delay as HCM suggested values might be obtained assumed the capacity to be 2400 vplph for the basic segment.

3.2.7 Traffic Characteristics: Truck Percentages

To test the impact of trucks on the operation of vehicles in the segment seven traffic composition cases with 0 to 20 percent truck traffic were tested. One-lane blockage incidents were modeled instead of shoulder blockage incidents to capture the impact of vehicle maneuvers. Maneuvers of trucks differ from those passenger cars and, therefore, it affects travel time and fuel consumption differently. Higher Percentages of trucks in traffic flow increase the travel delay and fuel consumption as expected (Table 4.9).

Table 3.9 Truck percentage analysis

percentage of trucks	Travel delay (vehicle-hour)			Fuel consumption (gal)		
	Passenger cars	Trucks	SUM	Passenger cars	Trucks	SUM
0.00	171.0673	0	171.0673	137.5791	0	137.5791
0.05	174.5893	13.296	187.8853	134.7476	13.50501	148.2526
0.10	166.5927	25.51267	192.1053	123.1948	25.98375	149.1785
0.12	160.7813	30.78933	191.5707	119.4744	31.20691	150.6813
0.15	149.6053	38.094	187.6993	112.8164	37.56797	150.3844
0.17	144.7567	42.16	186.9167	109.7824	42.52419	152.3066
0.20	140.1433	47.52067	342.1347	105.1306	49.08134	154.212

3.2.8 Simultaneous Changes of Factors

In the prior section, the effects of individual factors on travel delay and fuel consumption in the presence of incidents was studied. In reality, multiple factors will exist that will simultaneous the impact these measures under such incident conditions and their effects are often nonadditive. In brief, the factors that directly were considered in the travel delay and fuel consumption estimation models are: Incident duration, number of lanes, number of lanes blocked, prevailing traffic volume, FFS, percentage of trucks and gradient as determined in Sections 4.2.1 to 4.2.7.

No prior published study could be found that described a relationship between truck composition and/or roadway gradient with travel delay. Thus, additional analysis to test the independence of these factors and their impact on travel delay was completed. Simulation runs in which the number of lanes, truck percentage and/or segment gradient change concurrently were conducted. Results of these additional simulation runs indicated a constant increase in travel delay due to increased truck composition regardless of the number of lanes. The same pattern was found for segment gradient. These results infer that additional delay due to percentage of trucks and grade change on the three-lane freeway test segment can be added directly to estimate for segments with any number of lanes. However, this was not the case for fuel consumption.

3.3 Multiple-Regression Analysis

Multiple-regression relates two or more independent variables (x_i) to a dependent variable (*Y*). Seven multiple-regression models are presented for travel delay and fuel consumption of cars and trucks of different lane blockage incident scenarios based on a design sample of incidents. The general form of multiple regressions is shown in Equation 4.1 where dependent and independent variables are i dimensional vectors. The parameters β_i were estimated using a least squares method.

$$\mathbf{Y} = \boldsymbol{\beta_0} + \boldsymbol{\beta_1 x_1} + \boldsymbol{\beta_2 x_i} + \boldsymbol{\beta_3 x_3} + \cdots + \boldsymbol{\beta_n x_n} + \boldsymbol{\varepsilon}\,,\ \boldsymbol{i = 1, \ldots n} \qquad \textbf{Eq. 3.1}$$

To obtain the travel delay estimation models, the regression models were developed for different lane blockage scenarios as discussed in Section 4.2.1. In each category of lane blockage, two models are presented for light-duty and heavy-duty vehicles. Explanatory variables of the travel delay regression model were chosen to be incident duration, traffic volume, percentage of trucks and gradient of the roadway. The only parameter found insignificant in the conducted preliminarily experiments for fuel consumption was number of blocked lanes due to incidents. Thus, explanatory variables of fuel consumption regression model are: number of lanes in the segment, incident duration, traffic volume, , speed, percentage of trucks and gradient.

3.3.1 Minimum Sample Size

A balance between accuracy and computation time must be chosen in selecting an appropriate sample size of incident scenarios for simulation runs. The larger the sample size, the more accurate the model and the better the estimation of parameters, but the greater the computational effort. Determining the minimum sample size of incidents, thus, is necessary. For this study, the population means (μ) method is employed to determine the minimum sample size required for the multiple-regression models. With anticipated effect size (f^2) of 0.05, statistical power level of 0.95, four explanatory variables and probability level of 0.05, the minimum sample size required is 376 (Cohen et al. 2003). Thus, a sample size of 400 was used for each lane-blockage state. For the fuel consumption model 300 observations were used.

3.3.2 Designing a Sample of Incidents

To create a random sample of incidents for estimating the parameters of the multiple-regression models, the explanatory variables were used as the design criteria of each incident. Since the correlation between the explanatory variables is unknown, it was assumed that the explanatory variables are independent and uncorrelated with one another. Where this assumption invalid some incidents might have a low likelihood.

While some incident cases with very low probability may be generated in the sample used within the simulation and later to calibrate regression models, if appropriate modeling techniques are used, these samples will have little effect on the development of a regression model passing goodness-of-fit tests. In addition, if the domain of a variable is dependent to one another, the estimation model should be developed for that domain, since a general model of all points might have different local behavior. This issue is addressed here with using the real world ranges for generating the random variables and the appropriate probabilistic distributions best describing each criterion. The random values for each incident in the sample are generated as follows.

If incident duration is a random variable, it will have a probability density function (PDF). Statistical methods have been employed by researchers to explain and estimate incident duration when treating it as a random variable. These methods treat the random variables with probabilistic distributions, conditional probabilities, linear and non-linear regression models, time sequential and others as discussed in Chapter 3.

Golob et al. (1987), GIuliano (1989), Garib et al. (1997), Suvilllivan (1997) and Ozbay et al. (1999) found that the log-normal distribution very closely fit their freeway incident data. Ozbay et al. (1999) claimed that incidents with the same severity level have normal distributions, supporting the theory that incident duration is a random variable (Smith and Smith, 2002). Nam and Mannering (2000) found that the Weibull distribution is also capable to estimate incident duration of an incident sample. Smith and Smith (2002), however, found that required goodness-of-fit tests for log-normal and Weibull distributions failed.

To create a sample of incidents representing real data, therefore, incident duration cannot simply be generated randomly from a uniform distribution. The average and standard deviation of the incident durations used in the design sample for this study need to be close to the incidents to which SSP vehicles responded. Chou and Miller-Hooks (2008) found that the average incident duration of 80% of incidents that SSP vehicles responded to is 17.6 minutes in New York State with standard deviation of 18.07 minutes. First, the Weibull distribution was used to generate incident duration times for the sample, but calibration of its parameters to provide desirable average and standard deviation were not successful. MATLAB was employed for generating random variables from the inverse of the Weibull distribution. Boyles and Waller (2207) used a log-normal distribution with μ (mean)=3 and σ(standard deviation)=1.6 to describe the incident duration of the incidents. Herein, by searching within the vicinity of those parameters, a log-normal distribution with mean 2.8 and standard deviation of 1.4 was found that best fit the distribution parameters that were sought. Using the inverse of the defined distribution (Equation 4.2), a set of 400 random incident durations having a mean of 17.8 minutes, standard deviation of 16.9 minutes, maximum of 70 minutes, and minimum of 5 minutes was generated. The lognormal inverse function is defined in terms of its CDF as in Equation 4.2.

$$\boldsymbol{x} = \boldsymbol{F}^{-1}(\boldsymbol{p}|\mu, \boldsymbol{\sigma}) = \{\boldsymbol{x} : \boldsymbol{F}(\boldsymbol{x}|\mu, \boldsymbol{\sigma}) = \boldsymbol{p}\}, \qquad \textbf{Eq. 3.2}$$

where

$$\boldsymbol{p} = \boldsymbol{F}\,(\boldsymbol{x}|\,\mu, \boldsymbol{\sigma}) = \frac{1}{\boldsymbol{\sigma}\sqrt{2\pi}}\int_0^x \frac{e^{\frac{-(\ln(t)-\mu)^2}{2\sigma^2}}}{t}\,dt.$$

Hourly traffic volume is an important input used in the simulation runs. However, in travel delay studies, traffic volume is not often addressed directly and a factor that can be related to it is time-of-day variable: a.m. and p.m. peak hours on weekdays and off peak hours during weekdays and weekends. However, due to lack of information on the connection between time-of-day and volume, a uniform distribution is used to generate random traffic volumes in incident cases. Percentage of trucks in traffic composition, and gradient were assumed to be independent of one another and a uniform distribution was used to generate each of them. For fuel consumption sample, number of lanes also assigned to incident scenarios from a uniform distribution.

3.3.3 Multiple-Regression Models

As mentioned in Section 4.3.1, multiple-regression was selected to model travel delay and fuel consumption of both light- and heavy-duty vehicles in each lane blockage scenario. First, the linear regression models of travel delay and fuel consumption based on explanatory variables were obtained. Next, composition of variables is introduced to the model and a set of non-linear regression models are presented for validation by various goodness-of-fit tests. A stepwise technique is employed to find the best subset of explanatory variables for models.

The stepwise technique starts the regression with the best regressor. It then finds the next best variable to add to the model, and finally it checks all variables in each equation to see if the previously entered variables remain significant. Other techniques that might be used in place of the stepwise technique include MAXR which chooses the variables to add to the model so as to achieve the highest possible R-square value. The stepwise method terminates based on the Mallow's C_p statistics. Mallow's C_p is a goodness-of-fit test for regression that used ordinary least squares for estimating the parameters. When the expectation of C_p becomes close to the $P\ value$, the stepwise procedure terminates and the final set of explanatory variables are introduced.

SAS statistical software package was employed for the statistical analysis conducted herein. SAS is a combination of programs that were designed for statistical analysis of data. The package offers six variable selection methods. These methods present results in a set of candidate regression models from which the best is chosen. To choose the best estimation model for travel delay and fuel consumption from the set of candidates models, six approaches are exhibited as goodness-of-fit tests: coefficient of determination (R-square), adjusted R-square, Mallow's C_p, Akaike Information Criterion under the name of "an information criterion" (AIC), Bayesian Information Criterion (BIC) and Schwarz's Bayesian information criterion (SBC) as exhibited in Equations 5.1a to 5.1d.

The first method, the coefficient of determination method, is not always reliable. The goodness-of-fit increases with the number of regressors added to the model and, thus, the more explanatory variables, the better the model appears to be. The adjusted R-square method can be used to compare models with different numbers of explanatory variables, because regressors are added to the model only if their entry leads to statistically significant improvements in the model. Like the adjusted R-square technique, the AIC method penalizes any additional unnecessary estimators and discourages overfitting. Assuming the error term within the model is normally distributed, the maximum log likelihood was derived for each candidate models. The derived likelihood of each model is then to compute AIC, BIC and SBC (Equation 5.1b, 5.1c, 5.1d). From this set of candidate models, the one having minimum value of AIC, BIC and SBC would be selected as the final model. For example, to find the travel delay regression model having 8 explanatory variables, first using the stepwise and MAXR are used two sets of variables. Each set results regression model. The one best fit the data is identified throughout each of goodness-of-fits that may lead to a first choice model. If we decide to use R-square as goodness-of-fit test, the model which has higher R-square would be the best model,but if we want to use AIC as the goodness-of-fit test, the model that gives the lowest value of AIC would be presented as the final model.

$$C_p = \frac{SSE_p}{S^2} - \mathrm{N} + \mathrm{P} \qquad 5.1a$$

$$AIC = -2(MLL) + 2\,(k) \qquad 5.1b$$

$$BIC = -2(MLL) + P\,log(N) \qquad 5.1c$$

$$SBC = N \ln\left(\frac{SSE}{N}\right) + K \ln N \quad , \qquad 5.1d$$

where

N = number of observations,

SSE= Sum of squared errors,

P= number of explanatory variables,

K= number of free variables <= P+1, (k= # independent variables + intercept),

MML= Maximum log likelihood of the model.

3.3.3.1 Travel Delay Regression Models

Regression models were developed for each lane blockage scenario and vehicle type. Note that each scenario is assumed to arise with the same likelihood. Let *TTD* stand for total travel delay of an incident case, *ID* be incident duration, *vol* be traffic volume at the time of the incident, *PT* be percentage of trucks in the traffic composition and *G* represent the gradient of the road. First, the linear model is developed for light- and heavy-duty vehicles and the shoulder lane blockage scenario with four explanatory variables as shown in Equations 5.1a and 5.1b. All variables were found to be significant at the 0.15 level. The models have R-square values of 0.6772 and 0.5682, respectively.

LDV:

$$\mathbf{TTD = -37.391 + 0.02253(\mathit{ID}) + 16.86(\mathit{vol}) + 0.482(\mathit{PT}) + 4.222(\mathit{G})} \qquad \textbf{Eq. 3.3}$$

LDT:

$$\mathbf{TTD = -10.87 + 0.04167\ (\mathit{ID}) + 2.31\ (\mathit{vol}) + 0.588(\mathit{PT}) + 0.7841(\mathit{G})} \qquad \textbf{Eq. 3.4}$$

The above regression models are based on four assumptions related to the dependent variables: independence, normality, homoscedasticity (constant variance of response variable) and linearity.

The regression assumptions can be re-expressed in terms of modeling errors to validate the assumptions on which model is built. Random errors are independent, normally distributed, have constant variance σ^2 and zero mean (Equation 4.1). Having these conditions the random errors can be considered as a random sample from $N\ (0, \sigma^2)$. In addition, the best representation of errors is through standard residuals. Standard residuals are the difference between actual and predicted response variables for each observation with constant variance over different dependent variables. SAS calculates residuals with a variance of 1.

In general, any systematic pattern in residuals indicates a violation in assumptions and systematic error. Fit diagnostics for the models, including residual graphs for each parameter were obtained and analyzed. A summary of goodness-of-fit test results for travel delay of LDV is presented in Figure 4.7 as a sample of a full analysis. The behavior of other models and the analysis were very similar to this case. In this model, it appears that the linearity assumption is violated, because the residuals are not scattered randomly around zero and form a clear pattern. Also the variance of residuals seems to have two values and they value is not constant. It shows that the model does not have the same accuracy for all data points.

A Quantile-Quantile plot indicates that theoretical and actual data distributions do not agree, as the plotted points are not approximately on the $y=x$ line. The slope of the curve of the plotted points increases from left to right, which indicates that a theoretical distribution that is skewed to the right, such as a log-normal distribution, might better fit the data. In addition, the mild curve indicates a small shape parameter for the chosen distribution (i.e. σ for log-normal). Cook's D shows no outlier points, as all data points are within a distance of 2 of the zero line.

Figure 3.7 Summery of fit diagnostic for total travel delay of LDV

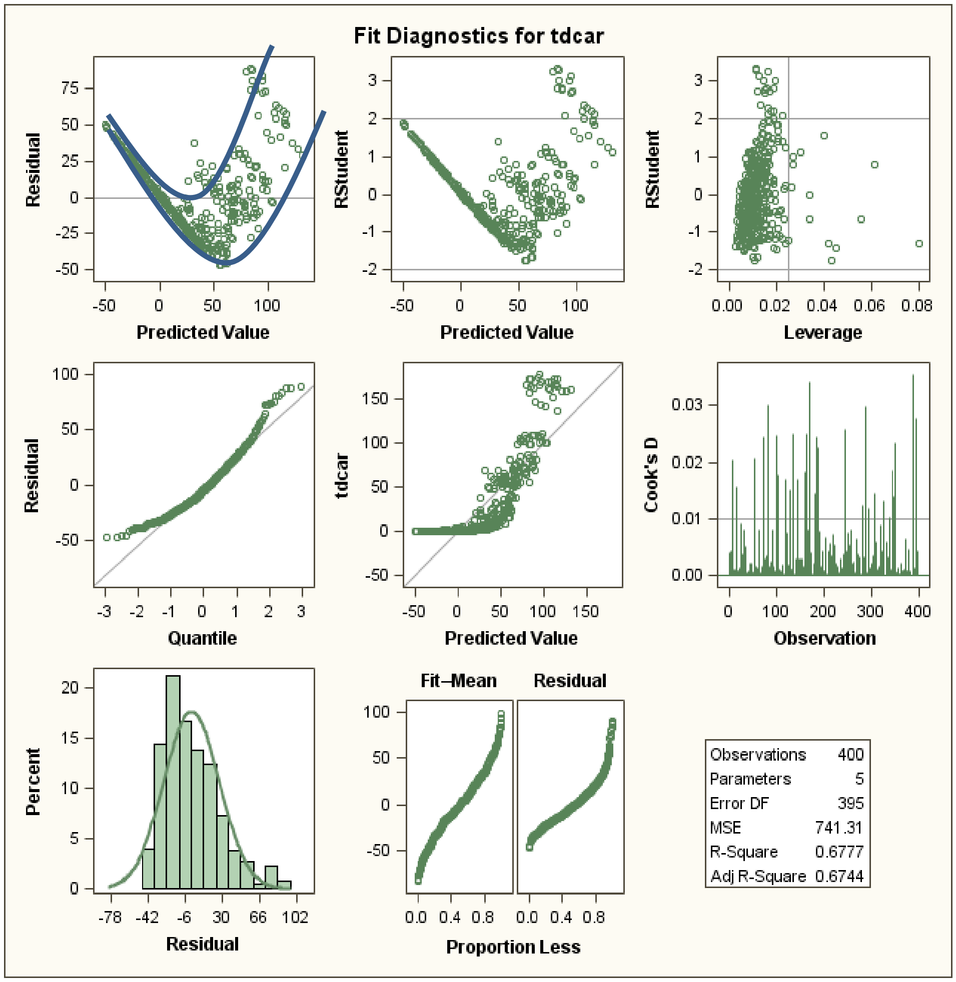

As part of additional analysis, the residuals are plotted separately for each explanatory variable (Figure 4.8). Since the variables are uncorrelated by design, each graph shows the direct relationship of dependent variable and explanatory variable. Incident duration has a random scatter plot matching its log-normal distribution. Residuals associated with the truck composition are also randomly scattered around zero, so the linear assumption seems reasonable. Residual graphs of volume and grade suggests a parabolic curve, then it may make sense to regress travel delay on the squared form of these two variables. Notice that the range of changes in truck composition is low inferring that the linear relationship with travel delay may be correct.

Figure 3.8 Scatterplots of residuals against explanatory variables

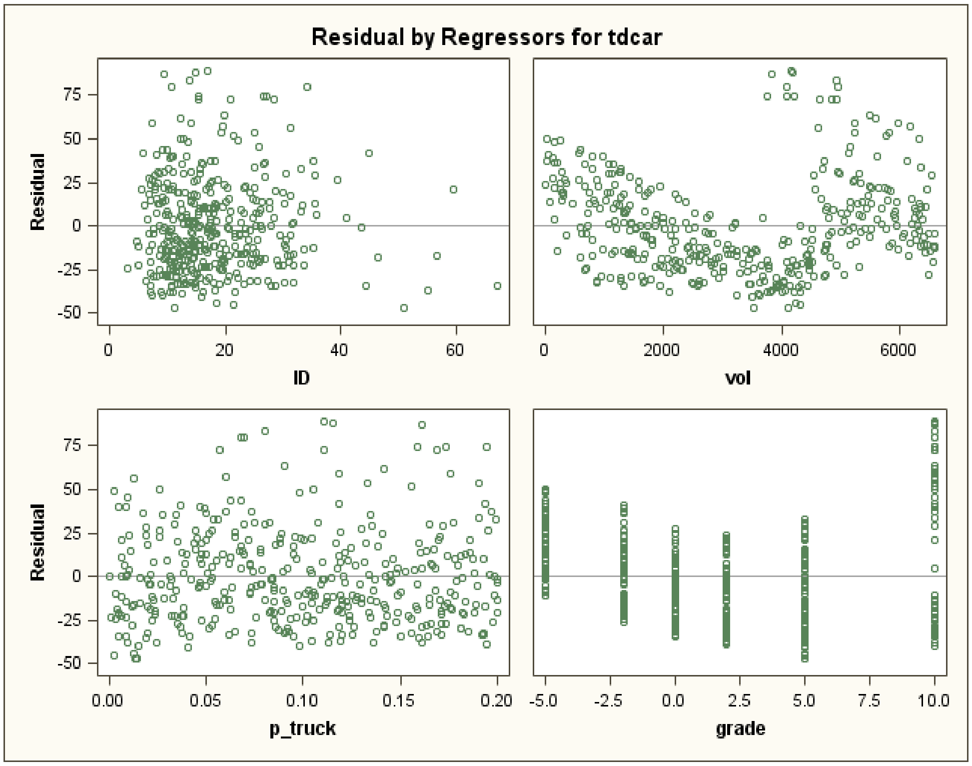

As a result, to improve the model, new variables are introduced. These variables are either the original variables squared (i.e. vol_sq indicates volume squared) or a multiple of two of the variables. Non-linear regression models were fitted to the data accordingly. The R-square of the models were improved slightly but the systematic errors were not eliminated.

Search for an appropriate multiple-regression model was repeated for one- and two-lane blockage incident cases using a similar procedure as described previously for the shoulder blockage case. The linear models are presented in Equations 4.5 to 4.8.

One-lane blockage travel delay linear regression model:

LDV:

$$\boldsymbol{TTD = 13.78 + 0.11521\,(ID) + \ 9.4(vol) + \ 0.102(PT) + \ 1.1135(G)} \qquad \textbf{Eq. 3.5}$$

LDT:

$$\boldsymbol{TTD = 0.055 + 0.033\,(ID) + \ 1.41\,(vol) + \ 0.278(PT) + \ 0.1754(G)} \qquad \textbf{Eq. 3.6}$$

Two-lane blockage travel delay linear regression model:

LDV:

$$\boldsymbol{TTD = 62.884 + 0.6914\ (ID) + \ 4.12(vol) - 1.293(PT) + \ 1.0186(G)} \qquad \textbf{Eq. 3.7}$$

LDT:

$$\boldsymbol{TTD = 5.644 + 0.132\ (ID) + \ 4.08(vol) + 0.2058(PT) - 0.2384(G)} \qquad \textbf{Eq.3.8}$$

Similar to the shoulder lane blockage category, non-linear regression models were calibrated for the one- and two-lane blockage incident categories. However, the travel delay estimation models of one- and two- lane blockage scenarios did not improve statistically compared with linear counterparts. The R-square of these non-linear models are presented in Table 4.16. A hybrid approach mentioned previously was established for improving travel delay regression models as described in the following section.

3.3.3.2 Hybrid Approach

In linear regression, the coefficient of a single variable will not change by removing or adding a new independent and uncorrelated variable to the model. In Section 4.2 truck percentage and segment grade were found to be uncorrelated with other explanatory variables. A hybrid approach in which travel delay obtained from simulated incidents is integrated with estimates obtained from developed regression models is created to reduce the error of the estimation models and capture the relationship between travel delay, number of lanes in the segment, incident duration, traffic volume and the speed of vehicles more accurately. In the hybrid approach, the primary linear regression model is broken into two parts: (a) a travel delay function on number of lanes, incident duration, traffic volume and speed and (b) a travel delay function on percentage of trucks in traffic composition and roadway gradient.

Assume an incident in which all the factors (the explanatory variables) are non-zero. The first part (a) is identical to the same incident case in which tucks percentage and gradient are zero. Travel delay associated with this incident ($TD_{i,v,s}^{k}$) was then directly computed from the simulation runs. The additional travel delay due to percentage of trucks and different gradients then was included in the model using linear regression estimation equations. For example, travel delay regression model for light-duty vehicles and shoulder blockage incidents (Equation 4.3) would be reformed as in Equation 4.9.

$$\mathbf{TTD} = \overset{\boxed{a}}{\left[\boldsymbol{TD^{k}_{i,v,s}}\right]} + \overset{\boxed{b}}{\left[\mathbf{0.48}(\boldsymbol{PT}) + \mathbf{4.2}(\boldsymbol{G})\right]} \qquad \textbf{Eq. 3.9}$$

To validate this hybrid approach, simulation runs for 300 incidents in a three-lane highway were completed. Incident durations and traffic volumes were set following the design described in Section 4.3.2. Truck percentage and gradient were set to random values from uniform distributions. Then, the equation 4.9 was applied to obtained travel delay data of the incidents with zero percentage of truck and grade, $TD^{k}_{i,v,s}$. Refer to these values as "predicted values" for the travel delay of designed incidents. Then, the coefficient of determination of the hybrid model can be computed as follows:

$$\boldsymbol{R^2 = 1 - \frac{SS_{err}}{SS_{tot}}}$$

where

$$SS_{err} = \sum_{i} (y_i - f_i)^2$$

$$SS_{tot} = \sum_{i} (y_i - Y_i)^2$$

SS_{err}= Residual sum of squares,

SS_{tot}= total sum of squares,

y_i= Observed values,

Y_i=Mean of observed values,

f_i= Predicted values by model.

The R-square of the linear regression for travel delay for shoulder incidents was 0.672 while the R-square of the hybrid model is 0.939. Thus, we can conclude that this estimation approach better captures travel delay. The same approach was applied to linear models of each of the six categories (3 lane blockage categories for each vehicle class) and the R-square was calculated. A comparison of R-square values between the linear regression models, non-linear regression models, and the hybrid approach is presented in Table 4.16. It can be noted that the R-square of regression models of all categories has improved significantly with the hybrid modeling approach given in Equation 4.9.

Table 3.10 Improved R-square comparison for new model

Lane blockage	Vehicle class	Linear model	Non-linear model	Hybrid Model
Shoulder lane blockage	LDV	0.677	0.878	0.939
	LDT	0.568	0.698	0.875
1-lane blockage	LDV	0.195	0.244	0.768
	LDT	0.153	0.236	0.719
2-lane blockage	LDV	0.142	0.141	0.784
	LDT	0.129	0.075	0.725

To use this hybrid approach in estimating travel delays in the SSP-BC Tool, simulation runs for all possible cases of number of lanes in a segment, number of lanes blocked due to the incident, incident duration, traffic volume, and speed of vehicles must be made. The travel delay obtained from the runs is then integrated with the regressed travel delay due to truck percentage and segment grade.

3.3.3.3 Fuel Consumption Regression Model

The same approach described in the previous section is used to obtain a fuel consumption prediction model for the light-duty vehicles. Later in Chapter 5 it is explained why the fuel consumption of LDT is not required for benefit computation of a SSP program. The linear model is presented in Equation 4.10 in addition to travel delay variables. Here, *spd* stands for speed of vehicles and *lane* is the number of lanes in the segment.

$$\boldsymbol{FC = 1 + 0.15\,(ID) - 3.616(100 * PT) + 19.23(g) + 0.05(vol) + 0.31(spd) + 15.43(lane)} \quad \textbf{Eq. 3.10}$$

The coefficient of determination of these linear models is 0.8210. The R-square for the light-duty vehicle model is very high, indicating excellent model fit to the data. However, it appears from Figure 4.9 that the linearity assumption is violated. This is indicated by a curve pattern in the residual scatterplot. Additionally, the variance of residuals increase indicates heteroscedasiticity assumption does not hold. From Figure

4.10, it can be seen that the residuals associated with volume are randomly scattered around zero, but the variance is not constant. This shows that the model is less accurate for some data points. Back in Figure 4.9, since the residual distribution is close to normally distributed and plotted points in the Q-Q chart are almost on the y=x line, it is reasonable to assume that the residuals are normally distributed

Figure 3.9 Summery of fit diagnostic of linear model of LDT fuel consumption

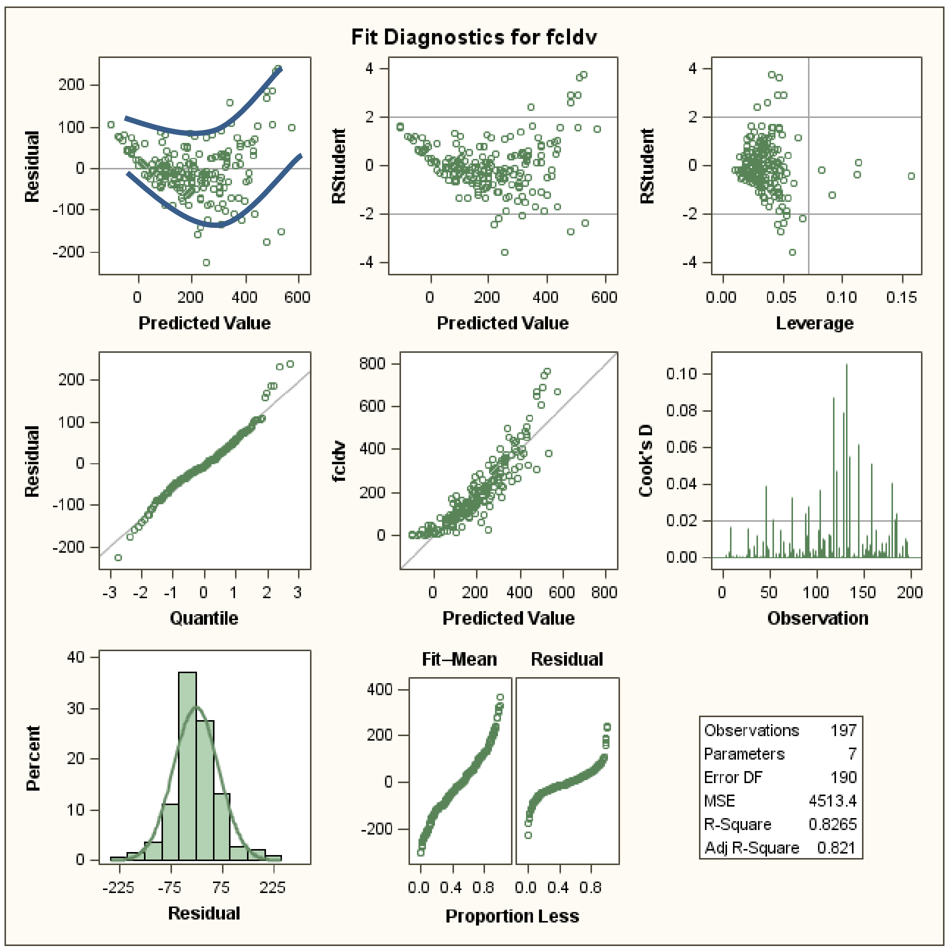

Figure 3.10 Scatterplots of residuals against explanatory variables

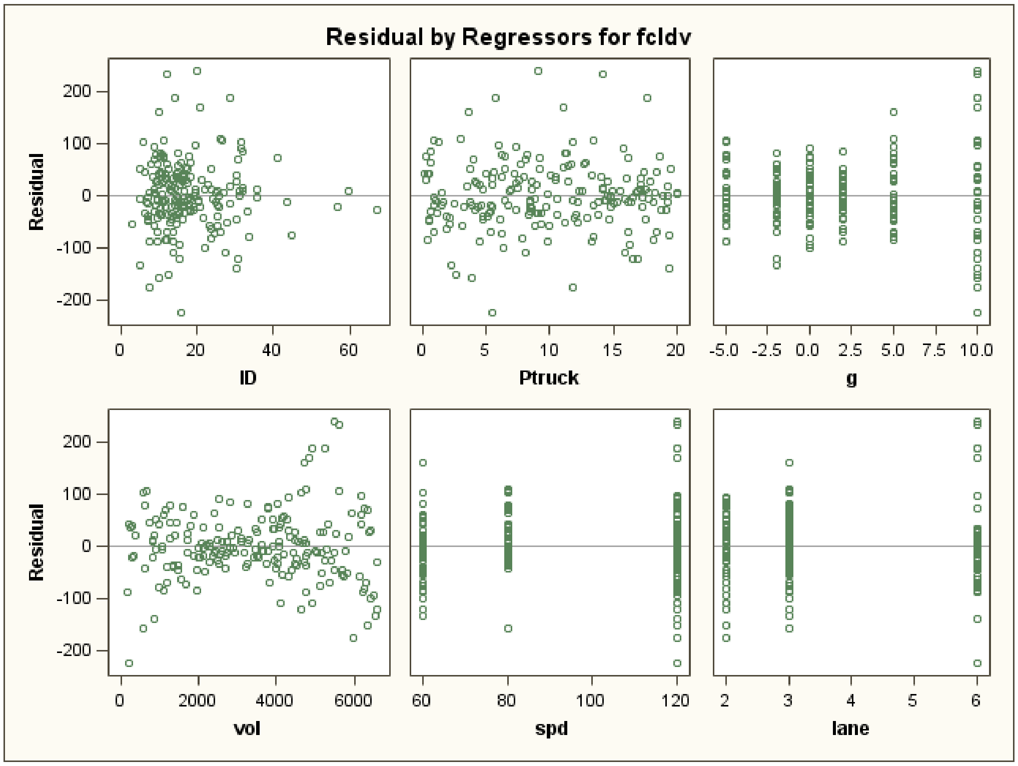

To address the linearity and variance problem, a set of non-linear models were derived and tested. From Figure 4.10, we can guess that a transform on gradient and speed might improve the model. Fuel consumption changes linearly with number of lanes in the segment ("lane") as found preciously in Section 4.3.2. Using the stepwise method, some parameters were chosen to enter the model. The final chosen nonlinear model for fuel consumption (Table 4.11) obtained after consideration of a variety of models.

Table 3.11 LDV fuel consumption

Root MSE	67.16175	R-Square	0.8293
Dependent Mean	200.47409	Adj R-Sq	0.8211
Coeff Var	33.50146		

Parameter Estimates			
Variable	DF	Parameter Estimate	Pr > |t|
Intercept	1	-255.22686	0.0368
vol	1	0.05440	<.0001
g	1	18.83305	<.0001
lane	1	15.77193	<.0001
spd	1	4.50066	0.0008
Ptruck	1	-3.56345	<.0001
ID	1	1.86832	0.0149
Spd^(2)	1	-0.02294	0.0233
ID^(1/6)	1	-0.18012	0.0928
gsq	1	0.08399	0.0050

The R-square of this model is not significantly improved by relaxing the linearity assumption. However, other goodness-of-fit tests show significant improvements and variables in the model agree with the similar studies in the same area, which make the model be adopted for the purpose of this study.

3.4 Summary

VISSIM was employed to estimate travel delay and fuel consumption of individual incidents in a segment. Impact of previously identified factors on travel delay and fuel consumption studied and multiple-regression models for estimating travel delay and fuel consumption were presented. A hybrid approach was introduced for improving the obtained travel delay models. Note that once fuel consumption is obtained, emissions can be computed (Section 3.4).

CHAPTER 5. B/C Ratio Estimation

This chapter discusses the computation of the B/C ratio, which is designed to provide insight into the return on investment received from operating a SSP program. Evaluation of the benefits in the B/C ratio requires a method for the amalgamation of chosen MOEs. In the developed tool, these are the savings in travel delay, fuel consumption, emissions and secondary incidents. These MOEs are given in a variety of units of measurement. Savings in travel delay is in vehicle-hours, savings in fuel consumption is in gallons of fuel, savings in emissions is in metric tons, and secondary incident savings is in number of prevented incidents. Thus, conversion to a common unit of measurement is required to develop a single numeric value for the numerator of the B/C ratio. Moreover, the unit of measurement must be commensurate with the units used in the B/C ratio's denominator, namely cost. Consequently, the most common approach is to convert the individual benefit measures to their monetary equivalents using monetary conversion factors. Methodologies for computing the total program savings associated with each of the chosen MOEs are provided in Section 5.1. Computation of the total benefit, i.e. the numerator of the B/C ratio, is discussed in Section 5.2. Section 5.3 describes total cost calculation in the deamination. This is followed by B/C ratio calculation in Section 5.4.

4.1 Savings Computation

To compute the benefit of a SSP program during a time period, benefits derived from each individual incident due to response by an SSP vehicle must first be determined. This is because the duration of the incident decreases as a result of the SSP vehicle response as explained in Section 3.2.4.2. To assess the value of the reduction in incident duration, travel delay, fuel consumption, and emissions can be estimated for the incident with reduced duration as a result of the SSP response "with-and-without" approach was employed (Section 2.2). Typically, it is the case that no such pre-program measurements were made. Thus, estimation of the "without" case must be made by assuming an increase in the duration of each realized incident. The amount of increase should be commensurate with the program's incident response time.

4.1.1 Savings in Travel Delay

To estimate travel delay of actual incidents in an area, using the travel delay hybrid model proposed in Section 4.3, simulation results from all studied incident scenarios are required. Simulation runs were made and travel delays associated with 14,784 incident scenarios were collected. The runs involved all possible combinations of 16 categories of incident duration, 11 categories of traffic volume and 6 speed categories, resulting in 1,056 combinations. For each combination, runs are including one of 3 types of lane blockage and one of 5 possible roadway sizes in terms of number of lanes. Results were saved in a table contained within the data base that supports the tool for further computations.

To estimate the travel delay associated with an incident with known characteristics using the proposed simulation-based procedure, the incident characteristics and associated traffic volume and speed must be known. As discussed in Chapter 3, the impact of the ramp density (Section 3.2.1.4), horizontal curvature (Section 3.2.2.1), and weather conditions (Section 3.2.5) on the capacity of the segment is captured through a reduction in FFS, affecting the speed category of the incidents. The maximum speed reduction due to existence of ramps, curvature, and adverse weather conditions determines the speed category of the incident. For example, consider an incident case for which speed in clear weather is 65 mph. To include the impact of heavy rain (a reduction in speed by 10-percent) and a full cloverleaf interchange in a one-mile segment (two on-ramps and two off-ramps in each direction, 5 mph reduction for each 2 ramps/mile),the employed speed for the incident cases in that segment would be 55 mph;

$$Actual\ speed = 65 - Max\{10\ \% * 65 = 6.5\ mph, 2 * 5 = 10\ mph\} = 65 - 10 = 55\ mph$$

When the final speed (after all reductions are taken) to be associated with an incident is determined, the estimation of travel delay for each incident can be completed with the use of the proposed regression models (Equations 4.3 to 4.8). The savings are computed from the difference between travel delays for the “without” and “with” incident cases. An overview of this procedure is provided in Figure 5.1.

Figure 4.1 Travel delay estimation procedure

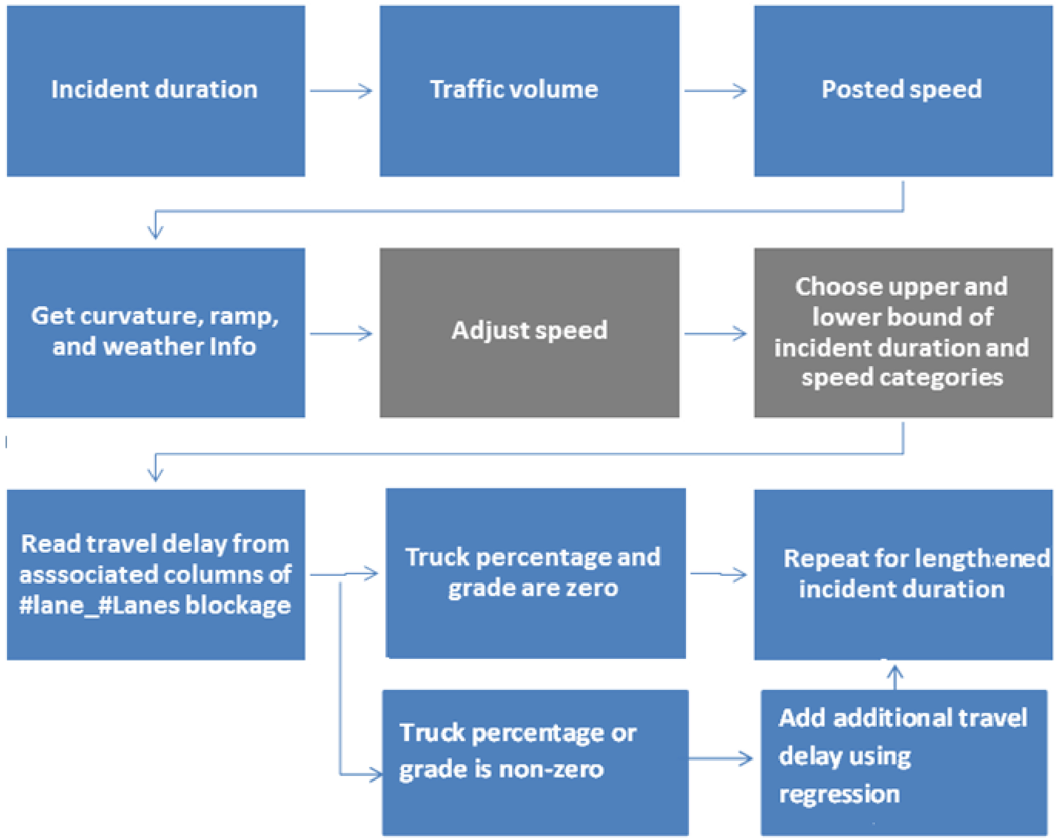

For incidents for which particular incident duration, traffic volume and speed is not one of the categories in above data set, travel delay is obtained by assuming linear changes in between upper and lower bound categories. If category of incident duration i, TD_i denotes travel delay of incident duration i and TD_l and TD_u stand for travel delay of lower and upper bound of the incident duration i category, respectively, Equation 5.1(a) can be used to obtain travel delay of desired incident duration.

$$TD_i = TD_l + \frac{TD_i - TD_l}{TD_u - TD_l}(TD_u - TD_l) \qquad \textbf{Eq. 4.1(a)}$$

Traffic volume is assumed to be rounded to nearest volume category. A similar linear estimation approach to incident duration was used to interpolate when given speeds outside the tested categories. Likewise, a similar equation to Equation 5.1(a) but for speed can be used as follows.

$$SP_i = SP_l + \frac{SP_i - SP_l}{SP_u - SP_l}(SP_u - SP_l)$$ **Eq. 4.2(b)**

Where in incident i, SP_i denotes speed of vehicles prior to incident i and SP_l and SP_u stand for the speed of lower and upper bound of the incident i, respectively, if neither incident duration nor speed associated with an incident were in the provided data set, by linear assumptions on speed and using Equation 5.1(b) for SP_u and SP_l, the travel delay associated with upper and lower bound on of incident duration, ID_u and ID_l, are computed and then Equation 5.1 is applied to compute the final travel delay. This process is shown in Figure 5.2.

Figure 4.2 Subcategory linear interpolation

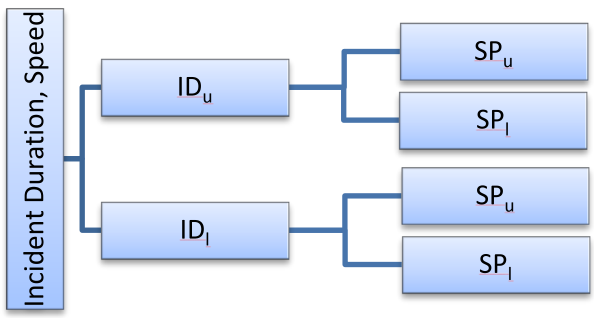

4.1.2 Saving in Fuel Consumption and Emissions

A similar with/without incident approach is taken to estimate fuel consumption savings associated with an incident scenario. Fuel consumption corresponding to each incident scenario is obtained directly from equations described in Tables 4.15 to 4.22. Emissions are calculated directly from equations 3.6-3.8 based on the fuel consumption estimates.

4.1.3 Saving in Secondary Incidents

The probability of occurrence of a secondary incident grows with an increase in the primary incident duration (Section 3.5). To estimate the number of prevented secondary incidents, the number of secondary incidents when SSP is not operating is assumed to be linearly correlated with the travel delay ratio of without and with incidents to which SSP responded in a period of time. This approach to estimating secondary incident savings is discussed in (Chou and Miller-Hooks, 2008). It supposes that total travel delay is a reasonable surrogate for impact area size of primary incidents in which incidents classifies as secondary. This relationship is shown in Equation 5.2.

$$\boldsymbol{N^{wo} = \frac{N^{w} * TD^{wo}}{TD^{w}},} \qquad \textbf{Eq. 4.2}$$

where

N^{wo} : Number of secondary incidents for extended incident duration case (without case),

N^{w}: Number of secondary incidents in base case (with case),

TD^{wo}: Travel delay for the extended case,

TD^{w}: Travel delay for the base case.

As discussed in Chapter 3, for this analysis, the number of secondary incidents (N^{w}) as a fraction of primary incidents must be known regardless of the chosen secondary incident classification method. TD^{wo} and TD^{w} are estimated as explained in Section 5.1.1.

Another method to calculate the benefits of SSP program in terms of prevented secondary incident is to consider the incident duration reduction contribution to likelihood of secondary incident occurrence as explained in Section 3.5. As mentioned in Section 3.5 Karlaftis et al. (1998) estimated the clearance time coefficient for winter and all other seasons as 0.017 and 0.031, respectively. Assuming that SSP vehicles reduce the incident duration by 20 minutes, the increase in the likelihood of a secondary incident occurrence would be 14.05% in winters and 18.59% in all other seasons.

$$odds\ ratio_{winter} \ = \ e^{20.0.017} \ = 1.405$$

$$odds\ ratio_{Other} \ = \ e^{20.0.031} \ = 1.859$$

The average increase in likelihood of occurrence of a secondary incident is %17.46. Using this method, the potential secondary incidents reduced due to SSP program can be computed as shown in Equation 5.3.

$$N = \left(\frac{3.e^{ID.0.031} + 1.e^{ID.0.017}}{4}\right) \times N^{p}, \qquad \textbf{Eq.5.3}$$

where

N: Number of reduced potential secondary incidents,

ID: Incident duration reduction due to SSP program operation in minutes,

N^p*:* Total number of incidents to which SSP vehicles responded.

4.2 Total Benefit Calculation

4.2.1 Monetary Values

To isolate a single unit for evaluation of a SSP program, congestion related travel delay (vehicle-hours), fuel consumption (gallons), and number of secondary incidents prevented are converted into their monetary equivalents. Monetary equivalents in the SSP-BC Tool proposed herein were provided by the American Transportation Research Institute (ATRI). Table 5.1 contains a list of the monetary equivalent variables, the variable's corresponding output, a description for each variable and data source. Four individual tables containing this information support the B/C ratio computation within the tool. They are also designed to be updatable.

Table 4.1 Summary of monetary equivalents (ATRI)

Variable	Corresponding Output	Description	Source
Average gasoline prices (Table B.1)	Gallons of fuel saved	Used to monetize the wasted fuel that would result from increased congestion if SSP did not exist NOTE: fuel is already factored into the Hourly Truck Cost, and the monetization of wasted fuel should only be performed on the passenger vehicle share	U.S. Energy Information Administration, Gasoline and Diesel Fuel Update; updated 5:00 p.m. every Monday; http://www.eia.doe.gov/oog/info/gdu/gasdiesel.asp
Average labor costs (Table B.2, B.3)	Hours of delay prevented	Used to monetize lost productivity of passenger vehicles resulting from increased congestion if SSP did not exist	U.S. Department of Labor, Bureau of Labor Statistics; State Occupational Employment and Wage Estimates; http://www.bls.gov/oes/current/oessrcst.htm
Commercial vehicle costs per hour	Hours of delay prevented; Gallons of fuel saved	Used to monetize lost productivity of commercial vehicles resulting from increased congestion if SSP did not exist.	An Analysis of the Operational Costs of Trucking: A 2011 Update; ATRI; http://www.atri-online.org/research/results/Op_Costs_2011_Update_one_page_summary.pdf Based on actual operational cost data collected from motor carriers across the country, representing a cross-Section of industry sectors.
Secondary incident cost	Number of secondary incidents averted	Represents only the cost of property damage. Used to monetize the cost of additional secondary incidents that would result from increased congestion if SSP did not exist.	The Economic Impact of Motor Vehicle Crashes: 2000. NHTSA.

While some previously developed B/C ratio estimates made for SSP programs have included monetized emissions equivalents in the savings computation, a review of the literature indicates that the available monetary equivalents are based largely on soft, intangible costs, as opposed to other more tangible costs (e.g. price of a gallon of fuel). Thus, tons of emissions saved are reported separately and are not included in the B/C ratio computed in the SSP-BC Tool.

Average hourly wages are used herein to convert savings in travel delay to a monetary equivalent. Wage values are available at metropolitan-levels and as a state average (Table B.3). Additionally, data containing the share of commercial VMT compared to total VMT by state were used for truck composition estimate for each state (Table B.4). This data is necessary to distinguish between the benefits derived from savings in travel delay due to passenger vehicles and commercial vehicles. Average operational cost of trucking for 2011 is obtained to be $59.61.

The B/C ratio is highly sensitive to the cost of secondary incidents. In this study, cost represents “property only damage” incidents and for 2011 it is assumed to be $4,736. Other costs associated with higher severity incidents and congestion due to secondary incidents were not considered.

4.2.2 Computing Total Benefit

To compute the total savings in travel delay, fuel consumption, emissions, and secondary incidents resulting from a SSP program in a segment over a period of time, information pertaining to the incidents arising along the studied roadway segment during the study period is needed. Specifically, the distribution of incidents with respect to lane blockage must be known (or approximated). Assuming any two incidents are independent, TS^j, the total savings of type *j*, where *j={total travel delay, fuel consumption, emission}* for every incident *i* arising during a period of time over a road segment as described in Equation 5.3 can be computed. When using this method, it is necessary to assume that the impact of an individual incident has no influence on other incidents on the road.

Furthermore, as described in Section 5.1.1, the speed of the incident scenario and so the savings in travel delay and fuel consumption is related to geometry characteristics of the study segment and weather condition in the time of the incident. The geometry characteristics are similar for all incidents in a study segment. However, the weather condition might vary incident by incident in a period of time. One incident under each weather conditions (Section 3.2.5) would have different final speed. Therefore, having the probability of each weather type, P_k, saving of one incident can be estimated as exhibited in equation 5.4.

$$\boldsymbol{TS^j = \sum_i \sum_k S^j_{i,k}\, P_k} \qquad \textbf{Eq. 5.5}$$

where

TS^j = Total saving j,

j = =Type of saving {Total travel delay, fuel consumption, emission pollutants},

i = Individual incidents,

k= Weather conditions {Clear, light rain, heavy rain, low visibility, snow, fog, icy

S_i^j = Saving type j in incident i of weather condition k.

Given monetary conversion rates for travel delay, fuel consumption, and secondary incidents, total program benefit can be computed. With these concepts, and assuming that benefits are uniformly distributed over length, the total benefit of the SSP program over the study period and roadway segment can be computed as in Equation 5.4.

$$\boldsymbol{B = \frac{\sum_{J=1,2} ME^j S^j}{10} * L + ME^j TS^j}, \qquad \textbf{Eq. 5.6}$$

where

B= Total benefit of a SSP program,

j = Total travel delay (1), Fuel consumption (2), Secondary incidents (3),

TS^j = Total savings of type j,

ME^j= Monetary equivalent of saving j,

L= the length of the study segment.

4.3 Cost Calculation

The total cost of a SSP program, *TC*, is a function of the number of roving SSP trucks along the study segment, hourly operating cost per truck, number of working hours, number of workdays in a year, fuel cost of each vehicle, cost of giveaway fuel to the vehicles that ran out of gas, and other costs such as vehicle maintenance cost as expressed by Equation 5.4. Moreover, for some SSP programs, most often the total annual cost of the whole SSP program is available and not the cost associated with the study segment. The total annual cost can be computed from Equation 5.4.

$$\boldsymbol{TAC = c \times n \times hr \times day + fuel + other,} \qquad \textbf{Eq. 4.3}$$

where

TC : Total annual cost for operating the SSP program in dollars,

c : Cost per truck-hour {hourly wage of driver, fuel cost of the vehicle},

n : Number of roving trucks,

hr : Number of working hours in each day,

day : Number of workdays in a year,

fuel: annual giveaway fuel cost.

The cost of many SSP programs can often be easily calculated, as many SSP programs are outsourced and the charges are provided contractually. The cost of the program by roadway segment may be less clear. Two general methodologies were considered herein for the computation of segment-based costs. First, given total program costs, costs associated with a given segment can be computed based on the proportion: number of the total incidents to which the SSP vehicles responded to those to which they responded arising only within the study segment. This computation is captured in Equation 5.8.

$$\boldsymbol{C_n = TAC \times (N_n/N_{tot}),} \qquad \textbf{Eq. 4.4}$$

where

C_n= Cost of operating the SSP program along study segment n,

TAC = Total annual cost of the SSP program,

N_n = Number of incidents along the study segment n to which the SSP program responded,

N_{tot}= Total number of incidents to which SSP program responded.

The second methodology is to compute cost associated with a given segment by the proportion of length of it to the total length of covered roads SSP vehicles covers. In this method, it is assumed that cost is uniformly distributed over length of the roads of the SSP service area. The first method is used in SSP-BC Tool.

Some SSP programs may operate a heterogeneous fleet of vehicles. Thus, those vehicles that are similar in response capability or with identical operational hours can be classified as falling within the same group. Total annual costs can be computed from costs computed for each category of vehicles.

4.4 The B/C ratio

The obtained benefit from Equation 5.5 and cost from Equation 5.7 are used to assess the segment-based B/C ratio for a given SSP program over the study period. The SSP-BC Tool provides multi-segment analysis. The B/C ratio of *n* segments is computed from the ratio of the sum of benefits to sum of costs for all segments as in Equation 5.6.

$$B/C_{tot} = \frac{\sum_n B_n}{\sum_n C_n}, \qquad \textbf{Eq. 4.5}$$

where

B/C_{tot} **=** B/C ratio of multiple segments,

B_n = Obtained benefit of segment n,

C_n= Obtained cost of segment n.

Recall that within the SSP-BC Tool, savings in emission pollutants are not translated to dollars and, thus, cannot be included in the B/C ratio. Emissions are given separately in the form of metric tons.

4.4.1 Additional Benefits

Additional savings that has not been quantified in this study are: improved safety not only in preventing secondary incidents, but in the improved feeling of security on the transportation system, congestion cost associated with the secondary incidents, improved freight transit system, environmental benefits, and benefits to other agencies like additional time available for troopers for more urgent tasks that the SSP programs cannot handle. A list of additional costs associated with incidents is:

Administrative costs: the cost (monetary and temporal) associated with investigating and documenting the primary, and any secondary, incidents. In the case of fatal incidents, costs increase exponentially. In addition, there are generally administrative costs associated with insurance claims.

Legal costs: Includes attorney fees and court costs associated with litigation resulting from primary and secondary incidents.

Rehabilitation costs: The cost of career retraining required as a result of disability caused by roadway incident. An additional cost in this category is, replacement employee costs. That is, employers often hire temporary help or compensate other staff by paying overtime to cover the position of an injured employee.

Disability/Retirement income: Should the employee suffer career-ending injury, the employer will have to make payments to fund the employee's disability pension.

Productivity reduction: this is the cost associated with lost wages and benefits over the victim's remaining lifespan.

Numerous additional sources of benefits in cost reduction have not been included in the computation of program benefits within the proposed SSP-BC tool. The exclusion of the many additional benefits from the benefit estimate used in the B/C ratio results in conservative B/C estimates.

CHAPTER 6. The Tool by Illustrative Example

The SSP-BC Tool interface was coded in Microsoft Visual Basic 2003. Data developed based on Chapter 4 is in microsoft Access (2010) format. Tables of monetary values for travel delay and fuel consumtion, and share of trucks in traffic volume were designed to be updated by the user.

The SSP-BC Tool is explained in Section 6.1. 693 incidents to which the SSP program in New York (H.E.L.P) responded over a 6-month period in 2006 is used as a case study for the tool and its outputs. A comparison between previously obtained B/C ratio by Chou and Miller-Hooks (2008) and use of the propesed generic SSP-BC Tool is made in the Section 6.2.

5.1 The SSP-BC Tool

The I-287 segment studied herein is approximately 10 miles in length, beginning at the junction with I-95 and continuing west to the Tappan Zee Bridge in New York. This segment is referred to as Beat 8-2 of the H.E.L.P. program. Incidents arising on this roadwaysegment will be handled by a H.E.L.P. vehicle driver, a trooper from Unit T or both. During the study period, 1,303 incidents arose along the study segment of I-287. 693 of these 1,303 incidents received service from the H.E.L.P. program during the H.E.L.P. hours of operation.

Figure 6.1 shows the main window of the SSP-BC tool including the information on SSP program level and number of segments. Total annual program cost is required here. In addition, a detailed cost list is provided in the “Cost” window (Figure 6.2) in which annual SSP program cost will be calculated automatically. The figure shows the cost information of the H.E.L.P program. Chou and Miller-Hooks (2008) used costs of $40 and $50 per truck-hour, two roving trucks operated within the study roadway segment with an eight-hour workday, 126 workdays within the 6 month study period (21 days/month). The annual cost using $40/truck-hour was $161,280. Up to 5 different categories of cost groups as explained in Section 5.3 are availble for different type of service vehicles or operational hours that might exist within a SSP program.

The next input is for finding the associated cost to the segment, total number of incidents arose in the segment in one year. If the annual cost was the estimated cost of total SSP program, not the program cost associated with the study segment like this example, the number of incidents to which the SSP program responded in a year has to be used as input here (Section 5.3).

Segments in a study area must be homogenouse in terms of geometry, weather and traffic volumes as explained in Chapter 3. The SSP-BC Tool is capable of analysing up to 30 segments at a time. This example has only 1 segment.

Figure 5.1 Main window

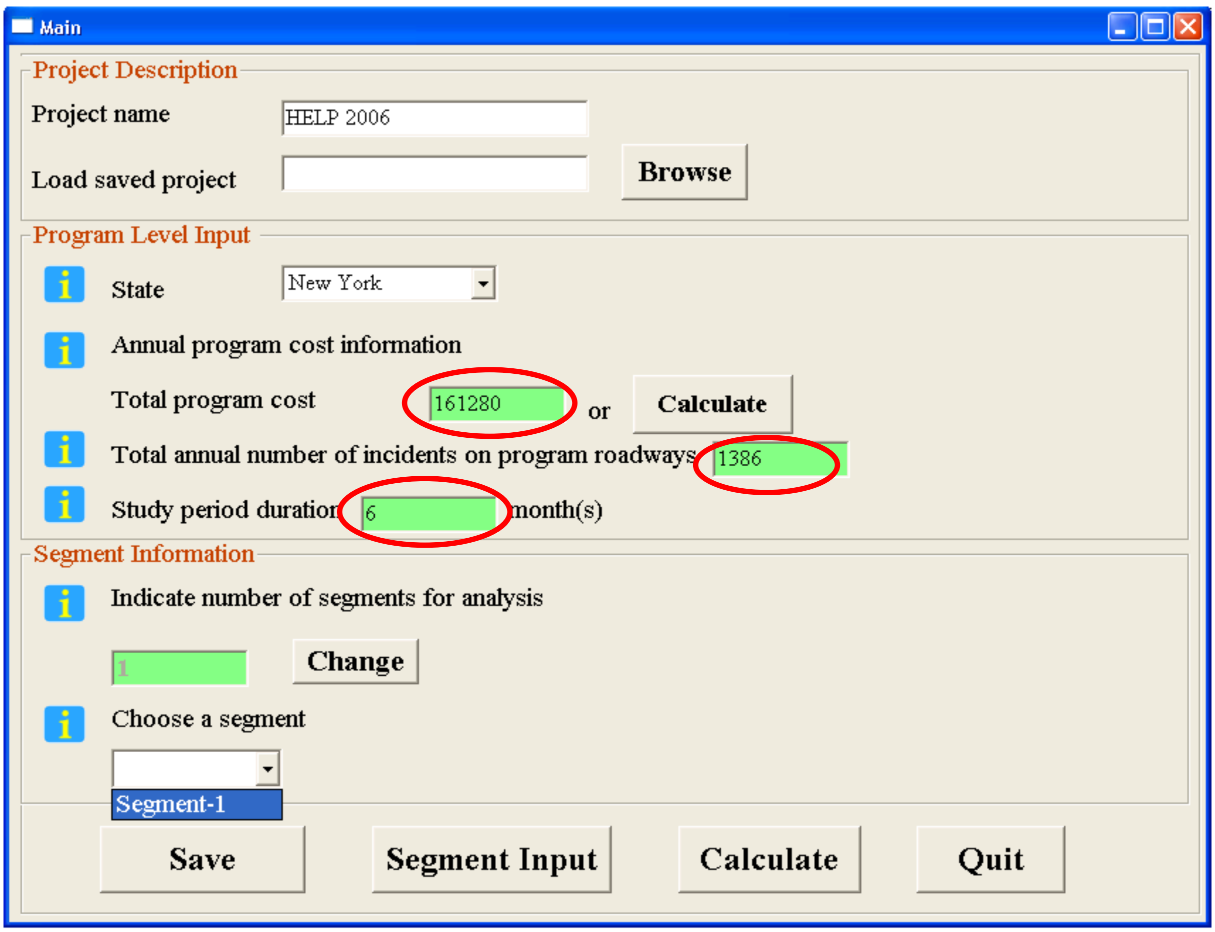

Figure 5.2 Program cost detail

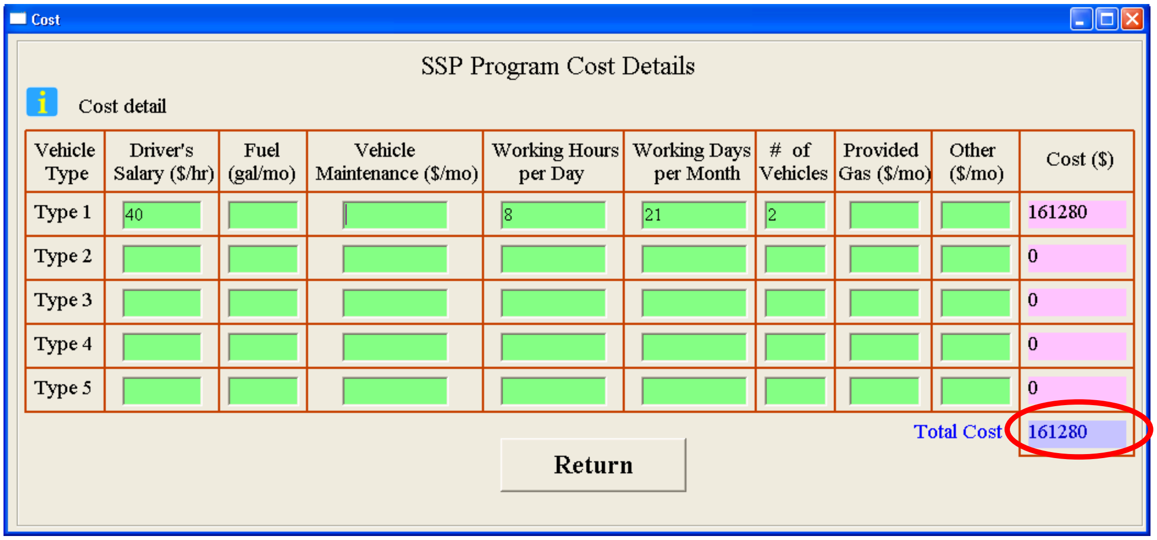

For each segment information pertaining to hours of operation weather, traffic conditions, SSP program average response time, roadway geometry, and incident distribution and duration must be entered. It is assumed that SSP programs operats within a single state. Regional data at the metropolitan level are applied in setting the monetary conversion rate. Average monetary values for the state are used when the region is set to "others".

Figure 5.3 Basic data in segment level

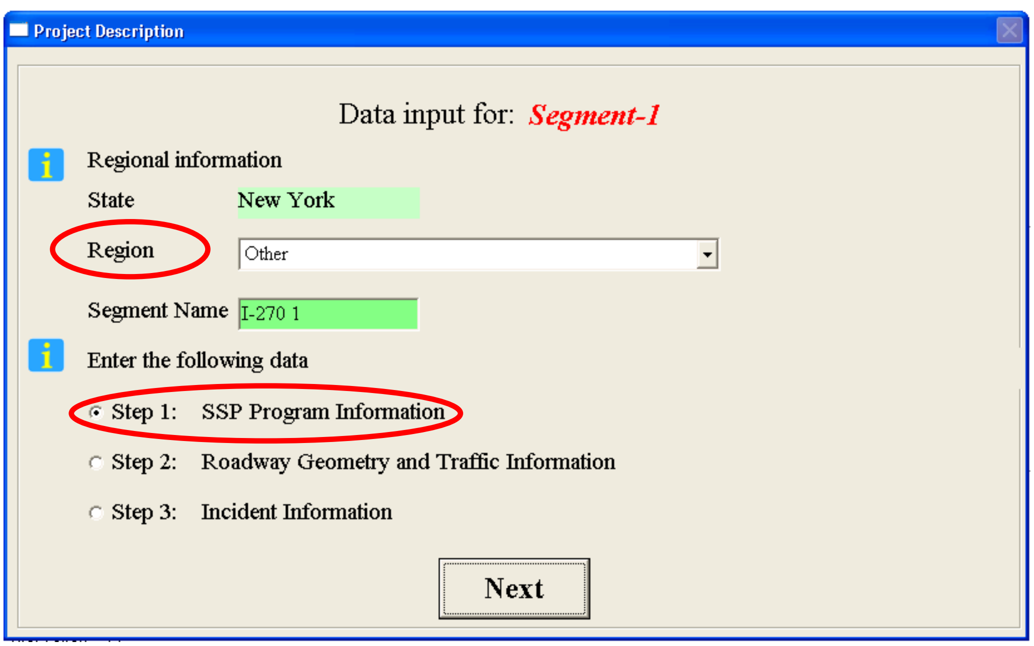

The program information window (Figure 6.4) contains details on operational hours and perfomance of the SSP program. Hour of operation are divided to four time categories. The user must to be consistant with her/his definition of each time category for analysis of each segment. For example, if she/he selects 7 to 10 AM as her/his AM peak hour, traffic and incident information for these hours must be used for the AM peak in following steps.

A key impact to the SSP-BC Tool is the average incident duration reduction offered by the program. Different approches for estimating this time reduction are discussed in detail in Chapter 2. In addition, the FSPE tool (Describe in Section 2.3) computes the arrival time of the SSP vehicles and ,thus, incidnet response time.

The savings in incident duration greatly depend on the severity of the incident or, as employed herein, on the number of lanes blocked as a result of incident occurence. The SSP-BC Tool assigns incident duration savings in each lane blockage category to the duration of the incidents in that category. The average value, as in the example, can also be used where sufficent data is not availble. Chou and Miller-Hooks (2008) founded an average savings of approximately 20 minutes in incident duration for incidents involving a collision and 19 minutes for incidents involving a disabled vehicle for the study area as a result of the presence of the H.E.L.P. program. The average incident duration savings of 20 minutes is used for the example solved here.

Figure 5.4 Program information window

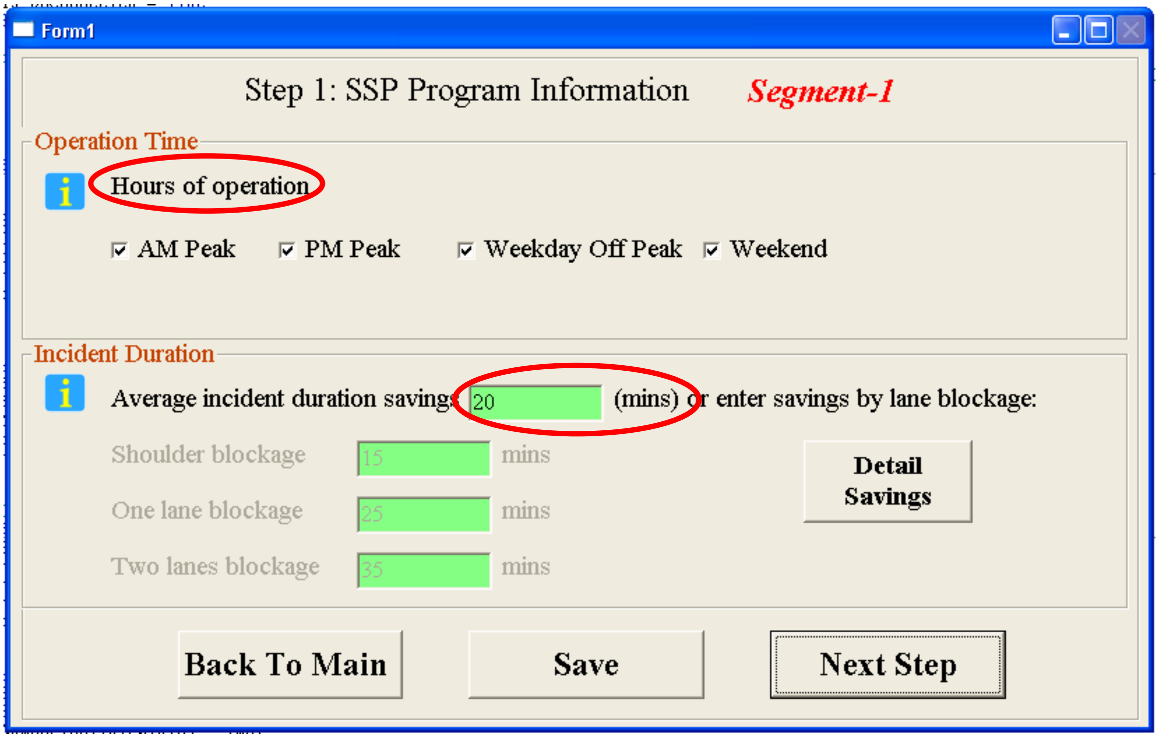

The SSP-BC Tool provides default values for incident duration and related savings to the due to SSP program based on previous studies in the area. The default values associated with roadway geometry and traffic information (Figure 6.5) are based on the numerical experiments used as described in Chapters 3 and 4 and summarized in Table 6.1.

Table 5.1 Geometry and traffic default values

Input	Default value
Segment length	10
Number of traffic lanes by direction	3
General terrain	Level
Horizontal curvature	straight
Number of ramps in segment	0
Posted main-lane speed limit	70
Percentages of trucks	3
Weather	clear

The H.E.L.P study segment length is 10 miles and number of lanes is 4. Default values of general terrain and road curvature were used. Total ramp density for the H.E.L.P study segment is 1.4 ramps/mile with14 on/off ramps within the segment.

Traffic volume data for the study roadway segment was employed for the same period, but in the following year. Average weekday and weekend traffic volumes by month were matched to the incidents by their date and time information. For each of the operational hour classes of the SSP program, one traffic volume was assumed in this example. Incidents for which prevailing traffic volume was between 0 and 600 vplph were categorized for the weekend, 600 to 1000 vplph for weekday off peak, 1000 to 1400 vplph as weekday PM peak, and 1400 to 2200 as weekday AM peak. The average for the prevailing incident traffic volumes in each category was set within a time class. For example for weekday PM peak, the average of 1200 vplph was used. The percentage of trucks set to 7.8% (Table B.4) for all operational hour classes. Weather was assumed clear for all incidents. Note that this classification of volume was done to fit the available data to the SSP-BC Tool. The operational hour of the H.E.L.P. program is weekday peak periods.

Figure 5.5 Roadway geometry and traffic information

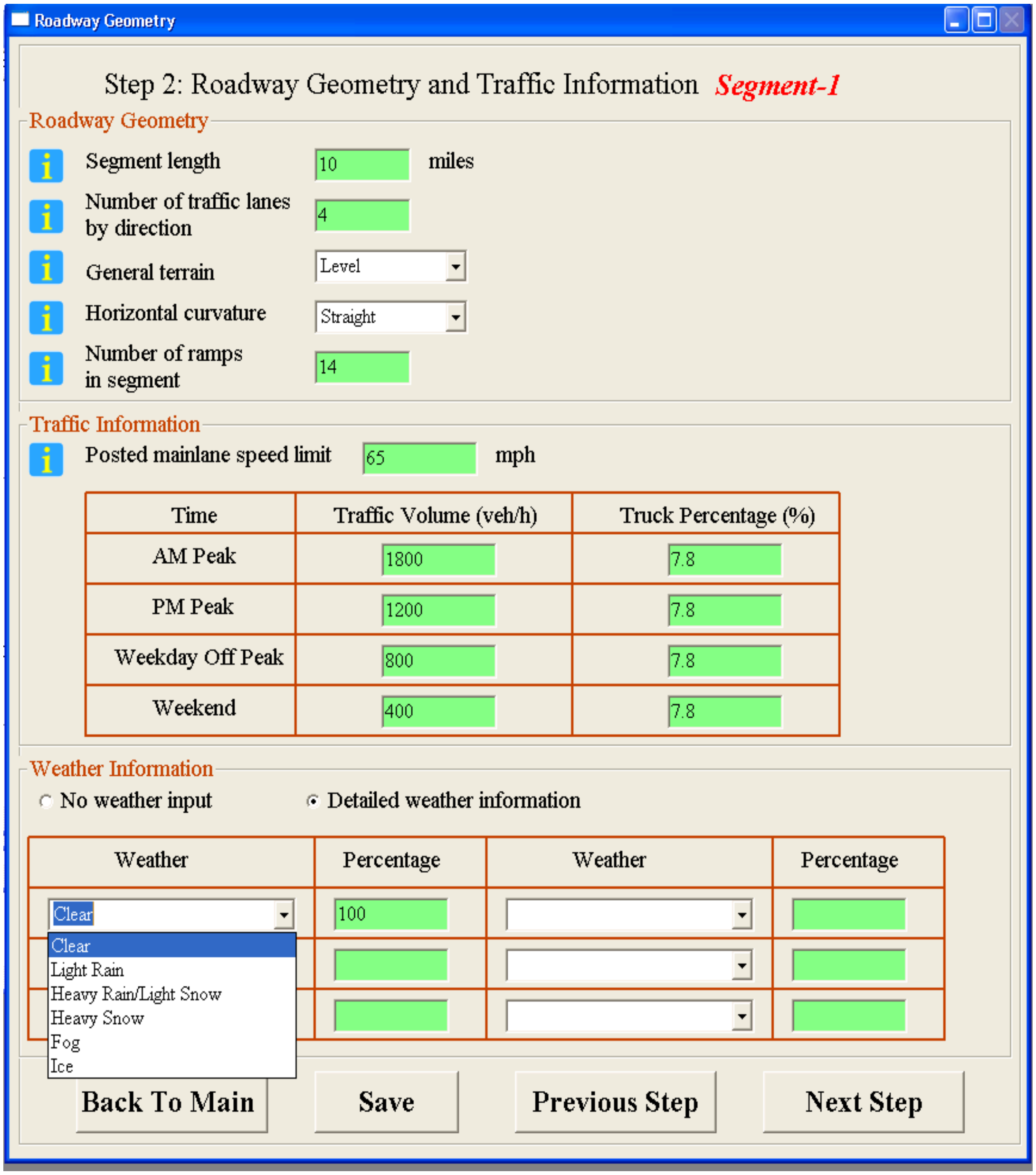

Incident information scenario is entered next. Average incident durations and number of incidents are required by lane blockage as shown in Figure 6.6. They are assumed to be identical for all operational hour classes for this example. Savings in prevented secondary incidents in the tool is calculated using the first method discussed in Section 5.1.3. The input is the percentage of secondary incidents out of primary incidents for the study segment.

Figure 5.6 Incident information window

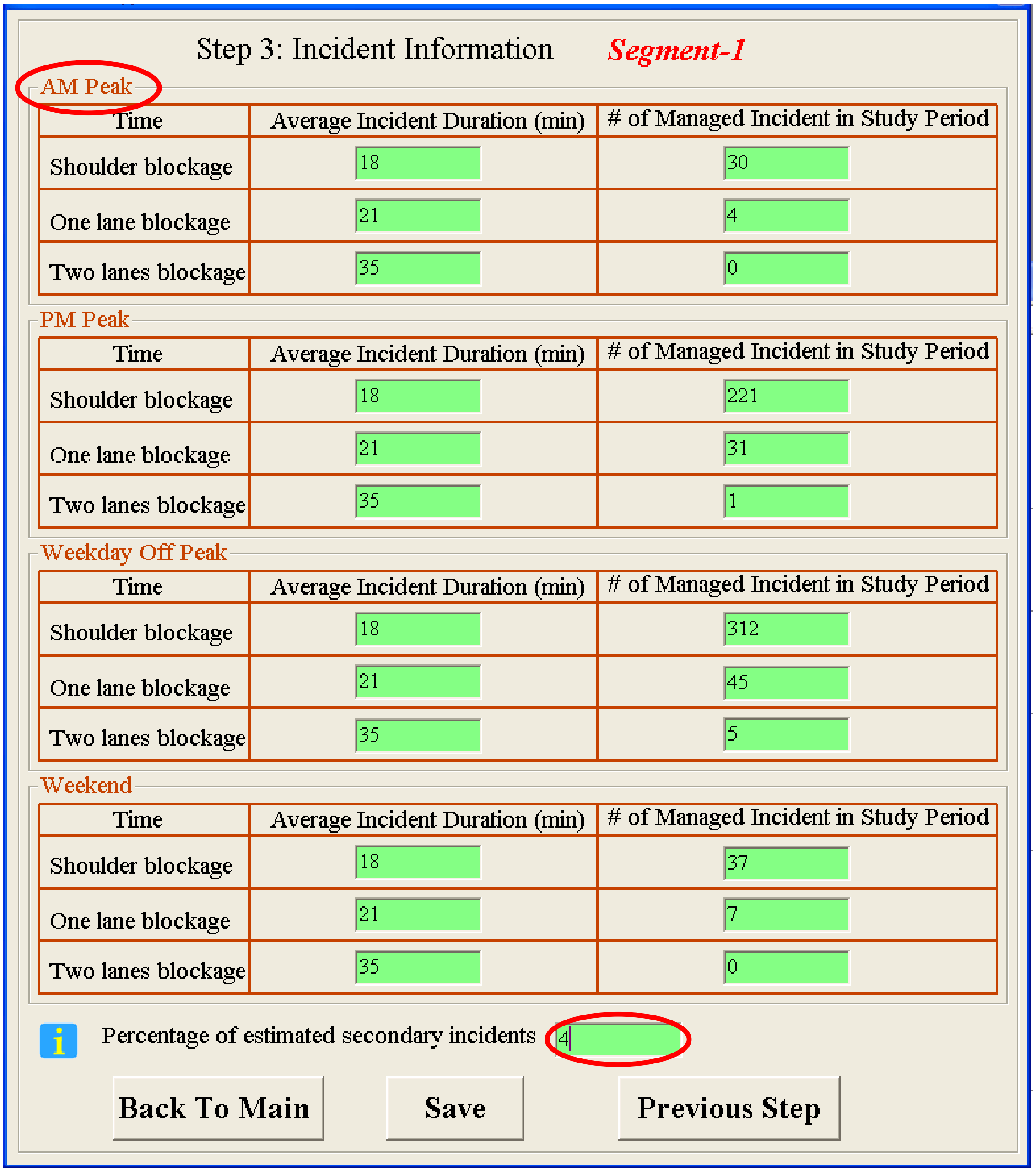

Since the example has only one segment, the B/C ratio can be ontained. The output window is shown in Figure 6.7. Users can choose one or more segments for the B/C ratio analysis. The outputs of the tool as described in MOEs, Section 3.1, are savings in travel delay in vehicle-hours, fuel of passenger cars and light-duty in gallons, number of prevented secondary incidents and emission pollutants in metric tones. The users specifies which MOEs (of travel delay, fuel consumption and secondary incidnes) to include in the

B/C ratio.The total benefit of the chosen segment is then calculated as described in Section 5.2.

For this example, 2006 monetary values are employed to compute the benefits for consistancy with the availble cost information of the program (Table 6.2).

Table 5.2 New York 2006 monetary values

State	Travel delay $/hr	Fuel (gas) $/gallon)	Carbon Monoxide (CO) $/ton	Hydrocarbons (HC) $/ton	Nitrogen Oxide(NO) $/ton
New York	15	2	6,360	6,700	12,875

Figure 5.7 Output window

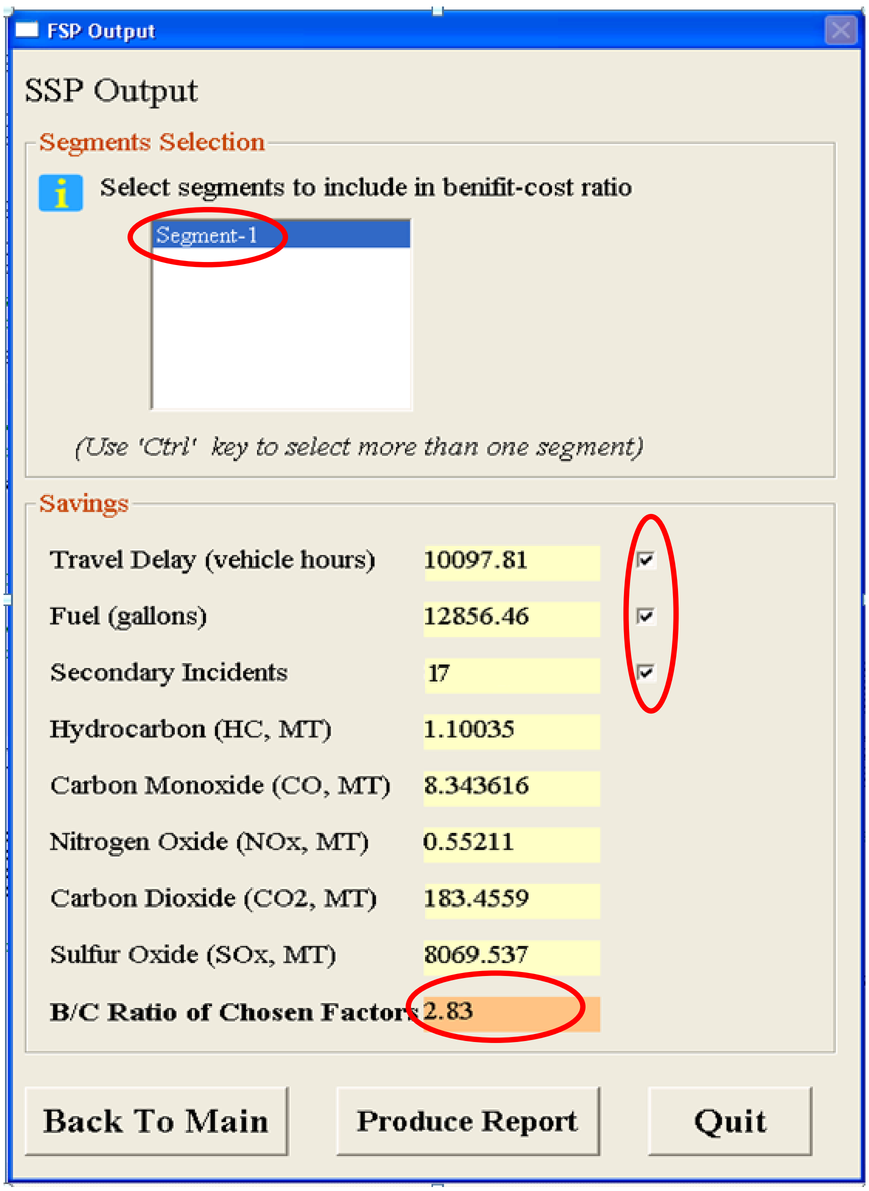

The B/C ratio of the H.E.L.P program was estimated to be 2.83 plus additional benefits derived from emisions savings. Adding emissions to the benefits increased the B/C ratio to 3.08. Chou and Miller-Hooks (2008) estimated the B/C ratio of the H.E.L.P program 2.68. In both B/C ratio estimates that included emissions, only benefits from savings in CO, HC, and NO were included. Monetary conversion rates used are given in Table 6.2. They used technique in which they replicated incidents in CORSIM and computed the travel delay using the same with/without approach (Section 5.1). They used conversion factors for fuel consumption and emissions from travel delay. In simulating incidents they did not includethe geometry characteristics of the segment, such as ramps. Table 6.3 contains obtained savings Chou and Miller-Hooks found for 20 minutes incident duration savings due to the operation of H.E.L.P. program.

Table 5.3 H.E.L.P result comparison

Type of saving	Chou et al. (2008)	SSP-BC
Travel delay (veh-hr)	12,182	10,097
Fuel consumption (gal)	1,451	12,856
Secondary incidents (#)	9	17
CO (ton)	1.79	8.34
HC (ton)	0.16	1.1
NO (ton)	0.08	0.55

Travel delay estimated by the SSP-BC Tool is slightly less than what Chou and Miller-Hooks obtained. On the other hand, Chou and Miller-Hooks estimated fewere saved secondary.

A comparison between VISSIM and CORSIM was completed to better understand difference in travel delay estimates. The study segment was simulated in both software products. Travel delay was gathered for different traffic volumes as plotted in Figure 6.8. It was found that CORSIM estimates higher travel delays compare to VISSIM when the simulated segment reaches its capacity. It seems that in CORSIM, the capacity of the roadway segment with defult parameters applied in Chou and Miller-Hooks, worked is lower compare to VISSIM using described calibrated parameters. Relate discussion can be found in Section 4.1.2. Where earlier studies note that VISSIM provides a better model of traffic than CORSIM.

Figure 5.8 CORSIM vs. VISSIM

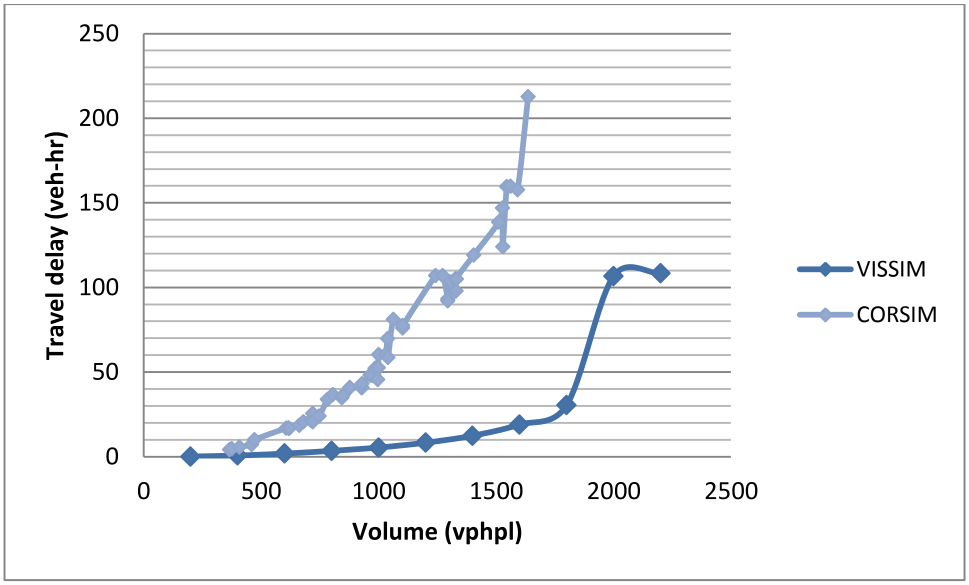

. The B/C ratio of the H.E.L.P program with 2011 monetary values (Appendix B),as current SSP-BC Tool monetary equivalent data, and asuming the truck-hour cost of $60 compare to $40 in 2006, total cost of the program would be $120,960, is 2.23.

CHAPTER 7. Conclusions and Limitations

The SSP-BC Tool was developed to fill the need for a standardized B/C ratio estimation methodology with wide applicability and substantiated and needed updatable monetary conversion rates. The tool was designed to support B/C ratio estimation for roadways with existing programs, but can also be used to test numerous what-if scenarios, including the introduction of a new program or the impact of improvements in service response times. A quicker and less data-intensive approach was developed so that it can be readily and widely utilized by all states around the US.

The SSP-BC Tool accounts for a wide array of traffic, environmental and program characteristics that influence benefit and cost estimates. The Factors, such as incident duration, traffic volume and composition, ramp density, horizontal and vertical alignments, and weather conditions that have been identified as important to travel delay fuel consumption and emissions estimation were included in this tool. Moreover, the per-second vehicle velocity and acceleration values were employed in the computation of fuel consumption and emissions.

Numerous experimental runs were completed and seven multiple-regression models for estimating travel delay and fuel consumption were developed. For experimental runs, the techniques to simulate different geometry, traffic, and weather characteristics were suggested and tested. Additional delay caused by two regression parameters, truck percentage and segment gradient, can be applied to any travel delay estimate in which traffic composition or gradient is not included.

6.1 Limitations

The SSP-BC Tool extensions are limited by a maximum incident duration of ninety minutes, that only up to two lanes can be blocked due to an incident and no consideration for roadway closure, and that any given segment has a maximum of six lanes. The SSP-BC Tool can be extended to include of longer duration or greater severity, and roadway with more than six lanes.

To complete a nationwide study, it would be ideal to have all input data associated with the entire national roadway system. As this is highly impractical, a statistical approach might be used in which a random sample of the required traffic and environmental data is taken. With this sample, a general estimation model can be created and calibrated based on statistical approaches. Unfortunately, this method is not an easy and cost effective method. In addition, obtaining one general estimation model for all states would not be reliable considering the fact that statistical models developed for the entirety of the nation will likely poorly fit the data of specific regions.

6.2 Contributions

In addition to the development of a nationwide tool for SSP program B/C ratio estimation, the contributions of this work include the identification of the significant factors affecting SSP program benefits, techniques for simulating these factors and development of regression models to estimate travel delay, fuel consumption and emissions given traffic, roadway geometry, program characteristics and weather conditions. For travel delay estimation, the developed enhanced regression methodology takes a hybrid approach to multiple-regression model construction. This approach combines parameters obtained through regression analysis for truck percentage and roadway grade, which were found to be independent of all other factors, with results from simulation runs. The simulation results and estimates from the regression models are developed into tables employed within the tool's database. For fuel consumption estimation, a multiple regression model is developed that is used directly within the tool. These developed regression models can be used directly where applicable.

APPENDIX A: Fuel Consumption Computation Tables

Table A.1 Calculation of Road-load coefficients

Vehicle Category	Source Mass (metric tons)	A (KW/mps)	B (KW/mps^2)	C (MW/mps^3)
LDV (passenger cars)	1.4788	0.156461	0.00200193	0.000492646
LDT (trucks, SUVs, etc)	1.86686	0.22112	0.00283757	0.000698282
LHD<=14K	7.64159	0.561933	0	0.00160302
LHD<=19.5K	6.25047	0.498699	0	0.00147383

Table A.2 Emission factors

Vehicle	Fuel Economy (mile/gal)[1]	Engine Displacement Volume, V (L)[3]	Emission Factor (EF in g/mi) for gasoline[2]			
			HC	CO	NOx	CO_2
LDV	22.1	1.3-3.1	2.8	20.9	1.39	451
LDT	17.6	2.5-5.3	3.51	27.7	1.81	637

Table A.3 Fuel properties

Fuel	Base Fuel	HV (KJ/g)[a]	ρ^b (g/gal)	SC_{Fuel} (ppm)
Gasoline	(Base fuel)	43.448	2834.95	80
Diesel	(Base fuel)	42.791	3210.98	500

Table A7.4 Transmission parameters for engine speed calculation (Source: PERE, 2005; EPA420-P-05-001)

LDV & LDT		
S = 35.6		
Speed (mph)	Gear	g/gtop
0-18	1	4.04
18-25	2	2.22
25-40	3	1.44
40-50	4	1
50+	5	0.9

APPENDIX B: Monetary Equivalents

Table B.1 Average gasoline prices

Area name	abb	Fuel price($)	Area name	abb	Fuel price ($)
Alabama	AL	3.163538462	Montana	MT	3.198192
Alaska	AK	3.514961538	Nebraska	NE	3.298904
Arizona	AZ	3.514961538	Nevada	NV	3.514962
Arkansas	AR	3.163538462	New Hampshire	NH	3.379346
California	CA	3.586	New Jersey	NJ	3.339615
Colorado	CO	3.163538462	New Mexico	NM	3.163538
Connecticut	CT	3.379346154	New York	NY	3.500981
Delaware	DE	3.339615385	North Carolina	NC	3.242577
District of Columbia	DC	3.339615385	North Dakota	ND	3.298904
Florida	FL	3.267	Ohio	OH	3.282615
Georgia	GA	3.242576923	Oklahoma	OK	3.298904
Hawaii	HI	3.514961538	Oregon	OR	3.514962
Idaho	ID	3.198192308	Pennsylvania	PA	3.339615
Illinois	IL	3.298903846	Rhode Island	RI	3.379346
Indiana	IN	3.298903846	South Carolina	SC	3.242577
Iowa	IA	3.298903846	South Dakota	SD	3.298904
Kansas	KS	3.298903846	Tennessee	TN	3.298904
Kentucky	KY	3.298903846	Texas	TX	3.167385
Louisiana	LA	3.163538462	Utah	UT	3.198192
Maine	ME	3.379346154	Vermont	VT	3.379346
Maryland	MD	3.339615385	Virginia	VA	3.242577
Massachusetts	MA	3.307923077	Washington	WA	3.492635
Michigan	MI	3.298903846	West Virginia	WV	3.242577
Minnesota	MN	3.303057692	Wisconsin	WI	3.298904
Mississippi	MS	3.163538462	Wyoming	WY	3.198192
Missouri	MO	3.298903846			

Table B.2 Average labor cost by state

Area name	Average wage ($/hr)	Area name	Average wage ($/hr)
Alabama	21.5	Montana	17.34
Alaska	24.21	Nebraska	18.42
Arizona	20.38	Nevada	19.82
Arkansas	17.05	New Hampshire	21.37
California	24.39	New Jersey	24.39
Colorado	22.48	New Mexico	19.26
Connecticut	24.96	New York	24.86
Delaware	22.53	North Carolina	19.47
District of Columbia	35.31	North Dakota	17.81
Florida	19.36	Ohio	19.66
Georgia	20.32	Oklahoma	17.76
Guam	15.02	Oregon	20.94
Hawaii	21.03	Pennsylvania	20.7
Idaho	18.56	Puerto Rico	12.92
Illinois	22.33	Rhode Island	22.08
Indiana	18.76	South Carolina	18.23
Iowa	18.14	South Dakota	16.53
Kansas	18.89	Tennessee	18.43
Kentucky	18.25	Texas	20.3
Louisiana	18.26	Utah	19.29
Maine	18.98	Vermont	20.21
Maryland	24.46	Virgin Islands	17.85
Massachusetts	25.82	Virginia	23

Michigan	20.81	Washington	23.53
Minnesota	21.86	West Virginia	17.01
Mississippi	16.31	Wisconsin	19.7
Missouri	19.13	Wyoming	19.96

Table B.3 Average wage by area

Area	Wage ($/hr)	Area	Wage ($/hr)
Anniston-Oxford AL	16.92	Duluth MN-WI	18.81
Auburn-Opelika AL	17.92	Fargo ND-MN	18.14
Birmingham-Hoover AL	19.82	Grand Forks ND-MN	17.81
Columbus GA-AL	17.83	La Crosse WI-MN	19.09
Decatur AL	17.72	Mankato-North Mankato MN	18.06
Dothan AL	16.59	Minneapolis-St. Paul-Bloomington MN-WI	23.63
Florence-Muscle Shoals AL	16.45	Rochester MN	23.43
Gadsden AL	15.93	St. Cloud MN	18.62
Huntsville AL	23.12	Northwest Minnesota nonmetropolitan area	17.28
Mobile AL	18.39	Northeast Minnesota nonmetropolitan area	17.2
Montgomery AL	18.43	Southwest Minnesota nonmetropolitan area	16.84
Tuscaloosa AL	18.26	Southeast Minnesota nonmetropolitan area	17.88
Northwest Alabama nonmetropolitan area	15.62	Gulfport-Biloxi MS	17.23
Northeast Alabama nonmetropolitan area	15.62	Hattiesburg MS	15.87
Southwest Alabama nonmetropolitan area	16.21	Jackson MS	17.7
Southeast Alabama nonmetropolitan area	16.73	Pascagoula MS	18.58
Anchorage AK	24.75	Northeast Mississippi nonmetropolitan area	15.78
Fairbanks AK	24.21	Northwest Mississippi nonmetropolitan area	14.8
Southeast Alaska nonmetropolitan area	22.33	Southeast Mississippi nonmetropolitan area	15.09
Railbelt / Southwest Alaska nonmetropolitan area	23.69	Southwest Mississippi nonmetropolitan area	15.97
Flagstaff AZ	18.89	Columbia MO	17.62
Lake Havasu City - Kingman AZ	16.97	Jefferson City MO	17.91
Phoenix-Mesa-Scottsdale AZ	20.89	Joplin MO	16.23
Prescott AZ	18.04	Springfield MO	17.02
Tucson AZ	20.27	Central Missouri nonmetropolitan area	15.51
Yuma AZ	16.4	North Missouri nonmetropolitan area	15.07

North Arizona nonmetropolitan area	16.99	Southeast Missouri nonmetropolitan area	14.67
Southeast Arizona nonmetropolitan area	19.48	Southwest Missouri nonmetropolitan area	14.67
Fayetteville-Springdale-Rogers AR-MO	18.7	Billings MT	18.06
Fort Smith AR-OK	16.09	Great Falls MT	16.62
Hot Springs AR	16.55	Missoula MT	17.5
Jonesboro AR	16	Eastern Montana nonmetropolitan area	16.43
Little Rock-North Little Rock-Conway AR	18.75	Central Montana nonmetropolitan area	16.36
Memphis TN-MS-AR	19.32	Southwestern Montana nonmetropolitan area	17.79
Pine Bluff AR	16.76	Western Montana nonmetropolitan area	16.66
Texarkana-Texarkana TX-AR	17.5	Lincoln NE	18.83
Central Arkansas nonmetropolitan area	15.21	Western Nebraska nonmetropolitan area	15.31
East Arkansas nonmetropolitan area	14.92	Central Nebraska nonmetropolitan area	15.96
South Arkansas nonmetropolitan area	15.17	Northeastern Nebraska nonmetropolitan area	15.86
West Arkansas nonmetropolitan area	14.33	Southeastern Nebraska nonmetropolitan area	16.01
Bakersfield CA	21.4	Carson City NV	21.85
Chico CA	19.54	Las Vegas-Paradise NV	19.59
El Centro CA	19.01	Reno-Sparks NV	20.52
Fresno CA	19.76	Western Central Nevada nonmetropolitan area	18.41
Hanford-Corcoran CA	20.71	Other Nevada nonmetropolitan area	20.7
Los Angeles-Long Beach-Glendale CA Metropolitan Division	24.16	Manchester NH	22.49
Los Angeles-Long Beach-Santa Ana CA	24.1	Northern New Hampshire nonmetropolitan area	16.73
Madera CA	20.78	Other New Hampshire nonmetropolitan area	19.85
Merced CA	18.79	Western New Hampshire nonmetropolitan area	21.76
Modesto CA	19.96	Southwestern New Hampshire nonmetropolitan area	20.11
Napa CA	23.86	Allentown-Bethlehem-Easton PA-NJ	20.38
Oakland-Fremont-Hayward CA Metropolitan Division	27.09	Atlantic City-Hammonton NJ	20.02
Oxnard-Thousand Oaks-Ventura CA	23.03	Camden NJ Metropolitan Division	22.26
Redding CA	19.88	Edison-New Brunswick NJ Metropolitan Division	24.57
Riverside-San Bernardino-Ontario CA	20.64	Newark-Union NJ-PA Metropolitan Division	25.74
Sacramento--Arden-Arcade--Roseville CA	24.08	New York-White Plains-Wayne NY-NJ Metropolitan Division	27.49
Salinas CA	20.61	Ocean City NJ	18.64
San Diego-Carlsbad-San Marcos CA	24.14	Trenton-Ewing NJ	26.93
San Francisco-Oakland-Fremont CA	28.76	Vineland-Millville-Bridgeton NJ	20.36
San Francisco-San Mateo-Redwood City CA Metropolitan Division	30.43	Albuquerque NM	19.96
San Jose-Sunnyvale-Santa Clara CA	32.62	Farmington NM	18.58
San Luis Obispo-Paso Robles CA	21.29	Las Cruces NM	18.45
Santa Ana-Anaheim-Irvine CA Metropolitan Division	23.93	Santa Fe NM	20.26

Santa Barbara-Santa Maria-Goleta CA	22.71	North and West Central New Mexico nonmetropolitan area	15.91
Santa Cruz-Watsonville CA	22.49	Eastern New Mexico nonmetropolitan area	17.01
Santa Rosa-Petaluma CA	23.3	Southwestern New Mexico nonmetropolitan area	16.6
Stockton CA	20.6	Los Alamos County New Mexico nonmetropolitan area	36.42
Vallejo-Fairfield CA	22.42	Albany-Schenectady-Troy NY	22.24
Visalia-Porterville CA	18.45	Binghamton NY	19.84
Yuba City CA	19.8	Buffalo-Niagara Falls NY	20.2
Mother Lode Region of California nonmetropolitan area	21.2	Elmira NY	19.37
Eastern Sierra Region of California nonmetropolitan area	19.07	Glens Falls NY	18.66
North Coast Region of California nonmetropolitan area	19.21	Ithaca NY	21.89
North Valley Region of California nonmetropolitan area	18.27	Kingston NY	19.75
Northern Mountains Region of California nonmetropolitan area	20.93	Nassau-Suffolk NY Metropolitan Division	24.45
Boulder CO	25.65	New York-Northern New Jersey-Long Island NY-NJ-PA	26.48
Colorado Springs CO	21.46	Poughkeepsie-Newburgh-Middletown NY	22.25
Denver-Aurora CO	23.77	Rochester NY	20.77
Fort Collins-Loveland CO	21.2	Syracuse NY	20.87
Grand Junction CO	19.02	Utica-Rome NY	18.58
Greeley CO	19.68	Capital/Northern New York nonmetropolitan area	18.3
Pueblo CO	18.02	East Central New York nonmetropolitan area	18.94
East and South Colorado nonmetropolitan area	16.33	Central New York nonmetropolitan area	18.46
West Colorado nonmetropolitan area	19.51	Southwest New York nonmetropolitan area	18
Northcentral Colorado nonmetropolitan area	20.49	Asheville NC	17.71
Central Colorado nonmetropolitan area	17.87	Burlington NC	17.07
Bridgeport-Stamford-Norwalk CT	28.03	Charlotte-Gastonia-Concord NC-SC	21.46
Danbury CT	23.27	Durham NC	25.59
Hartford-West Hartford-East Hartford CT	25.13	Fayetteville NC	17.56
New Haven CT	24.37	Goldsboro NC	16.35
Norwich-New London CT-RI	21.31	Greensboro-High Point NC	19.05
Springfield MA-CT	21.4	Greenville NC	18.17
Waterbury CT	22.07	Hickory-Lenoir-Morganton NC	16.86
Worcester MA-CT	23.11	Jacksonville NC	16.42
Northwestern Connecticut nonmetropolitan area	21.4	Raleigh-Cary NC	21.54
Eastern Connecticut nonmetropolitan area	19.91	Rocky Mount NC	16.5
Dover DE	18.81	Virginia Beach-Norfolk-Newport News VA-NC	19.92
Wilmington DE-MD-NJ Metropolitan Division	24.12	Wilmington NC	18.43
Sussex County Delaware nonmetropolitan area	17.34	Winston-Salem NC	19.62
Washington-Arlington-Alexandria DC-VA-MD-WV Metropolitan Division	29.95	Northeastern North Carolina nonmetropolitan area	16.49

Washington-Arlington-Alexandria DC-VA-MD-WV	29.58	Other North Carolina nonmetropolitan area	16.39
Cape Coral-Fort Myers FL	18.68	Western Central North Carolina nonmetropolitan area	17.09
Crestview-Fort Walton Beach-Destin FL	19.08	Western North Carolina nonmetropolitan area	15.98
Deltona-Daytona Beach-Ormond Beach FL	16.96	Bismarck ND	18.23
Fort Lauderdale-Pompano Beach-Deerfield Beach FL Metropolitan Division	20.2	Far Western North Dakota nonmetropolitan area	18.63
Gainesville FL	20.55	West Central North Dakota nonmetropolitan area	17.43
Jacksonville FL	19.73	East Central North Dakota nonmetropolitan area	16.04
Lakeland-Winter Haven FL	17.5	Far Eastern North Dakota nonmetropolitan area	16.57
Miami-Fort Lauderdale-Miami Beach FL	20.3	Akron OH	19.74
Miami-Miami Beach-Kendall FL Metropolitan Division	20.21	Canton-Massillon OH	17.54
Naples-Marco Island FL	19.15	Cleveland-Elyria-Mentor OH	20.59
North Port-Bradenton-Sarasota FL	18.62	Columbus OH	21.03
Ocala FL	17.14	Dayton OH	20.39
Orlando-Kissimmee FL	18.71	Lima OH	18.29
Palm Bay-Melbourne-Titusville FL	20.67	Mansfield OH	17.62
Palm Coast FL	16.61	Parkersburg-Marietta-Vienna WV-OH	17.23
Panama City-Lynn Haven FL	17.14	Sandusky OH	16.64
Pensacola-Ferry Pass-Brent FL	17.72	Springfield OH	17.84
Port St. Lucie FL	18.09	Steubenville-Weirton OH-WV	16.39
Punta Gorda FL	17.17	Toledo OH	18.98
Sebastian-Vero Beach FL	18.09	Wheeling WV-OH	16
Tallahassee FL	19.73	Youngstown-Warren-Boardman OH-PA	17.42
Tampa-St. Petersburg-Clearwater FL	20.07	West Northwestern Ohio nonmetropolitan area	17.35
West Palm Beach-Boca Raton-Boynton Beach FL Metropolitan Division	20.63	Other Ohio nonmetropolitan area	16.78
Northwest Florida nonmetropolitan area	15.96	Eastern Ohio nonmetropolitan area	16.45
Northeast Florida nonmetropolitan area	16.57	Southern Ohio nonmetropolitan area	17.01
South Florida nonmetropolitan area	16.37	Lawton OK	16.75
Albany GA	17.15	Oklahoma City OK	18.83
Athens-Clarke County GA	19.15	Tulsa OK	18.65
Atlanta-Sandy Springs-Marietta GA	22.33	Northeastern Oklahoma nonmetropolitan area	15.85
Augusta-Richmond County GA-SC	19.35	Northwestern Oklahoma nonmetropolitan area	15.99
Brunswick GA	17.91	Southwestern Oklahoma nonmetropolitan area	16.17
Chattanooga TN-GA	18.39	Southeastern Oklahoma nonmetropolitan area	15.7
Dalton GA	16.73	Bend OR	19.05
Gainesville GA	18.73	Corvallis OR	22.65
Hinesville-Fort Stewart GA	18.02	Eugene-Springfield OR	19.66
Macon GA	17.6	Medford OR	18.96

Rome GA	18.17	Portland-Vancouver-Beaverton OR-WA	22.58
Savannah GA	19.07	Salem OR	19.5
Valdosta GA	15.46	Coastal Oregon nonmetropolitan area	17.38
Warner Robins GA	20.6	Southern Oregon nonmetropolitan area	17.59
North Georgia nonmetropolitan area	15.71	Eastern Oregon nonmetropolitan area	17.49
Middle Georgia nonmetropolitan area	16.11	Linn County Oregon nonmetropolitan area	18.72
East Georgia nonmetropolitan area	15.63	Altoona PA	16.51
South Georgia nonmetropolitan area	15.68	Erie PA	17.69
Honolulu HI	21.68	Harrisburg-Carlisle PA	20.72
Hawaii / Maui / Kauai nonmetropolitan area	19.21	Johnstown PA	17.05
Boise City-Nampa ID	19.52	Lancaster PA	18.81
Coeur d'Alene ID	17.22	Lebanon PA	18.41
Idaho Falls ID	19.19	Philadelphia PA Metropolitan Division	23.69
Lewiston ID-WA	17.85	Philadelphia-Camden-Wilmington PA-NJ-DE-MD	23.47
Logan UT-ID	16.71	Pittsburgh PA	20.44
Pocatello ID	17.47	Reading PA	19.57
North Idaho nonmetropolitan area	17.16	Scranton--Wilkes-Barre PA	17.73
Southwest Idaho nonmetropolitan area	16.29	State College PA	20.4
Southcentral Idaho nonmetropolitan area	16.81	Williamsport PA	17.28
East Idaho nonmetropolitan area	20.05	York-Hanover PA	19.05
Bloomington-Normal IL	22.11	Far Western Pennsylvania nonmetropolitan area	17.43
Cape Girardeau-Jackson MO-IL	17.06	West Central Pennsylvania nonmetropolitan area	16.54
Champaign-Urbana IL	21.64	Northeastern Pennsylvania nonmetropolitan area	17.01
Chicago-Naperville-Joliet IL Metropolitan Division	23.62	East Central Pennsylvania nonmetropolitan area	18.09
Chicago-Naperville-Joliet IL-IN-WI	23.32	Aguadilla-Isabela-San Sebastian PR	11.04
Danville IL	17.7	Fajardo PR	11.71
Davenport-Moline-Rock Island IA-IL	18.87	Guayama PR	13.69
Decatur IL	19.15	Mayaguez PR	11.73
Kankakee-Bradley IL	18.04	Ponce PR	11.7
Lake County-Kenosha County IL-WI Metropolitan Division	23.33	San German-Cabo Rojo PR	10.88
Peoria IL	19.56	San Juan-Caguas-Guaynabo PR	13.25
Rockford IL	19.73	Yauco PR	10.87
St. Louis MO-IL	20.9	Puerto Rico nonmetropolitan area 1	11.72
Springfield IL	21.17	Puerto Rico nonmetropolitan area 2	11.13
Northwest Illinois nonmetropolitan area	17.81	New Shoreham Town Rhode Island nonmetropolitan area	17.03
West Central Illinois nonmetropolitan area	17.09	Anderson SC	17.27
East Central Illinois nonmetropolitan area	16.87	Charleston-North Charleston-Summerville SC	19.21
South Illinois nonmetropolitan area	17.9	Columbia SC	19.39
Anderson IN	16.69	Florence SC	17.49

Bloomington IN	17.14	Greenville-Mauldin-Easley SC	18.8
Cincinnati-Middletown OH-KY-IN	20.5	Myrtle Beach-Conway-North Myrtle Beach SC	14.84
Columbus IN	19.95	Spartanburg SC	18.55
Elkhart-Goshen IN	17.75	Sumter SC	16.11
Evansville IN-KY	18.78	Low Country South Carolina nonmetropolitan area	17.17
Fort Wayne IN	18.74	Upper Savannah South Carolina nonmetropolitan area	17.26
Gary IN Metropolitan Division	19.08	Pee Dee South Carolina nonmetropolitan area	15.44
Indianapolis-Carmel IN	20.54	Lower Savannah South Carolina nonmetropolitan area	16.44
Kokomo IN	20.29	Rapid City SD	16.64
Lafayette IN	18.94	Sioux Falls SD	17.77
Louisville-Jefferson County KY-IN	19.39	Central South Dakota nonmetropolitan area	15.14
Michigan City-La Porte IN	16.79	Eastern South Dakota nonmetropolitan area	15.69
Muncie IN	18.06	Western South Dakota nonmetropolitan area	15.27
South Bend-Mishawaka IN-MI	18.89	Cleveland TN	16.21
Terre Haute IN	16.92	Jackson TN	16.8
Northeast Indiana nonmetropolitan area	16.56	Johnson City TN	17.08
Northwest Indiana nonmetropolitan area	16.48	Kingsport-Bristol-Bristol TN-VA	17.73
Southwest / Southeast Indiana nonmetropolitan area	17.08	Knoxville TN	18.8
Ames IA	20.08	Morristown TN	15.75
Cedar Rapids IA	19.77	Nashville-Davidson--Murfreesboro--Franklin TN	19.57
Des Moines-West Des Moines IA	20.72	Western Tennessee nonmetropolitan area	15.76
Dubuque IA	17.34	South Central Tennessee nonmetropolitan area	16.68
Iowa City IA	20.11	North Central Tennessee nonmetropolitan area	15.18
Omaha-Council Bluffs NE-IA	19.76	Eastern Tennessee nonmetropolitan area	15.54
Sioux City IA-NE-SD	16.14	Abilene TX	16.72
Waterloo-Cedar Falls IA	17.87	Amarillo TX	18.14
Northeast Iowa nonmetropolitan area	16.22	Austin-Round Rock TX	22.18
Northwest Iowa nonmetropolitan area	16.16	Beaumont-Port Arthur TX	19.1
Southwest Iowa nonmetropolitan area	15.62	Brownsville-Harlingen TX	15.25
Southeast Iowa nonmetropolitan area	16.59	College Station-Bryan TX	18.89
Kansas City MO-KS	21.18	Corpus Christi TX	17.35
Lawrence KS	17.55	Dallas-Fort Worth-Arlington TX	21.89
Manhattan KS	17.09	Dallas-Plano-Irving TX Metropolitan Division	22.53
St. Joseph MO-KS	16.83	El Paso TX	16.88
Topeka KS	18.62	Fort Worth-Arlington TX Metropolitan Division	20.36
Wichita KS	19.02	Houston-Sugar Land-Baytown TX	22.26
Kansas nonmetropolitan area	15.93	Killeen-Temple-Fort Hood TX	17.74

Bowling Green KY	17.38	Laredo TX	16.14
Clarksville TN-KY	16.91	Longview TX	17.83
Elizabethtown KY	17.9	Lubbock TX	17.38
Huntington-Ashland WV-KY-OH	17.06	McAllen-Edinburg-Mission TX	15.61
Lexington-Fayette KY	18.92	Midland TX	20.76
Owensboro KY	16.91	Odessa TX	18.91
West Kentucky nonmetropolitan area	17.09	San Angelo TX	17.05
South Central Kentucky nonmetropolitan area	15.69	San Antonio TX	18.95
West Central Kentucky nonmetropolitan area	17	Sherman-Denison TX	17.48
East Kentucky nonmetropolitan area	17.25	Tyler TX	17.72
Alexandria LA	16.89	Victoria TX	17.5
Baton Rouge LA	18.9	Waco TX	17.64
Houma-Bayou Cane-Thibodaux LA	18.24	Wichita Falls TX	16.66
Lafayette LA	17.87	Northwestern Texas nonmetropolitan area	16.58
Lake Charles LA	17.43	North Central Texas nonmetropolitan area	16.62
Monroe LA	16.7	Eastern Texas nonmetropolitan area	16.09
New Orleans-Metairie-Kenner LA	19.72	Central Texas nonmetropolitan area	16.19
Shreveport-Bossier City LA	17.62	Southern Texas nonmetropolitan area	15.72
Hammond nonmetropolitan area	16.48	Gulf Coast Texas nonmetropolitan area	16.52
Natchitoches nonmetropolitan area	16.14	Ogden-Clearfield UT	18.4
Winnsboro nonmetropolitan area	16.1	Provo-Orem UT	18.67
New Iberia nonmetropolitan area	17.61	St. George UT	16.43
Bangor ME	18.68	Salt Lake City UT	20.47
Lewiston-Auburn ME	17.84	Northern Utah nonmetropolitan area	18.96
Portland-South Portland-Biddeford ME	20.52	West Central Utah nonmetropolitan area	16.28
Portsmouth NH-ME	23.15	South Western Utah nonmetropolitan area	16.11
Rochester-Dover NH-ME	20.6	Eastern Utah nonmetropolitan area	18.02
Northeast Maine nonmetropolitan area	16.73	Burlington-South Burlington VT	21.98
Southwest Maine nonmetropolitan area	18.39	Southern Vermont nonmetropolitan area	19.76
Baltimore-Towson MD	24	Northern Vermont nonmetropolitan area	18.79
Bethesda-Frederick-Gaithersburg MD Metropolitan Division	28.06	Blacksburg-Christiansburg-Radford VA	18.57
Cumberland MD-WV	17.99	Charlottesville VA	21.8
Hagerstown-Martinsburg MD-WV	18.64	Danville VA	16.64
Salisbury MD	19.61	Harrisonburg VA	17.71
Upper Eastern Shore nonmetropolitan area	17.85	Lynchburg VA	17.48
Garrett County Maryland nonmetropolitan area	16.31	Richmond VA	21.41
St. Mary's County Maryland nonmetropolitan area	29.12	Roanoke VA	18.26
Barnstable Town MA	21.31	Winchester VA-WV	19.28
Boston-Cambridge-Quincy MA-NH	27.19	Southwestern Virginia nonmetropolitan area	16.24
Boston-Cambridge-Quincy MA NECTA Division	28.56	Southside Virginia nonmetropolitan area	15.83
Brockton-Bridgewater-Easton MA NECTA Division	22.22	Northeastern Virginia nonmetropolitan area	20.48

Framingham MA NECTA Division	27.86	Northwestern Virginia nonmetropolitan area	17.02
Haverhill-North Andover-Amesbury MA-NH NECTA Division	21.7	Bellingham WA	19.92
Lawrence-Methuen-Salem MA-NH NECTA Division	21.58	Bremerton-Silverdale WA	22.44
Leominster-Fitchburg-Gardner MA	19.67	Kennewick-Pasco-Richland WA	22.91
Lowell-Billerica-Chelmsford MA-NH NECTA Division	26.67	Longview WA	20.4
Nashua NH-MA NECTA Division	23.36	Mount Vernon-Anacortes WA	20.13
New Bedford MA	19.84	Olympia WA	22.19
Peabody MA NECTA Division	22.73	Seattle-Bellevue-Everett WA Metropolitan Division	26.25
Pittsfield MA	20.28	Seattle-Tacoma-Bellevue WA	25.57
Providence-Fall River-Warwick RI-MA	21.62	Spokane WA	20.24
Taunton-Norton-Raynham MA NECTA Division	21.67	Tacoma WA Metropolitan Division	21.94
Nantucket Island and Martha's Vineyard nonmetropolitan area	21.93	Wenatchee WA	18.56
Southwest Massachusetts nonmetropolitan area	18.66	Yakima WA	18.38
Northwest Massachusetts nonmetropolitan area	20.16	Northwestern Washington nonmetropolitan area	19.4
North Central Massachusetts nonmetropolitan area	23.64	Southwestern Washington nonmetropolitan area	18.7
Ann Arbor MI	23.44	Central Washington nonmetropolitan area	18.66
Battle Creek MI	19.78	Eastern Washington nonmetropolitan area	20.5
Bay City MI	18.1	Charleston WV	18.25
Detroit-Livonia-Dearborn MI Metropolitan Division	22.85	Morgantown WV	17.78
Detroit-Warren-Livonia MI	22.64	Southern West Virginia nonmetropolitan area	16.21
Flint MI	19.37	North Central West Virginia nonmetropolitan area	16.08
Grand Rapids-Wyoming MI	19.72	Appleton WI	18.95
Holland-Grand Haven MI	18.67	Eau Claire WI	17.84
Jackson MI	19.29	Fond du Lac WI	18.49
Kalamazoo-Portage MI	18.92	Green Bay WI	19.42
Lansing-East Lansing MI	21	Janesville WI	18.43
Monroe MI	19.13	Madison WI	21.8
Muskegon-Norton Shores MI	18.03	Milwaukee-Waukesha-West Allis WI	21.64
Niles-Benton Harbor MI	18.89	Oshkosh-Neenah WI	19.44
Saginaw-Saginaw Township North MI	18.99	Racine WI	18.34
Warren-Troy-Farmington Hills MI Metropolitan Division	22.49	Sheboygan WI	18.92
Upper Peninsula of Michigan nonmetropolitan area	17.49	Wausau WI	18.48
Northeast Lower Peninsula of Michigan nonmetropolitan area	15.99	Eastern Wisconsin nonmetropolitan area	17.69
Northwest Lower Peninsula of Michigan nonmetropolitan area	17.51	West Central Wisconsin nonmetropolitan area	17.92
Balance of Lower Peninsula of Michigan nonmetropolitan area	17.97	South Central Wisconsin nonmetropolitan area	16.54
		Southwestern Wisconsin nonmetropolitan area	16.96

		Northern Wisconsin nonmetropolitan area	16.61
		Casper WY	20.37
		Cheyenne WY	19.57
		Northwestern Wyoming nonmetropolitan area	18.14
		Southwestern Wyoming nonmetropolitan area	21.03
		Northeastern Wyoming nonmetropolitan area	20.32
		Southeastern Wyoming nonmetropolitan area	18.73

Table B.4 Truck percentage by state

State	Percentage of trucks	State	Percentage of trucks
Alabama	11.8%	Montana	13.0%
Alaska	9.5%	Nebraska	12.9%
Arizona	12.0%	Nevada	8.4%
Arkansas	16.8%	New Hampshire	7.4%
California	8.6%	New Jersey	7.6%
Colorado	6.7%	New Mexico	19.7%
Connecticut	6.5%	New York	7.8%
Delaware	8.9%	North Carolina	10.9%
Dist. of Col.	3.5%	North Dakota	17.8%
Florida	8.7%	Ohio	11.1%
Georgia	9.8%	Oklahoma	15.0%
Hawaii	3.9%	Oregon	12.1%
Idaho	14.6%	Pennsylvania	10.5%
Illinois	12.0%	Rhode Island	4.7%
Indiana	14.5%	South Carolina	10.1%
Iowa	15.2%	South Dakota	13.3%
Kansas	12.6%	Tennessee	11.6%
Kentucky	13.8%	Texas	12.2%
Louisiana	15.7%	Utah	19.2%
Maine	9.0%	Vermont	8.8%
Maryland	8.5%	Virginia	7.6%
Massachusetts	5.0%	Washington	10.4%
Michigan	7.5%	West Virginia	12.7%
Minnesota	6.7%	Wisconsin	13.2%
Mississippi	13.7%	Wyoming	19.9%
Missouri	14.5%	USA Average	10.6%

References

Bachman, W. H. (1997). *Toward a GIS-Based Modal Model of Automobile Exhaust Emissions*. EPA Cooperative Agreement #: CR823020. Georgia Institute of Technology. Atlanta, Georgia. Available at: <http://www.epa.gov/nrmrl/pubs/600r98097/600R98097.pdf. Last Accessed: December, 2011.

Barth et al, (2000). *The Development of a Comprehensive Modal Emissions Model*. NCHRP Project 25-11 Final report. Available at: http://onlinepubs.trb.org/onlinepubs/nchrp/nchrp_w122.pdf. Last Accessed: September, 2011.

Bertini, R.L., Tantiyanugulchai, S., Anderson E., Lindgren, R., & Leal, M. (2001). Evaluation of Region 2 Incident Response Program Using Archived Data. Portland State University, Research Report PSU-CE-TRG-01-01.

Blumentritt, C.W., Pinnell, C., McCasland, W.R., Ross, D.W., and Glazer, J. for Selection of Ramp Control Systems. NCHRP Report No. 232.

Boyles, S., Fajardo, D., & Fajardo., D. (2006), Naïve Bayesian Classifier for Incident Duration Prediction

Boyles, S., S. T. Waller. (2007). A Stochastic Delay Prediction Model for Real-Time Incident Management, *ITE Journal* 77, 18-24.

Chang, G.L. & Rochon, S. (2006). Performance Evaluation of CHART – the Real Time Incident Management System in Year 2006. Maryland Department of Transportation.

Cohen, J., & Cohen, P. (1983). Applied multiple regression/correlation analysis for the behavioral sciences (2nd ed.). Hillsdale, NJ: Lawrence Erlbaum Associates.

Chou, C., & Miller-Hooks, E. (2008). Benefit-cost Analysis of Freeway Service Patrol Programs: Methodology and Case Study. *Presentation at the 88th Annual Meeting of the Transportation Research Board*, Maryland, 20.

Chou, C. and E. Miller-Hooks, E. (2010). Violations Modeling in Studies of Concurrent-Flow Lanes. Transportation Research Record 2196, 75-82.

Chou, C., & Miller-Hooks, E. (2010). Simulation-Based Secondary Incident Filtering Method. *Journal of Transportation Engineering*, Vol. 136, No.8, 746-754.

CMEM, (2010). *Comprehensive Modal Emissions Model (CMEM)*. Center for Environmental Research and Technology. Riverside, California. Available at: <http://www.cert.ucr.edu/cmem/>. Last Accessed: December, 2011.

Cuciti, P., & Janson, B. (1995). Incident Management via Courtesy Patrol: Evaluation of a Pilot Program in Colorado. *Transportation Research Record, 1494*. Transportation Research Board, National Research Council, Washington DC.

Donnell, E., Patten, M., & Mason, J. (1999). Evaluating a Roadside Assistance Program: Penn-Lincoln Parkway Service Patrol. *Transportation Research Record: Journal of the Transportation Research Board*, 1683(-1), 143-149.

Dougald, L.E., Demetsky, M.J., (2008). Assessing Return on Investment of Freeway Safety Service Patrol Programs. *Transportation Research Record: Journal of the Transportation Research Board*, 2047, 19-27.

Garib, A., Radwan, A.E., & Al-Deek, H. (1997). Estimating magnitude and duration of incident delays. Journal of Transportation Engineering 123 (6), 459–466.

GREET (2008). *GREET Transportation Fuel Cycle Analysis Model, GREET 1.8b*. Argonne National Laboratory. USDOE. 2008. Available at: <cta.ornl.gov/bedb/.../Lower-Higher_Heating_Values_for_Various_Fuels.xls>. Last Accessed: January, 2012.

Guin, A., Porter, C., Smith, B., & Holmes, C. (2007). Benefits Analysis for Incident Management Program Integrated with Intelligent Transportation Systems Operations: Case Study. *Transportation Research Record: Journal of the Transportation Research Board*, 2000, 78-87.

Hadi, M., Sinha, P., & Wang, A. (2007). Modeling Reductions in Freeway Capacity due to Incidents in Microscopic Simulation Models. *Transportation Research Record: Journal of the Transportation Research Board, 1999*(-1), 62-68. Choa, F. , Milam , R. T. , & Stanek D. (2002).

Hagen, L., Zhou, H., & Singh, H. (2005). Road Ranger Benefit Cost Analysis. Florida Department of Transportation.

Haghani, A., Iliescu, D., Hamedi, M. & Yang, S. (2006). Methodology for Quantifying the Cost Effectiveness of Freeway Service Patrol Programs: A Case Study. University of Maryland.*Guidelines*

Han, L. D., Chin, S., & Hwang, H. (2003). Estimating Adverse Weather Impacts on Major U.S. Highway Network, Transportation Research Board, Washington, D.C.

Hani S. Mahmassani, Jing Dong, Jiwon Kim, Roger B. Chen and Byungkyu (Brian) Park (2009). Incorporating Weather Impacts in Traffic Estimation and Prediction Systems, Final Report.

Hawkins, P. (1993). Evaluation of the Southwest Freeway Motorist Assistance Program in Houston. Texas Transportation Institute, Texas Department of Transportation, Report No. 1922-1F.

Hirunyanitiwattana, W., & Mattingly, S. (2006). Identifying Secondary Crash Characteristics for California Highway System. Presented at 85th Annual Meeting of the Transportation Research Board, Washington, D.C.

Hobeika, A.G. & Dhulipala, S. (2004). Estimation of Travel Times on Urban Freeways under Incident Conditions, *Transportation Research Record*: *Journal of the Transportation Research Board 1867*, TRB, National Research Council, Washington D.C., 97-106

International Panel on Climate Change (IPCC), (2006). *2006 IPCC Guidelines for National Greenhouse Gas Inventories*. Available at: <http://www.ipcc-nggip.iges.or.jp/public/2006gl/index.html>. Last Accessed: November, 2011.

Karlaftis, M. G., Richards, N. J., Latoski, S. P., & Sinha, K. C. (1998). Empirical analysis of secondary crash causes. Proc., 77th Annu. Meeting, Transportation Research Board, Washington, D.C.

Karlaftis, M., S. Latoski, N. Richards, & K. Sinha. (1999). ITS Impacts on Safety and Traffic Management: An Investigation of Secondary Crash Causes. ITS Journal, Vol. 5, No. 1, 39–52.

Khattak, A., J. Schofer, and M. Wang. (1995) A simple time-sequential procedure for predicting freeway incident duration. *IVHS Journal*, Vol. 2, , 113-138.

Khattak, A., Wang, X., & Zhang, H. (2008). Are Incident Durations and Secondary Incidents Interdependent *Presented at the 2009 Transportation Research Board Annual Meeting,* Washington, D.C.

Kim, W., Chang, G., & Rochon, S. M.(2008)Analysis of Freeway Incident Duration for ATIS Application, Presented the 15th world congress on intelligent transportation system, New York

Koupal et al., (2005). Koupal, J, Landamn,l, Nam,E, Scarbro,C, Glover,E and Ginannelli, R. *MOVES Energy and Emissions Inputs*. Office of Transportation and Air Quality. Available at: http://www.epa.gov/otaq/models/ngm/420p05003.pdf. Last Accessed: December, 2011.

Latoski, S. P., Pal, R., & Sinha K.C. (1999). Cost-Effectiveness Evaluation of Hoosier Helper Freeway Service Patrol. *Journal of Transportation Engineering*, 125(5), 429-437.

Lindley, J.A. (1987). Urban Freeway Congestion: Quantification of the Problem and Effectiveness of Potential Solution. *ITE Journal 57 (1)*, 27-32.

Martin Fellendorf , Peter Vortisch, (2001) Validation of the Microscopic Traffic Flow Model VISSIM in Different Real-Workd Situations. Annual Meeting TRB.

Masinick, J. P., & Tang, H. (2004).An analysis on the Impact of Rubbernecking onUrban Freeway Traffic, Research Report No. UVACTS-15-0-62.

Mauch, M., Ahn, S., Chung, K., & Skabardonis, A. (2005). Baseline Evaluation of the Freeway Service Patrol (FSP) I-710 Big-Rig Demonstration Program. Institute of Transportation Studies, University of California-Bekerley, Working Paper UCB-ITS-WP-2005-3.

Minnesota Department of Transportation, (2004). FIRST Program Evaluation. ITS annual report.

Moore, J., G. Giuliano, & Cho, S. (2004). Secondary Accident Rates on Los Angeles Freeways. *Journal of Transportation Engineering*, Vol. 130, No. 3, 280–285.

Murty, A. S. R., & Verma, A. K. (1986). Inverse normal and lognormal distributions for reliability design. *Reliability Engineering*, 15(1), 55-60.

Nam, D., & Mannering, F. (2000). An exploratory hazard-based analysis of highway incident duration. Transportation Research Part A: Policy and Practice 34 (2), 85–102.

Office of Transportation and Air Quality (OTAQ), 2012. *Regulations and Standards*. Available at: <http://www.epa.gov/otaq/climate/regulations.htm>. Last Accessed: January, 2012.

Pulugurtha, S., Dangeti, M., Nambisan, S., & Kaseko, M.(2002). Simulating and Analyzing 27 Incidents Using CORSIM and VISSIM Traffic Simulation Software. Proceedings of the 28 Seventh International Conference, Applications of Advanced Technologies in Transportation.

Rakha, H., Farzaneh, M., Arafeh, M., Hranac, R., Sterzin, E. & Krechmer, D. (2007). Empirical Studies on Traffic Flow in Inclement Weather, Final Report - Phase I.

Raub, R. A., (1997). Occurrence of Secondary Crashes on Urban Arterial Roadways. Transportation Research Record 1581, TRB, National Research Council, Washington, D.C., 1997. pp. 53–58.

Roadway Design Manual, 2010.

Saka, A. A., Jeihani, M., & James, P. A. (2008) Estimation of Traffic Recovery Time for Different Flow Regimes on Freeways. Final Report No. SP708B4L. July 2008

Shankar, V., Mannering, F., & Barfield, W. (1995). Effect of roadway geometrics and environmental factors on rural freeway accident frequencies. *Accident Analysis & Prevention, 27*(3), 371-389.

Skabardonis, A., & Mauch, M. (2005). SSP Beat Evaluation and Predictor Models: User's Manual. Institute of Transportation Studies, University of California-Berkeley, Research Report: UCB-ITS-RR-2005-XX.

Skabardonis, A., Noeimi, H., Petty, K., Rydzewski, D., Varaiya, P., & Haitham, A. (1995). Freeway Service Patrol Evaluation. Institute of Transportation Studies, University of California-Berkeley, California PATH Research Report No. UCB-ITS-PRR-95-5.

Skabardonis, A., Petty, K., Varaiya, P., & Bertini, R. (1998). Evaluation of the Freeway Service Patrol (FSP) in Los Angeles. Institute of Transpotation Studies, University of California-Berkeley, California PATH Research Report No. UCB-ITS-PRR-98-31.

Smith, K., & Smith, B.L., (2001). Forecasting the Clearance Time of Freeway Accidents. No. STL-2001-01, Center for Transportation Studies (University of Virginia), Charlottesville, VA.

Sun, C. (2007). Secondary Accident Data Fusion for Assessing Long-Term Performance of Transportation Systems. Midwest Transportation Consortium, Center for Transportation Research and Education, Cedar Falls, Iowa.

Sun, C., Chilukuri, V., Ryan, T., & Trueblood, M. (2010). Evaluation of Freeway Motorist Assist Program. University of Missouri-Columbia, Final Report RD 09-004.

Sun,C., Chilukuri, V., (2010). Dynamic Incident Progression Curve for Classifying Secondary Traffic Crashes. *Journal of Transportation Engineering*, Vol. 136, No. 12, 1153-1158.

Traffic Incident Management Handbook, 2000

USDOE, (2011). *Alternative Fuels & Advanced Vehicles Data Center*. Energy Efficiency & Renewable Energy. USDOE. Available at: <http://www.afdc.energy.gov/afdc/>. Last Accessed: December, 2011.

USDOE, (2012). *Fuel Economy*. Energy Efficiency & Renewable Energy. USDOE. Available at: < http://www.fueleconomy.gov/feg/findacar.shtml>. Last Accessed: January, 2012.

USEPA, (2004). *Update of Methane and NitroUSOxide Emission Factors on On-Highway Vehicles.* USEPA Report Number: EPA420-P-04-016. Available at: < http://www.epa.gov/otaq/models/ngm/420p04016.pdf >. Last Accessed: January, 2012.

USEPA, (2006). *High Global Warming Potential (GWP) Gases*. Available at: http://www.epa.gov/highgwp/scientific.html. Last Accessed: January, 2011.

USEPA, (2007). *Emission Facts: Average Annual Emissions and Fuel Consumption for Passenger Cars and Light Trucks*. Consumer Information. USEPA. Available at: < http://www.epa.gov/oms/consumer/f00013.htm> . Last Accessed: January, 2012.

USEPA, (2009). *Transportation and Air Quality*. Available at: http://www.epa.gov/otaq/. Last Accessed: August, 2011.

USEPA, (2011). *Motor Vehicle Emissions Model (MOVES)*. Modeling and Inventories. USEPA. Available at: <http://www.epa.gov/otaq/models/moves/index.htm>. Last Accessed: January, 2012.

Wang, Y.H., Hallenbeck, M., & Cheevarunothai, P. (2008).Quantifying Incident-Induced 21 Travel Delays on Freeways Using Traffic Sensor Data Washington State Department of 22 Transportation, Report No. TNW2008-02, 23

Wirasinghe, S. C. (1978) Determination of traffic delays from shock-wave analysis. Transportation Research 12, 343-348.

Zhan, C., A. Gan, and M. Hadi., (2009). Identifying Secondary Crashes and Their Contributing Factors. In *Transportation Research Record: Journal of the Transportation Research Board*, No. 2102, Transportation Research Board of the National Academies, Washington, D.C., 68-75.

Zhan, C., Shen, L., Hadi, M., and Gan, A. (2008) . Understanding the characteristic of secondary crashes on freeways. CD-ROM, Transportation Research Board, Washington, D.C.

Zhang, H., & Khattak, A. (2010). Analysis of Cascading Incident Event Durations on Urban Freeways. *Transportation Research Record: Journal of the Transportation Research Board*, No. 2178, Transportation Research Board of the National Academies, Washington, D.C., pp. 30–39.